UNIVERSITÄTSKLINIKUM HAMBURG-EPPENDORF

Klinik für Pädiatrische Hämatologie und Onkologie

Prof. Dr. med. Stefan Rutkowski

The transcriptional co-activator and lysine acetyltransferase CBP in brain and tumor development

Dissertation

zur Erlangung des Doktorgrades Dr. rer. biol. hum. / PhD
an der Medizinischen Fakultät der Universität Hamburg.

vorgelegt von:

Melanie Schoof
aus Henstedt-Ulzburg

Hamburg 2020

**Angenommen von der
Medizinischen Fakultät der Universität Hamburg am:**   23.06.2020

Veröffentlicht mit Genehmigung der Medizinischen Fakultät der Universität Hamburg.

Prüfungsausschuss, der/die Vorsitzende: Prof. Dr. Ulrich Schüller

Prüfungsausschuss, zweite/r Gutachter/in: Prof. Dr. Dietmar Kuhl

Parts of this work have been published as:

TABLE OF CONTENTS

1 INTRODUCTION

1.1 THE MOUSE AS A MODEL ORGANISM

Today, the mouse (*Mus musculus*) is the most common research mammal in all biological disciplines all over the world. The importance of the mouse as a model system is reflected by the fact that until 2019, 180 of the 216 Nobel Prize laureates in physiology and medicine involved research based on mouse models [1].

The history of the mouse as a model system started in the 18th and 19th century, when the first mice were bred and traded by wealthy collectors as a domestic animal. During the 19th century, the first scientists became interested in the mouse genetics. The breeding was mostly done to generate different coat colors and the mouse became the first mammal in which the genetic doctrine proposed by Gregor Mendel was applied [2]. In order to reduce genetic variability, the first inbred strain was developed in the early 20th century. In the 1920s, Clarence Cook Little bred the C57Bl/6J strain, which is still one of the most commonly used mouse strains in research today. In 1929, Little founded the *Jackson Laboratory*, which helped understanding the mouse genome as it was an independent research institution collecting information and mouse strains [3]. Then, in 2002, the mouse genome was sequenced and it was revealed that mice and men share 85 % of their protein coding genome [4].

1.1.1 THE CRE-LOXP SYSTEM

An important step in the history of the mouse as a model system was the development of the cre-loxP system. Since the beginning of the employment of the mouse in biological research, animals were used in cancer research in order to study the role of specific proteins in development and disease. For this purpose, knockout mice lacking one or two copies of the respective gene were bred [5]. Those mouse models helped gaining a lot of information but have their inherent limitations. If a protein is essential for development, a homozygous knockout is not viable and therefore the organism cannot be studied. Additionally, a conventional knockout does not allow a space and time specific knockout of a gene of interest.

Therefore, the cre-loxP system is used today. It allows a cell and time specific manipulation of a target gene which can be achieved by either activation through cre-driven excision of a STOP-cassette in front of a target gene or the inactivation of a transgene.

Sternberg et al. discovered the cre-loxP system in 1981 [6]. They studied the bacteriophage P1 and discovered that it carries an enzyme, which cuts and recombines DNA at a defined position. This enzyme was called cre (causing recombination) and its recognition sites loxP (locus for crossing over(x), P1). This system was then employed in different biological systems for a targeted gene activation or inactivation. In 1988, it was first used in a mammalian cell line and in 1993, the first mouse strain using the cre-loxP system was developed [7, 8].

The principle of the cre-loxP system is simple: The cre recombinase is able to recognize its specific target sequences, the loxP sites, binds them and cuts out the DNA sequence between the two loxP sites. The region which is excised by the recombinase is called floxed (flanked by loxP).

1.2 CENTRAL NERVOUS SYSTEM DEVELOPMENT

The central nervous system (CNS) consists of the brain and the spinal cord and controls all body functions.

The CNS derives from the germinal layer ectoderm in a process called neurulation. It starts as early as gestational day 19 in humans with the establishment of the neural plate. During development, the lateral edges of the neural plate move towards each other and fuse in the midline. Thereby, they form the neural tube, which is the precursor for the brain and the spinal cord. Neurulation is completed at the end of the fourth week of pregnancy in humans and at embryonic day (E) nine in mice [9, 10]. After neural tube formation, three primitive vesicles are formed which build the three main regions later in development. These are the prosencephalon, the mesencephalon and the rhombencephalon.

Neurogenesis and the general brain architecture are largely completed at birth of both, mice and men, with the exception of the cerebellum, which develops also postnatal. Additionally, the maturation of glial cells, synaptogenesis, synapse pruning and myelination happen after birth [11]. The main mechanisms of development, migration and differentiation are conserved between human and mouse, only the time scale is shifted between species [12]. Therefore, the mouse is a frequently used model for mammalian brain development. One main difference between rodents and primates is the existence of a highly folded (gyrated) cortex in primates in comparison to a smooth (lisencephalic) cortex in rodents. This allows a larger number of neurons in the same area leading to a higher neuron density in primates. The main difference in the development of a lisencephalic compared to a gyrated cortex is the existence of an outer subventricular zone (oSVZ) in primates. It consists of a second layer of proliferating intermediate progenitor cells and thereby increases the number of neurons

which can be produced from the radial glia cells [13]. Despite these differences, the mouse is believed to model many aspects of human brain development, and many important findings throughout the last decades were made in the mouse as a model organism.

1.3 THE NEOCORTEX

The mammalian brain can be divided into fore-, mid- and hindbrain, which develop from the different primitive vesicles. The forebrain consists of the cerebral hemispheres and the underlying diencephalon. It is essential for complex cognitive processes and voluntary movements. The cerebral hemispheres are composed of a layer of grey matter, the cerebral cortex or neocortex, and underlying white matter. The neocortex is distinct from the more ancient paleo cortex and archicortex and is the largest structure for neural integration in the CNS [14, 15]. The paleocortex and the archicortex are phytogenetically older structures and build up the olfactory bulb (OB) and the hippocampus, respectively. The neocortex is strictly organized in six distinct layers in all mammals, a common feature already described in the early 20th century [16, 17]. All cell layers have a characteristic cell shape: Layers II/III and V contain pyramidal neurons, and the layers IV and VI consist of stellate and multiform cells, which do not show the typical neuron morphology. Layer I contains Cajal-Retzius cells, which are among the first neurons in the developing cortex and that are important for neuron migration. Thus, the correct establishment of cortex morphology is highly dependent on these cells (Fig. 1 b).

The biggest class of neurons in the cortex are pyramidal neurons. They can be found in all mammals, but also in birds, fish and reptiles. The name derives from the typical morphology with the cell soma shaped like a rounded pyramid. They usually have one or more longer dendrites emerging from the upper part of their soma, the apical dendrites, and a cluster of shorter dendrites on the other site of the soma (basal dendrites). The axon is also located on the basal site of the cell. On the dendrite, the synapses are organized on "dendritic spines" [18].

Four classes of dendritic spines are described which represent different differentiation stages and flexibility. The most stable and differentiated spines are mushroom spines which are defined by a large head where the synapses are located and a short, thin neck. In comparison, long thin spines are defined by a long neck and no recognizable head. They are thought to be more flexible and often built and retracted. Due to their lifespan, the stable mushroom spines are thought to be more important for long-term memory whereas the flexible thinner spines are needed for short term memory [19]. It was shown that neuron morphology is disturbed in mental retardation. Additionally, it was proposed that the morphology of the neuron is correlated to the behavioral phenotype in patients. Abnormalities

in neuron morphology are described in Down-, Rett-, Fragile-X-, Pitt-Hopkins- and other intellectual disability (ID) syndromes. The changes in morphology are different between the syndromes, which correlates well with the individual symptoms of ID in patients [20-22].
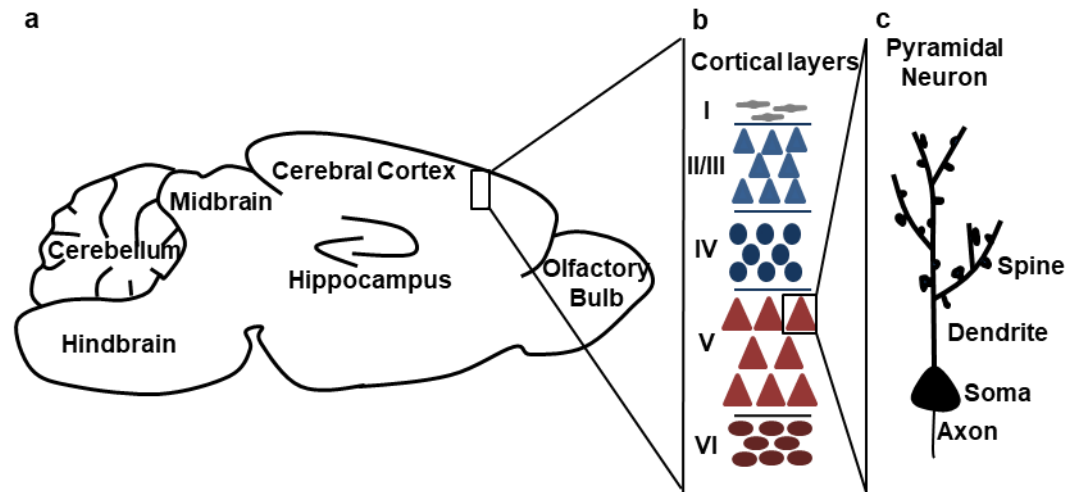
Figure 1: Forebrain architecture

(a) Schematic drawing of the mouse brain. Major brain structures are labeled. (b) Schematic drawing of the cell composition of the mammalian neocortex. The cortex is built from six distinct cell layers consisting of specific neurons. The layers can be distinguished by their cell morphology and split into the deeper layers V and VI (red) and the upper layers II/III and IV (blue) based on their time of development. The outermost layer I consists of Cajal-Retzius cells (grey) which are important for correct cortex development and among the first neurons to be produced. [23, 24] (c) Drawing of a pyramidal neuron e.g. from the cortical layer V. It is characterized by the pyramidal shaped cell soma and a prominent apical dendrite. Dendritic spines are small protrusions on the dendrites. The axon is located on the basal site of the cell [18].

1.4 NEURONAL MIGRATION

The migration of neural progenitor cells (NPCs) is one of the key mechanisms in the development of the CNS. The cells are migrating through the reconstruction of the cytoskeleton in response to extracellular cues. Thereby the procedure of cell movement follows a conserved structure: First, the cell extends a neurite which is preceded by a growth cone. Then the nucleus is translocated into the neurite and the trailing process is retracted. This is regulated by a large interactive signaling network and always involves the cytoskeleton as the mechanical unit performing the movement and extracellular signals guiding it. These signals can be long-distance guidance cues or short-distance instructive molecules [25].

There are two modes of neural precursor migration in the mammalian brain: radial migration from the progenitor zone to the surface, following the radial layout of the neural tube; and tangential migration, which is orthogonal to the radial migration direction [26].

Radial migration is important for the construction of laminated structures of the brain like the cerebral and cerebellar cortex, the spinal cord and the striatum and thalamus. One of the best studied migration process in the developing brain occurs during the development of the neocortex.

All neurons which build the cerebral cortex derive from the ventricular zone (VZ) and the subventricular zone (SVZ) [27-30]. The "classical" model of neocortex development proposes the radial glia (RG) as a neural stem cell (NSC) residing in the VZ, lining the ventricle. These cells divide, like other stem cells, asymmetrically. In each division, one RG daughter cell and a transit amplifying progenitor cell (TAP) are produced. The TAP divides symmetrically for a defined number of divisions before differentiating into a non-dividing neural cell. The neurons produced by TAPs migrate to their final position along the fibers of the RG to the cortical plate. Thereby, the cortical layers are formed in an inside out fashion (Figure 2) [13, 31-33]. In mouse cortical development, the first wave of neural migration to build the cortex happens around E11. The produced neurons build the preplate in the developing cortex. The second wave of migration around E13 builds the marginal plate and the subplate. Afterwards, successive waves of migration build up the layers in the cortical plate with the earliest neurons constructing the deepest layers [34, 35].
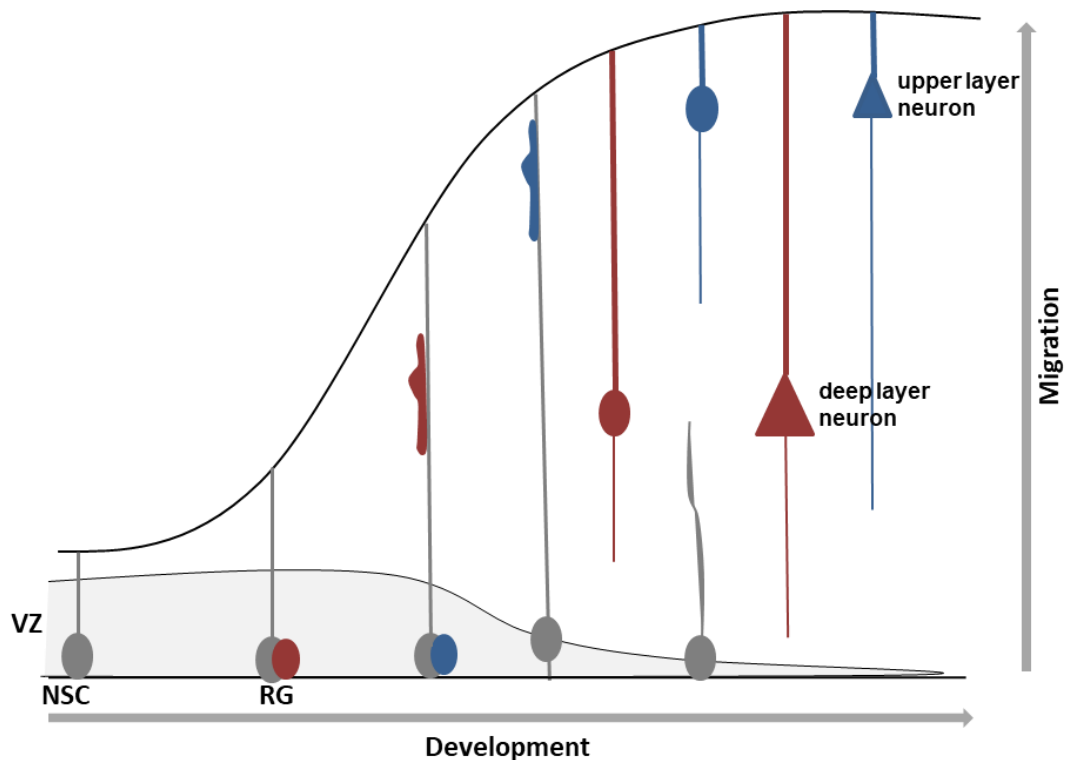
Figure 2: Radial migration in neocortex development

(a) Schematic drawing of mouse neocortex development. NSCs residing in the ventricular zone elaborate processes towards the cortical surface. During neurogenesis between E11 and E16, specific NSCs, RGs, produce neural precursor cells (NPCs) by asymmetric division. Precursor cells then migrate along the process of the RG towards the cortical surface and build up the neocortex in an inside out fashion in which early born neurons (red) build up the deeper layers and later born neurons (blue) build the upper layers. Neurons migrate to their final destination in the cortex, where they differentiate and establish their final morphology. The NSCs which remain in the VZ switch to the production of glial cells after neurogenesis is completed. Afterwards, they give rise to a layer of ependymal cells and astrocytes. Adapted from [36].

Tangential migration is known from two main regions in the forebrain: the migration from the medial ganglionic eminence (MGE) towards the neocortex and hippocampus and from the lateral ganglionic eminence (LGE) towards the OB via the rostral migratory stream (RMS). The latter route is also one of the two areas of postnatal neurogenesis in the mouse brain. It was proposed that neural migration and neurodevelopment are co-dependent processes not only in the embryonic brain but also in adult neurogenesis [25]. In the mouse, adult neurogenesis in the OB is a key example for such a process. Interneurons of the OB (granule and periglomerular cells (PGs)) are constantly generated throughout life. The precursors of those cells are generated in the SVZ at the lateral ventricle and migrate through the RMS towards the OB. This migration is found in different species like rodents, primates and humans [37-40]. RMS migration is one of the largest and fastest routes in CNS development [41]. Additionally, it is highly productive as postnatally produced neurons in the

SVZ incorporate into the OB circuitry with a daily turnover rate of 1 % [26, 37, 42-44]. The origin of the stem cell compartment constituting the SVZ and thereby the RMS lie within the embryonic LGE. The alignment of cells in the region of the latter RMS can be found as early as E15 in the rodent brain [45].

The RMS itself is composed of different cell types. The majority of cells are migrating neuroblasts (Type A cells) which organize themselves into chains. In the postnatal brain, the type A cells are surrounded by a so called "glial tube" composed of specialized astrocytes. A key difference between the tangential migration in the RMS and the radial migration in the embryonic cortex is the dependence on glial processes for migration. In the developing cortex, precursor cells migrate along the fibers of the RG towards their final position in the cortical plate [34]. In the RMS, the glial tube is formed postnatally, so prenatal migration has to be completely independent of glial processes [46]. Thus, the astrocytes surrounding the RMS have both signaling and scaffolding functions for the migrating cells but are not essential for the migration. Additionally, the (postnatal) RMS is surrounded by endothelial cells. The blood vessels in close proximity to the RMS are organized in parallel to the migration route and deliver signaling molecules as well as providing an additional scaffold for the migrating cells.

The migration in the RMS can be divided into three steps: Initiation, migration and termination. The initiation starts in a specialized stem cell niche in the SVZ adjacent to the lateral ventricle. The NSCs residing there (Type B cells) divide slowly and asymmetrically, and produce TAP cells (Type C cells). These progenitors in turn produce numerous migrating Type A cells before finally differentiating into Type A cells themselves [47]. The migration towards the OB is then directed and influenced by numerous factors including cell-cell adhesion and extracellular matrix (ECM) interactions, chemo-attractive and chemo-repulsive signals, as well as local influences by astrocytes and blood vessels [48]. Once the cells reach the OB, the third step in migration starts. During termination, the cells detach from their migration chains and migrate radially along glial processes towards their final position in the granular and periglomerular layer. The differentiation of precursor cells in the OB is a multistep process which ends in the formation of γ-aminobutyric acid (GABA)-ergic neurons in the granular layer or dopaminergic neurons in the periglomerular layer [48].
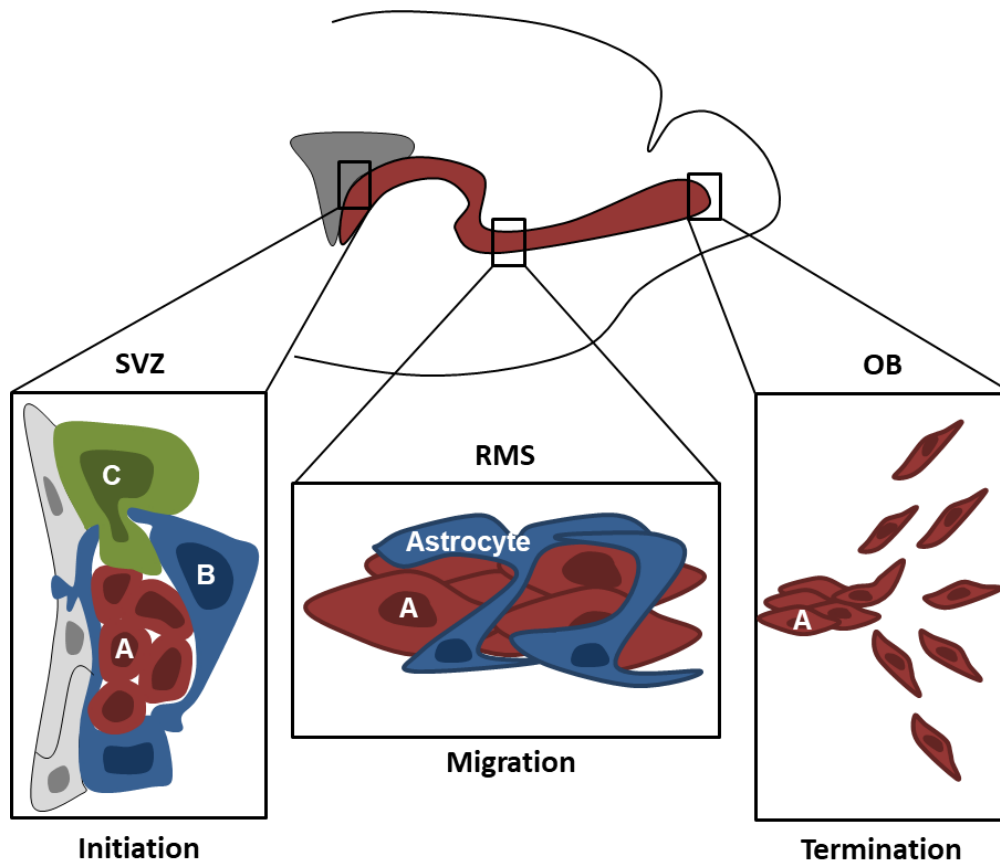
Figure 3: Migration in the mouse rostral migratory stream

Schematic drawing of the different phases of neural precursor migration in the mouse RMS. The cells start their migration in the SVZ, where ependymal cells (grey) line the lateral ventricle. Three cell types of precursor cells can be found within the SVZ. Type B cells (blue) are the local stem cells with astrocytic characteristics expressing GFAP residing in this neurogenic niche. These cells produce transit-amplifying precursor cells (Type C, green) which then in turn give rise to migratory neuroblasts (Type A cells, red). After initiation, Type A cells start their migration in the RMS towards the olfactory bulb (OB). The migrating cells organize themselves in chains which are ensheathed by astrocytes (blue). Once arrived at the OB, cells terminate their migration by detaching from the chains and switching to a radial migration until they reached their final position and integrate into local circuitry in the OB. Adapted from [49, 50] (for [49] Copyright 2003 Society for Neuroscience).

1.5 THE CYCLIC AMP-RESPONSIVE ELEMENT BINDING PROTEIN BINDING PROTEIN

The cyclic AMP-responsive element binding protein (CREB) binding protein (CREBBP/CBP) is a ubiquitously expressed protein. Its coding gene *CREBBP/CBP* is located on chromosome 16.3 and produces a protein of 2442 amino acids and 265 kDa. CBP was first described in 1993 as a transcriptional co-activator interacting with CREB, c-Fos and c-Jun [51]. More recently, interactions of CBP with more than 400 nuclear proteins were described [52].

In 1996, it was shown that CBP has an additional intrinsic lysine acetylation activity [53]. CBP and its close homologue, the E1A Binding Protein P300 (p300), build their own family among the lysine acetyl transferases (KATs, formerly known as HATs). Lysine acetylation is a ubiquitous posttranslational modification which is involved in many different signaling pathways (reviewed for example in [54]). The opposing enzymes to KATs are lysine deacetylases (KDACs) which remove the acetyl group from the lysine. Lysine acetylation is known for two main functions. The first function comprises the acetylation of lysine residues in the tail of histones, also called histone acetylation. This process facilitates the access of transcription factors (TFs) and the basal transcription machinery to the DNA and is essential for high-level gene expression [55]. The second main function is the acetylation of lysine residues in various proteins independent of histones, which is also described as an important posttranslational modification, for example for p53, nuclear factor 'kappa-light-chain-enhancer' of activated B-cells (NF-kB) and DNA-directed RNA polymerase II subunit RPB1 [56-58].

CBP as a large protein consists of different domains for protein-protein interactions and lysine acetylation as well as for transactivation (Fig. 3) [59, 60]. It functions as a molecular scaffold through physical interaction with a TF and opening of condensed DNA by acetylation.

			Chromatin association and modification region			
CH1			CH2		CH3	
NRID	TAZ1	KIX	Bromo / PHD	KAT11	TAZ2	Q
Exons 1	2	3-4	5-9	10-16 / 17	18-30	31
Interaction partners NRs Stat1	Mdm2 Pit1 HIF1 Stat2		CREB BRACA c-myb ATF2/4 c-Jun	ATF-2	C-Fos E1A MyoD PCAF TFIIB TBP	p/CIP SRC1
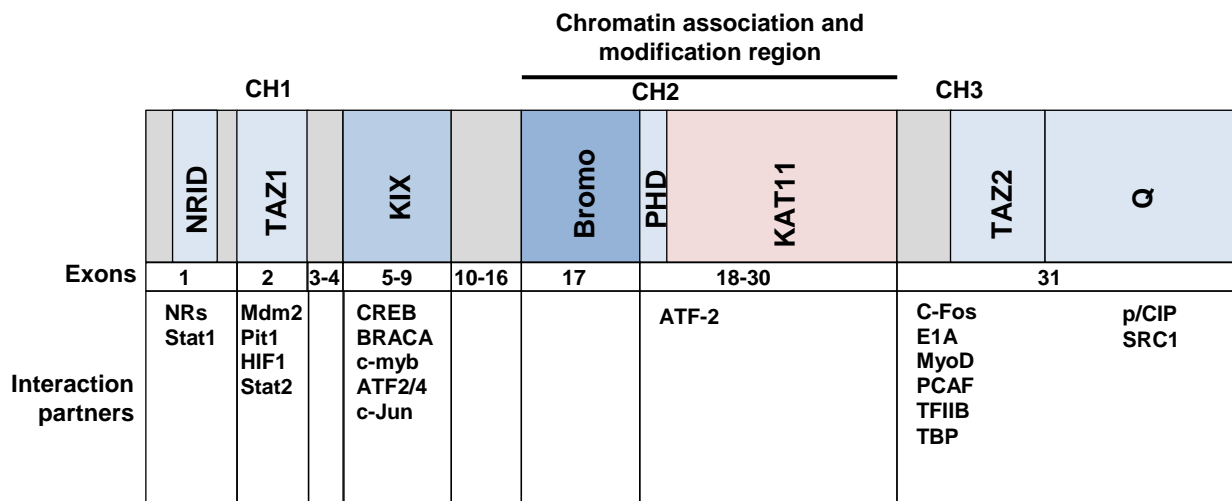
Figure 4: Linearized structure of the CBP protein.
Depicted are important protein domains: NRID – Nuclear hormone receptor interaction domain, TAZ – transcriptional adapter zinc-binding domain 1&2, KIX – CREB binding domain, Bromo – bromodomain, PHD – plant homeodomain, KAT11 – lysine acetyltransferase, Q – polyglutamine stretch, CH 1-3: cystein/histidine-rich region 1-3. The exons coding for the respective domains are depicted as well as examples of interaction partners. Adapted from [60].

1.6 THE RUBINSTEIN-TAYBI SYNDROME

The Rubinstein-Taybi syndrome (RTS/RSTS; OMIM 180849/613684) is a congenital neurodevelopmental disorder first described in 1963 [61]. It affects 1/100,000 to 125,000 newborns and more than 90 % of patient survive into adulthood [62]. In 1995, *CBP* mutations were found to be responsible for the syndrome [63]. Ten years later, in 2005, mutations in the strongly homologous *EP300* were identified as an additional cause for RSTS [64]. Mutations in both genes are dominant and the majority of mutations are *de novo* in one of the two responsible genes [65-67]. All kinds of *CBP* mutations are described to cause RSTS with point mutations being the most frequent type of mutation. Mutations in *CBP* are identified in 50 – 70 % and *EP300* mutations in about 3 % of patients [64, 68, 69]. For the remaining patients, the genetic cause of the syndrome remains unclear. Some patients might carry mutations in the regulatory regions of the genes which are usually not included in the standard sequencing procedures [70].

The clinical manifestations of RSTS includes a multitude of symptoms and involve all major body parts [71]. Frequent symptoms are short statue, facial abnormalities including microcephaly, broad nasal bridge and a highly arched palate, heart malformations (affecting 1/3 of patients [72]), abnormalities in the extremities leading to the term "broad thumbs and hallux syndrome" [73], motor deficits [74], cancer predisposition especially for neuronal and embryonal tumors [75, 76] and an ID with an intelligence quotient (IQ) between 35 and 50 [77].

The multitude of neurological symptoms together with the microcephaly as a main feature of RSTS led to a focus on brain anomalies in RSTS patients [78]. Despite this, only very few autopsies of brains of RSTS patients have been conducted in the late 1960s and early 1970s. They describe anomalies in different brain regions, for example in the corpus callosum (CC), the hippocampus and especially a less differentiated neuron morphology of cortical neurons [79-81]. The anomalies of the CC and the hippocampus are also reflected in several magnet resonance imaging (MRI) studies. The largest series of MRIs of RSTS patients so far was conducted in 2018 by Ajmone et al. in 23 Italian RSTS patients [82]. This study describes dimorphisms in the CC, brain stem, hippocampus and OB hypo- or aplasia.

1.7 CBP FUNCTION IN RSTS

CBP is important for hematopoietic stem cells and interacts with developmentally relevant TFs like CREB, suggesting that CBP might be generally important for cell differentiation [51, 83]. However, the exact functions of CBP causing the multiple symptoms of RSTS are still a subject of research. A focus, also in this study, is placed on the cognitive deficits observed in

RSTS and thus the roles of CBP during neural development and brain homeostasis. The few existing neuropathological examinations described neurons in the brains of RSTS patients as less differentiated and immature but these reports were all collected in the late 1960 and early 1970s [79-81]. Therefore, no genetic analysis of these patients exists which would have been important as *CBP* mutations are identified in only 50-70 % of diagnosed RSTS patients.

CBP is important for cortical precursor and interneuron differentiation as well as for experience-induced changes in adult neurogenesis [84-86]. Still, it is not clear whether the lysine acetylation or the co-activation of specific TFs is the essential function of CBP in neural differentiation and cognition. On the one hand, an increased CREB function is able to rescue a CBP knockout phenotype at least partly [87, 88] and on the other hand, KDAC inhibitors can reverse the phenotype of CBP knockout mice [84, 85, 88, 89]. The significance of the KAT function of CBP is also supported by the KAT domain being a mutational hotspot in RSTS and by the fact that Ajmone et al. only detected abnormalities in the MRI of RSTS patients with mutations within the KAT domain [82, 90]. Therefore, the current hypothesis is that the combination of both functions makes CBP such an important protein in brain development and homeostasis. The integration of environmental signals into gene expression, which is proposed to be the essential function of KATs, could be the explanation for the phenotypic variability of RSTS and similar developmental disorders. Additionally, it might explain the missing of a clear genotype-phenotype correlation [54].

1.8 MOUSE MODELS OF RSTS

In order to understand RSTS and CBP function, different mouse models have been generated which helped gaining knowledge about RSTS. The first model was described in 1997 [91]. This conventional heterozygous mouse model, genetically resembling the human situation of a heterozygous germline mutation, could mirror many aspects of the human syndrome, such as memory deficits and specific facial features [92, 93]. This is also visible in MRI studies of these mice, showing microcephaly and other features described in RSTS patients [94].

Mice with a homozygous deletion of *Cbp* or *Ep300* are not viable and die prenatally between E9 and E12 [95-97]. Death of the animals is due to abnormal vessel formation, exencephaly and failure in heart development. These findings indicate an essential function of both proteins in the development of different organs. Interestingly, double heterozygous mice carrying only one copy of *Cbp* and one copy of *Ep300* also die prenatally [95].

In order to further understand CBP function, mice with mutations in specific domains of CBP, were generated. Homozygous mutations in the KAT, in the CH1 (a protein-protein interaction

domain), as well as in the KIX domain are embryonically lethal suggesting the importance of all those domains for prenatal development [98-100].

Heterozygous global knockout models are the most exact resemblance of the human disorder but do not allow the exact study of protein function. Therefore, conditional mouse models have been generated and also employed in this study. These conditional models are based on the cre-LoxP system and combine the cre-driven recombination in a specific tissue with a floxed *Cbp* allele. Target cells for the deletion described so far were for example postmitotic neurons (*CaMKV*-promoter) or CNS precursor cells (*Nestin* promoter) [101, 102].

All those mouse models show cognitive deficits, which emphasizes the importance of CBP in cognitive functions. The combination of information generated in different mouse models will hopefully help to understand the processes leading to an ID in RSTS patients.

1.9 CBP FUNCTION IN CANCER

The first indications that CBP is associated with cancer development and might act as a tumor suppressor in different entities were collected in RSTS patients. After the description of the syndrome in 1963, the analysis of patients 30 years later revealed an increased cancer risk among RSTS patients. Those tumors were mostly hematological malignancies and embryonic and CNS tumors [75]. Shortly after this discovery, translocations involving *CBP* were associated with the development of different forms of leukemia [103-106]. This was complemented with the finding that mutations in *CBP* are present in different hematologic malignancies [107, 108]. Experimental evidence suggests the function of CBP as a classical tumor suppressor: In mice, a heterozygous knockout of *Cbp* leads to the development of hematologic malignancies which are characterized by a loss of the remaining *Cbp* allele [92, 93]. Apart from malignancies of the hematopoietic system, mutations in *CBP* were also identified in non-small cell lung cancer, colorectal adenocarcinoma, breast and bladder carcinoma and other solid tumor entities [109, 110]. Additionally, recurring mutations in *CBP* were found in sequencing studies of medulloblastoma (MB) and glioma [111-116]. Large sequencing studies revealed that CBP is altered in about 3 % of all human cancers, which makes it an important protein in cancer research and a potential target for therapy [109, 110].

A role of CBP in the development of brain tumors, especially in MB, has been described in the last few years [113-115]. In the COSMIC database, 25 % of all collected *CBP* mutations were found in CNS malignancies. The largest group among those tumors is the MB with 48 % of all recognized cases, followed by glioma with 42 % [109, 110].

MB is the most common malignant brain tumor in children. They are divided molecularly into four different subgroups based on their specific gene expression and methylation pattern

[117]. Additionally, it has been proposed that they derive from distinct cells which might also explain their differences [118]. Two of these subgroups are defined by the activation of an oncogenic signaling pathway, the sonic hedgehog (SHH)-pathway or the wingless/Int-1 (WNT)-pathway. In the other two groups, no such superordinate signaling was identified although their gene expression signature and methylation patterns are distinct (group 3 and 4). *CBP* mutations are particularly frequent in adult SHH MBs, and Merk et al. showed that CBP has a tumor suppressive role only upon a postnatal knockout in a SHH-MB mouse model [115]. Additionally, it was observed that RSTS patients do not develop SHH MBs but group 3 and group 4 MBs [76, 119]. The combination of both observations suggests that CBP has different roles during development. Therefore, the distinct cells of origin for the subgroups of MBs might have a different vulnerability window for *CBP* mutations in the malignant transformation.

Glioma is another entity in which frequent mutations of *CBP* were identified through sequencing studies [111]. Glioma are the most common malignant brain tumors and account for 75 % of all malignant primary brain tumors [120]. This large family of tumors arises from glial or glial precursor cells and include astrocytoma, oligodendroglioma, glioblastoma, ependymoma and other rare entities [121]. Gliomas range from tumors with a low aggressiveness and good prognosis to rather aggressive tumors which are associated with short survival and high metastatic probabilities. The first description of a morphological basis for tumor characterization of glioma was published in 1926 [122]. Today, tumors are distinguished based on histology and molecular features, which allows a more and more exact description of different tumor entities and thereby enables a more personalized medicine [121].

1.10 THE PROTO-ONCOGENE *MYCN*

MYCN (protein product N-myc, Neuroblastoma-Derived V-Myc Avian Myelocytomatosis Viral Related Oncogene) is a member of the MYC family of TFs, which are all known proto-oncogenes. The MYC family and its network is important in several signaling networks and regulates cell growth, differentiation and apoptosis [123]. Given its important role in essential processes in cell development, it is not surprising that aberrant MYC signaling is associated with numerous different cancers [124, 125].

N-myc itself is a 60 – 63 kDa sized protein. The protein coding gene was discovered in 1963 as a paralogue to *cMyc* [126]. N-myc is essential during embryonic development as homozygous knockout mice die between E10.5 and E12.5 from multiple abnormalities in organ development [127, 128]. In wild type mice, N-myc expression peaks in the neural tube,

sensory neural-crest derived structures as well as in the fore- and hindbrain. Additionally, N-myc is essential for the rapid proliferation of progenitor cells in the CNS [129].

The important function of N-myc in embryonic development in general and especially in neural development is also represented by the frequent mutations or amplifications of *MYCN* in CNS tumors, especially MBs and glioma [130].

1.11 OBJECTIVE OF THIS STUDY

This study was conducted to gain more information about the role of CBP during brain development and brain tumor growth. CBP is a ubiquitously expressed transcriptional co-activator and lysine acetyltransferase. It is known to interact with multiple different TFs and other proteins and to influence the global gene expression of a cell. Germline mutations in *CBP* are causing RSTS, a neurodevelopmental disorder leading to CNS abnormalities and an ID.

In the first part of the project, we wanted to elucidate mechanisms and molecular functions which cause the ID of RSTS patients. Different mouse models have been developed in order to study CBP functions and to explain the ID of patients, but the exact mechanisms are still not completely understood. As almost no data on the histology of the brains RSTS patients exists, the knowledge must be generated in model organisms. Therefore, we generated a new mouse model. We employed the cre-loxP system driven by the *human glial fibrilliary acidic protein* (*hGFAP)*-promoter to achieve a CNS specific knockout and a floxed *Cbp* allele leading to a loss of protein function. We were interested in the morphological consequences of a *CBP* deletion on brain structure level as well as on a cellular level. The histologic characterization of the ID might help to understand the mechanisms and thereby improve patient care. Additional to the morphologic characterization, we wanted to determine molecular mechanisms how a loss of CBP function leads to an ID in patients.

In a second part of the project, we investigated the role of CBP in tumor development. A tumor predisposition in RSTS patients was proposed, but could not been recapitulated in a mouse model. As also the number of patients is small, the existence of a predisposition is still under debate. The role of CBP in tumor development seems to be highly dependent of timing: Sporadic mutations in *CBP* have been associated with the development of MBs, especially adult SHH MB and an early loss of CBP is not tumor suppressive at least in the context of SHH MBs. This might suggest that CBP does not act as a tumor suppressor in MB development in RSTS patients as the causing *CBP* germline mutations affecting the entire neurogenesis. However, RSTS has been proposed to predispose to group 3 and group 4 MBs. This led to the hypothesis that the timing and cell of origin is important for the role of CBP. We wanted to model the development of tumors in RSTS patients and therefore

combined the loss of CBP with the expression of the known oncogenic driver N-myc. Developing brain tumors were analyzed for their gene expression and by histology.

Taken together, the role of CBP in brain development and tumor development, especially in the context of RSTS, was investigated by different histological and functional analysis. Through this, more information was collected to understand this complex disease which might one day help to improve patient care.

2 MATERIAL AND METHODS

2.1 CHEMICALS AND REAGENTS

All chemicals employed in this study have been purchased by Merk, Carl Roth and Sigma Aldrich. All buffers were prepared using ddH_2O.

2.1.1 CELL CULTURE REAGENTS

Table 1: Cell culture reagents

Cell culture reagent	Vendor
bFGF (#100-18B)	Peprotech
Hank's balanced salt solution (HBSS)	Gibco / Thermo Fisher Scientific
HEPES	Life Technologies / Thermo Fisher Scientific
L-Glutamin	Life Technologies / Thermo Fisher Scientific
N2	Gibco / Thermo Fisher Scientific
Penicillin/Strepomyocin (P/S)	Life Technologies / Thermo Fisher Scientific
Non-essential amino acids	Sigma-Aldrich
Trypsin inhibitor	Carl Roth
Trypsin/EDTA	Life Technologies / Thermo Fisher Scientific
DNase I from bovine pancreas	Sigmal-Aldrich
Matrigel	Corning
Neurobasal	Gibco / Thermo Fisher Scientific
B27	Gibco / Thermo Fisher Scientific
mEGF (#315-09)	Peprotech
DMEM/F12	Gibco / Thermo Fisher Scientific
Trypsin inhibitor from soy beans	Carl Roth
StemPro Accutase Cell Dissociation Reagent (Accutase)	Gibco/ Thermo Fisher Scientific

2.2 GENERAL MOLECULAR BIOLOGY AND BIOCHEMISTRY METHODS

2.2.1 RNA ISOLATION

Ribonucleic acid (RNA) was isolated from fresh mouse tissue for gene expression analysis. The guanidinium thiocyanate-phenol-chloroform extraction (Trizol) method was used [131]. Mouse tissue was freshly dissected and minced in Trizol reagent (Thermo Fisher Scientific). After a 5-minute incubation at room temperature (RT), trichloromethane was added and the

16

mixture was incubated for 3 minutes at RT. Then, the phases were separated by centrifugation (12,000 x g, 15 minutes, 4 °C). The clear phase, containing the RNA, was mixed with an equal volume of Isopropyl alcohol and incubated at RT for 10 minutes. The RNA was then precipitated via centrifugation (12,000 x g, 10 minutes, 4 °C) and washed with 75 % ethanol followed by a final centrifugation step (8,000 x g, 10 minutes, 4 °C). The pellet was dried at RT and the RNA was dissolved in water. The dissolved RNA was stored at -80 °C.

2.2.2 RNA QUANTIFICATION AND QUALITY CONTROL

In order to quantify the RNA, a spectrophotometer "Nanodrop" (Thermo Fisher Scientific) was used. The amount of RNA is quantified by the absorption of ultraviolet light which differs between RNA and deoxyribonucleic acid (DNA). Thereby, the amount and purity of the nucleic acid can be determined. Additionally, the integrity of the RNA was determined with the "Bioanalyzer" (Agilent). This system is an automated electrophoresis tool which allows the determination of the RNA integrity number (RIN). This number reflects purity and integrity of RNA and is essential for high throughput RNA experiments, as RNA quality is considered to be essential for high quality sequencing data.

2.2.3 IGF1 QUANTIFICATION VIA ELISA

The amount of insulin-like growth factor-1 (IGF1) was determined with a commercially available enzyme-linked immunosorbent assay (ELISA). The utilized kit was the Mouse/Rat IGF-I/IGF-1 Quantikine ELISA Kit from R&D systems according to the manufacturer`s instructions. Briefly, a standard curve was prepared with recombinant IGF1 supplied in the kit. The samples were diluted with a solution provided by the kit and incubated for 2 hours at RT on an orbital shaker. Afterwards, the wells were washed with washing buffer and the supplied conjugate was applied. After 2-hour incubation on an orbital shaker at RT, the wells were washed again. Then, the substrate-solution was added and incubated for 30 minutes in the dark. The reaction was stopped by a specific solution and the color change is measured in a spectrophotometer at 450 nm.

2.3 TRANSGENIC ANIMALS

2.3.1 MOUSE MODELS

In this work, different transgenic mouse models were used: *hGFAP-cre* [132, 133], *CBP*$^{Fl/Fl}$ [134] and *lsl-MYCN*$^{Fl/Fl}$ [135]. All animal procedures were approved by the state of Hamburg (Reference 113/116). Animals were kept in a 12-hour-light/dark cycle and had food and

water *ad libitum*. Adult animals were anaesthetized with CO_2 and sacrificed by cervical dislocation. Younger animals up to postnatal day (P) 14 were sacrificed by decapitation.

2.3.2 GENOTYPING

For genotyping, genomic DNA was extracted from tail-tips (young animals) or ear biopsies (adult animals). The tissue was lysed with lysis buffer containing 200 mM NaCl, 100 mM Tris-HCl pH 8.3, 5 mM EDTA, 0.2 % SDS and 200 µg/ml Proteinase K for 2 h at 56 °C and 1000 rpm. Thereafter, samples were centrifuged (4 °C, 14,000 rpm) and the supernatant was mixed with an equal volume of ice-cold Isopropanol. Thereby, genomic DNA was precipitated and then pelleted at 4 °C and 14,000 rpm. The pellet was resuspended in TE-buffer (20 mM Tris-HCl pH 8.3, 1 mM EDTA in ddH2O) and the DNA was stored at 4 °C.

The, the DNA was employed for genotyping using primer pairs described for the mouse strains. A list of the primers used in this work can be found in Table 2. The PCR was performed as shown in Table 3. All primers were purchased by Metabion and used in a final concentration of 100 mM. The PCR was performed with Taq-polymerase (GoTaq polymerase, Promega) and a reaction buffer (Green GoTaq reaction buffer) supplied by the manufacturer.

Table 2: Primer sequences employed for genotyping of animals

Transgene	Forward Primer	Reverse Primer
Cre	TCCGGGCTGCCACGACCAA	GGCGCGGCAACACCATTTT
Ntf3	CTGAGTGACAGCACCCCTTT	GTTTCCTCCGTGGTGAGGTT
CBP	CCTCTGAAGGAGAAACAAGCA	ACCATCATTCATCAGTGGACT
MYCN WT	CTCTTCCCTCGTGATCTGCAACTCC	CATGTCTTTAATCTACCTCGATGG
MYCN Mu	ACCACAAGGCCCTCAGTACC	TGGGACGCACAGTGATGG

Table 3: PCR program employed for genotyping of animals

PCR Step	Temperature [°C]	Duration [s]	No. of repeats
Denaturation	95	120	1
Denaturation	95	30	
Annealing	60/65	30	35
Elongation	72	60	
Elongation	72	120	1
Stop	4	-	

After PCR, the DNA was analyzed using 2 %-agarose gels, stained with ethidium bromide and visualized with a Gel documentation system (BioDocAnalyzer, Biometra).

2.3.3 BEHAVIOR TESTING

In order to analyze possible behavioral abnormalities in our mouse model, an open field test was performed. Therefore, young adult mice (postnatal day (P) 30) were placed into a standard cage filled with bedding and their behavior was videotaped for 2 minutes. Siblings of both sexes were used as no sex specific differences were expected.

The videos were then analyzed manually by tracking the animal's movements throughout the 2 minutes. The center of the cage was defined as the area 7.5 cm from the cage walls. The time spent in the different areas, the time spent rearing out of the cage as well as the total distance travelled was recorded.

2.3.4 MAGNET RESONANCE IMAGING

We investigated the overall brain morphology using MRI. Mice were freshly sacrificed and measurements were taken at the rodent MRI facility at the UKE Hamburg under supervision of Jan Sedlacik. MRI was performed using a dedicated small animal 7T MRI (ClinScan, Bruker) with a receiver phased array surface coil with 4 elements closely covering the mouse head and a linear polarized rat body transmit coil. A 2D T2 weighted Turbo Spin Echo (TSE) sequence in coronal orientation was scanned with echo time 50 ms, repetition time 6304.6 ms, flip angle 180°, readout bandwidth 100 Hz/pixel, field of view 20x15 mm^3, matrix 192x144, turbo factor or echo train length 9, slice thickness 0.2 mm, number of slices 82, no gap between slices, 4 averages and 6:56 minutes scan time. At least 3 animals per genotype were used. Pictures were analyzed by manual quantification using MRIcro software (Chris Rorden, Version 1.40).

2.3.5 PERFUSION

For the analysis of the ultra-structure of neurons with electron microscopy, animals were perfused with 4 % paraformaldehyde (PFA). For perfusion, the animals were anaesthetized, and then the left heart ventricle and the right atrial auricle were opened. The circulatory system was then flushed with phosphate buffered saline (PBS) until the liver was completely discolored. After washing, 4 % PFA was applied to the circulatory system for 2-3 minutes. After fixation, the brain was extracted from the skull and placed in a solution of 2 % PFA and 2 % Glutaraldehyde and stored at 4 °C until further processing for electron microscopy (*2.4.3*).

2.3.6 PRIMARY CELL CULTURE

2.3.6.1 SVZ Explant Culture

In order to analyze the migration behavior of NPCs *in vitro,* we employed an assay described first in 1997 [136]. Briefly, young postnatal mice (2 – 5 days old) were decapitated, the brains dissected, cut on a vibrating microtome (Leica) in 400 µm thick slices and the SVZ was dissected. The SVZ was then cut and placed into Matrigel (Corning). The explants in Matrigel were covered by "SVZ-Medium" (Neurobasal supplemented with B27, L-Glutamine, P/S). After 48 hours of culture (humidified incubator, 37 °C, 5 % CO2), the explants were photographed and fixed with 4 % PFA for 20 minutes at RT. Pictures were taken with a Leica DM IL microscope.

For analysis of the migration of precursor cells, the migration distance from the explant was measured at 10 different spots around the explant using ImageJ. Additionally, the number of single cells in a circle around the explant was counted using ImageJ (Fiji).

2.3.6.2 SVZ-OB-Co-culture

In an attempt to recapitulate the migration behavior of NPCs in the presence of external signaling molecules, we co-cultured explants from the SVZ with explants from the OB. The procedure for preparing the explants was as described in 2.3.6.3. Additionally, small pieces of the OB were placed next to the SVZ explant in the Matrigel without direct contact. The explants were cultured for 48 h, pictures were taken and the number of single cells around the SVZ explant was counted.

2.3.6.3 SVZ-OB-Medium Exchange culture

Additional to the co-culture experiments of the SVZ and the OB, we incubated SVZ explants with conditioned medium from the OB. Therefore, SVZ explants were prepared as described in 2.3.6.3 and simultaneously, explants of the OB were prepared, placed in a drop of Matrigel and incubated in SVZ explant medium. After 24 hours, the medium of the SVZ explants was discarded and the medium of the OB was added to the SVZ explants. For the growth factor supplementation experiments, 100 ng human brain-derived neurotrophic factor (BDNF, recombinant human protein, abcam ab9794) or 200 ng insulin-like growth factor-1 (IGF1, recombinant murine protein, peprotech 250-19) were added to the medium. The SVZ explants were cultured in the OB-conditioned medium for another 24 h. Afterwards, the cultures were fixed with 4 % PFA, pictures were taken and the number of single cells around the explant was counted.

2.3.6.4 Tumor sphere culture

For tumor sphere generation, adult *hGFAP-cre::CBP^{Fl/Fl} lsl-MYCN^{Fl/Fl}* mice and control siblings without cre (*CBP^{Fl/Fl} lsl-MYCN^{Fl/Fl}*) were sacrificed and the brain was extracted. The OBs and the hind- and midbrain were dissected and the meninges were removed. Then, the tissue was cut into small pieces and digested with Trypsin/EDTA for 40 minutes at 37 °C. The reaction was stopped by the addition of an equal volume of trypsin inhibitor (1 mg/mL). After washing with fresh medium, the cells were mechanically dissociated and the suspension was filtered with a 40 μm cell strainer. Afterwards, the cell suspension was seeded in a cell culture flask in neurosphere medium (Neurobasal, B27, L-Glutamine, P/S, 20 ng/mL EGF, 10 ng/mL FGF) and grown in a humidified incubator at 37 °C and 5 % CO_2. The cultures were supplemented with new growth factors every 2 days. Once a week, the spheres were pelleted (150xg, 3 min), dissociated mechanically and split in an appropriate ratio into new flasks. For dissociation of tumor spheres, the suspension was centrifuged (150xg, 2 min), washed with PBS (150xg, 2 min), resuspended and incubated for 10 min at RT with Accutase. Afterwards, the suspension was mechanically dissociated further and the cells were pelleted (200xg, 4 min). The cell pellet was resuspended in an appropriate volume and seeded in a new tissue culture flask.

2.4 Histological Methods

2.4.1 Immunohistochemistry

Tissue for histological examination was freshly dissected and fixed in 4 % PFA at RT for at least 12 hours. For the histological analysis of cultivated cells, cells were fixed in 4 % PFA at RT for 20 min. Afterwards, the cells were pelleted (2 min, 21,000 x g) and washed with PBS. Then, cells were embedded in low-melting point agarose (SOP 2.3.12 Institute of Neuropathology, University medical center Hamburg-Eppendorf). Afterwards, the fixed tissue or embedded cells, were dehydrated and embedded in paraffin according to standard procedures (SOP 2.4.1 Institute of Neuropathology, University medical center Hamburg-Eppendorf). Paraffin embedded tissues were cut into 4 μm sections. For overall morphological examination, Hematoxylin & Eosin (H&E) staining was used. The staining was performed using standard protocols. All pictures of histological stains were made with an Olympus BX43 microscope.

For immunohistological stains, automated staining using the Ventana system (Roche) was used according to manufacturer's instructions or manual staining was performed. The Ventana system is an automated staining system for histology. Stainings were conducted by

the Institute of Neuropathology at the University medical center Hamburg-Eppendorf (SOP 2.6.8).

For manual staining, the slides were first deparaffinized in a descending ethanol row. Afterwards, antigen demasking was performed by boiling for 20 min in Citrate buffer (pH 6). Then, endogenous peroxidases were blocked by incubation in 5 % hydrogen peroxide in methanol for 20 minutes. All washing steps were performed at RT with PBS-T (PBS supplemented with 10 % Triton X100). After washing, the slides were incubated with blocking solution (5 % BSA in PBS-T) for 1 h at RT. The primary antibody was diluted in blocking solution and incubated at 4 °C overnight in a humid environment. After primary antibody incubation, the slides were washed in PBS-T. Then, detection was performed with the SuperVision 2 Kit (DCS Diagnostics) according to manufacturers´ instructions. The kit bases on the chromogenic reaction of a secondary antibody polymer coupled horseradish peroxidase with 3,3'-Diaminobenzidine (DAB) leading to a brown signal in cells carrying a labeled antigen. After incubation with a specific enhancer, the secondary antibody polymer and a DAB solution, a counter staining with hematoxylin was performed. After the completed staining, the slide was dehydrated using an ascending ethanol row and mounted with a specific xylol-based mounting medium (DPX Mountant for histology, Sigma-Aldrich).

Table 4: Antibodies employed for immunohistochemistry

Antibody	Vendor	Number	Dilution	Target
Sox2	Abcam	ab97959	1:200	Sex determining region Y-box 2 (Sox2)
NeuN	Millipore	Mab377	1:25	Neuronal nuclear protein (NeuN)
Ki67	Abcam	ab16667	1:100	Marker of proliferation Ki-67 (Ki67)
DCX	Abcam	ab18723	1:100	Doublecortin (DCX)
CBP	Santa Cruz	sc-7300	1:50	CyclicAMP-responsive element binding protein binding protein (CBP)
Prox1	Abcam	ab1999359	1:500	Prospero homeobox protein 1 (Prox1)
N-myc	Cell signaling technologies	51705S	1:600	v-myc avian myelocytomatosis viral oncogene neuroblastoma derived homolog (N-myc)
Neurofilament	Dako	M0762	1:800	Intermediate filament of neurons (Neurofilament)
GFAP	Dako	M0761	1:200	Glial fibrillary acidic protein (GFAP)
S100	Dako	Z0311	1:100	S100 protein (S100)
Map2c	Sigma-Aldrich	M4403	1:3000	Microtubule-associated protein 2c
Olig2	Merck-Millipore	AB9610	1:200	Oligodendrocyte transcription factor (Olig2)
Otx2	Thermo-Fisher	1H12C4B5	1:2000	Orthodenticle homeobox 2 (Otx2)
Nestin	BD Biosciences	611658	1:200	Neuroectodermal stem cell marker (Nestin)

2.4.2 GOLGI-COX-STAINING

In order to stain the entire cell body of neurons, Golgi-Cox staining was used. For this, the FD Rapid GolgiStain Kit (FD NeuroTechnologies) was employed according to manufacturers` instructions. Briefly, mouse brains were dissected and impregnated with a premade solution of mercuric chloride, potassium dichromate and potassium chromate for one week. Afterwards, the brains were embedded in 4 % agarose gel and sliced with a microtome with

a vibrating blade (VT1000S, Leica) into 200 µm thin frontal sections. The impregnation was visualized by a premade solution provided in the kit.

2.4.3 ELECTRON MICROSCOPY

For electron microscopy, animals were anaesthetized and perfused with 4 % PFA for optimal tissue fixation and preservation (s. 2.3.5). After perfusion, the brain was immediately dissected and stored in a solution of 2 % PFA and 2 % glutaraldehyde at 4 °C until further processing. The tissue was processed for electron microscopy at the Institute for Neuropathology at the University Medical Center Hamburg-Eppendorf under supervision of Prof. Christian Hagel following standard protocols. Briefly, samples were washed in 0.1 M cacodylate buffer (Sigma-Aldrich), incubated for 2 hours in 1 % osmium tetroxide (Science Services), dehydrated in an ascending series of ethanol, and embedded in Epon 812 (Serva). Ultrathin sections were counterstained with uranyl acetate (Polyscience) and lead citrate (Riedel-de Haën), and analyzed with a LEO 912 AB OMEGA electron microscope (Leo Elektronenmikroskopie).

2.4.4 IMAGING

Imaging was performed according to the experimental setup on an Olympus BX43, Leica DM IL or Nikon Eclipse Ti2 microscope.

2.5 GLOBAL GENE EXPRESSION ANALYSIS

2.5.1 RNA SEQUENCING

Total RNA was sequenced in the HPI Sequencing Core facility in cooperation with Dr. Daniela Indenbirken. Briefly, the RNA integrity was analyzed with the RNA 6000 Nano Chip on an Agilent 2100 Bioanalyzer (Agilent Technologies). From total RNA, mRNA was extracted using the NEBNext Poly(A) mRNA Magnetic Isolation module (New England Biolabs) and RNA-Seq libraries were generated using the NEXTFLEX Rapid Directional qRNA-Seq Kit (Bioo Scientific) as per the manufacturers` recommendations. Concentrations of all samples were measured with a Qubit 2.0 Fluorometer (Thermo Fisher Scientific) and fragment lengths distribution of the final libraries was analyzed with the DNA High Sensitivity Chip on an Agilent 2100 Bioanalyzer (Agilent Technologies). All samples were normalized to 2 nM and pooled equimolar. The library pool was sequenced on the NextSeq500 (Illumina) with 1 x 75 bp, with 16.1 to 18.6 million reads per sample. For each sample, the sufficient quality of the raw reads was confirmed by FastQC v0.11.8 [137]. Afterwards, the reads were aligned to the mouse reference genome GRCm38 with STAR v2.6.1c [138] and

simultaneously counted per gene by employing the *quantmode GeneCounts* option. Counts are based on the Ensembl annotation release 95. Differential expressed genes were estimated with DESeq2 v1.22.2 [139].

2.6 STATISTICS

The Prism 7 software (GraphPad) was used for statistical analysis. Survival data were analyzed through Kaplan-Meier curves. P-values < 0.05 were considered as significant. When comparing two groups the unpaired two-tailed t-test was conducted. If percentages should be compared they were arcsin transformed to enable the t-test. Each experiment was performed at least three times. Pictures for quantifications were chosen to be representative and the observer was blinded for the genotype of the sample.

3 RESULTS

3.1 A KNOCKOUT OF CBP IN THE CNS LEADS TO BEHAVIORAL AND ANATOMICAL ABNORMALITIES IN THE MOUSE BRAIN

RSTS is a developmental disorder caused in 70 % of patients by mutations of *CBP* in which an ID is observed in 100 % of patients. The strong effect of CBP on the CNS function is also reflected by the finding that all described mouse models for RSTS so far show abnormalities in memory and motor functions. The different mouse models generated until now helped gaining information about the functions of CBP, but the exact mechanisms, especially for the ID, remained unclear [70].

The most prominent mouse models for RSTS are conventional heterozygous knockouts of either the whole CBP protein or specific domains [91-93]. The advantage of these models is the most exact resemblance of the genetic situation in patients. Nevertheless, the heterozygosity does not allow the study of exact protein function because intact protein is still present in the cells. We used a tissue specific knockout mouse model, allowing the homozygous knockout of *Cbp* while retaining viability of the animals.

We employed a CNS specific knockout mouse model driven by the cre/loxP system. The cre recombinase is expressed under the *hGFAP* promoter. This promoter is active from E13.5 onwards in NSCs and astrocytes of the mouse brain. *hGFAP*-activity drives the expression of the cre recombinase in those cells and leads to recombination between the loxP sites flanking exon 7 of *Cbp*. The cre driven recombination induces the excision of exon 7, which then generates a new STOP codon within the mRNA of CBP. The translation of the mRNA finally results in a severely truncated protein in which 24 of its 31 exons are missing including the KAT domain (Fig. 5 a).

We wanted to detect phenotypic abnormalities of our mutant mice. The mice appeared smaller than their wild type littermates. Therefore, as a first measurement we weighed the mice throughout their development from birth until P30 and determined that the body weight of the mutants is significantly reduced from P7 onwards (Fig. 5 b,c). Before P7, the weight is comparable to the weight of the wild type littermates.

Neurodevelopmental disorders, including RSTS, often lead to behavioral symptoms in patients. In order to analyze if our mouse model can model those aspects of the disease, we performed an open field test. In this test, we compared CBP deficient animals with their CBP competent siblings for their anxiety related behavior. The animals were placed in an empty cage and their behavior was recorded. We showed that the *hGFAP-cre::CBP^{Fl/Fl}* mice

traveled a similar distance as the control animals but spent significantly less time in the center of the cage. Furthermore, they reared significantly less often out of the cage (Fig. 5 d). By this, we showed that CBP deficiency does affect mouse behavior and leads to an increase in anxiety. In addition to the increased anxiety in the animals, we noticed that the mutants seemed to be easily stressed upon handling. This strong reaction to change prevented further behavioral tests to assess the memory function of our CBP deficient mouse model.

As we saw phenotypic abnormalities in the mice, we wanted to investigate the brain of the transgenic animals further. For a first overview of the CBP deletion induced changes on the brain, sagittal sections were made and stained by H&E. The analysis of the stains revealed anomalies in the hippocampus, the RMS and OB (Fig. 5 e). These regions are areas in which adult neurogenesis in the mouse brain is described [140].

In the analysis of the brain sections, we noticed that the hippocampus and other brain regions appear severely smaller in the mutant mice compared to the wild type controls. Thus, we supplemented our analysis with MRI to be able to quantitatively asses the size abnormalities in *hGFAP-cre::CBP^{Fl/Fl}* mice. Thereby, we showed that *hGFAP-cre::CBP^{Fl/Fl}* mice have a significant brain hypoplasia. We also detected a size reduction of the hippocampus, the CC and an OB hypoplasia (Fig. 5 f).

Taken together, the first analysis of our mouse model revealed strong phenotypic abnormalities in the brain. Therefore, we concluded that our mouse model is suitable to study the effects of a CBP deletion on the CNS and conducted further experiments.
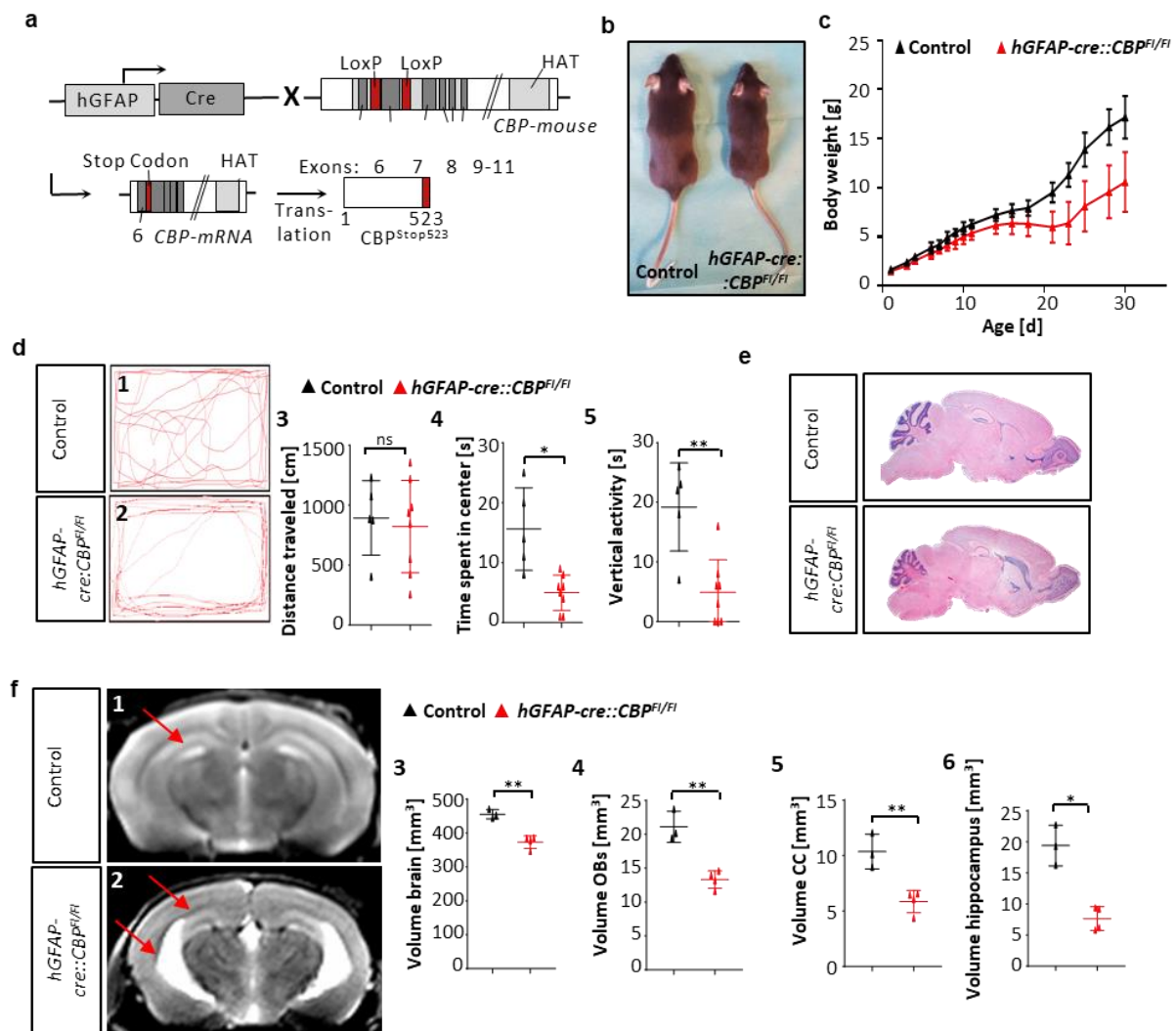
Figure 5: CNS-specific deletion of CBP affects mouse behavior and anatomy

(a) In *hGFAP-cre::CBP^Fl/Fl* mice, CBP^Stop523 is expressed in cells that express the cre-recombinase under the *hGFAP* promoter. CBP^Stop523 does not contain the KAT domain. LoxP: Cre-recombinase recognition and incision site, KAT: Lysine acetyltransferase domain. (b) *hGFAP-cre::CBP^Fl/Fl* mice are visibly smaller than their wild type littermates. (c) The growth retardation of *hGFAP-cre::CBP^Fl/Fl* mice becomes visible from P7 onwards. (d1-5) Open field test: tracked mouse movements in the open field test for one representative control and mutant animal. Movement analysis shows that transgenic mice spend significantly less time in the center and show significantly less vertical activity. (e) Phenotypic abnormalities of *hGFAP-cre::CBP^Fl/Fl* mice are obvious in sagittal H&E stains of adult mice. Those abnormalities include a cerebellar, hippocampal and olfactory bulb hypoplasia and a cell accumulation at the RMS. (f1-5) Representative coronal T2 weighted brain MRIs of transgenic and control animals with arrows marking the hypoplastic hippocampus and the widened lateral ventricle in the mutant. Volumetric analysis unveiled significantly reduced brain volume, OB size, CC volume and hippocampus size after early loss of CBP. $*p < 0.05$, $**p < 0.01$, $***p < 0.001$

3.1.1 A CNS-SPECIFIC CBP KNOCKOUT ALTERS HIPPOCAMPAL MORPHOLOGY

We observed in the MRI that the hippocampus of *hGFAP-cre::CBP^{Fl/Fl}* mice is significantly smaller. Therefore, we concluded that the hippocampus is a structure which is highly affected by the CBP loss. This can in part be explained by the activity of the *hGFAP*-promoter which is active throughout the whole hippocampal development [133]. Also, it was shown that the embryonic hippocampus is also highly affected by the CBP deletion [141]. Furthermore, the hippocampus is a structure which is important in learning and memory processes and is impaired in many neurodevelopmental disorders. Therefore, we decided to study the morphology of this anatomic structure in further detail. In frontal sections, we confirmed the size reduction already obvious in the MRI (Fig. 5 e,f). The overall structure of the hippocampus with the dentate gyrus (DG) and the cornu ammonis (CA) is preserved even without functional CBP.

Apart from overall morphology, we were especially interested in the cellular composition and adult neurogenesis in the hippocampus. Therefore, we used immunohistochemistry to detect the different cell populations in the hippocampus. Previous work was able to show that the stem cell compartment of the hippocampus is disturbed in *hGFAP-cre::CBP^{Fl/Fl}* mice and that less stem cells are found in the adult hippocampus of these animals [141]. This seems to root in the disturbed embryonic development of the hippocampus in *hGFAP-cre::CBP^{Fl/Fl}* mice. We wanted to analyze the different cell populations especially in the DG to investigate if the reduction in stem cells leads to a disturbed cell population or only a size reduction of the DG (Fig. 6 a,e). First, we showed that all cells of the DG are affected by the CBP loss and are clearly negative in the staining whereas in the control, all cells in this region express CBP (Fig. 6 b,f). Despite the reduction in stem cells, the cells in the DG differentiate and express the neuronal marker NeuN as well as the DG granule cell marker Prox1 (Fig. 6 c-d; g-h). We also employed the progenitor marker doublecortin (DCX) to identify the NPCs in the hippocampus (Fig. 6 i,j). In the wild type, cells expressing DCX are located in the inner cell layers of the DG and build a cell band lining the entire DG. In contrast to that, in the mutant only a small percentage of cells express DCX (18 % positive cells in the mutant vs. 38 % in the control) (Fig. 6 k). Additional to the reduction in cell number, DCX-positive cells are in the correct orientation and general location but appear in cell clusters rather than building up a cell layer. This different arrangement of DCX positive cells is most likely due to the reduction in stem cells which produce new progenitors. Usually, the stem cells are equally distributed throughout the DG and therefore, a cell band of progenitors lines the DG. We hypothesized that the developing NPCs are not evenly distributed but are rather found in clusters around their stem cells as the stem cells in the mutant are not equally distributed among the entire hippocampus.
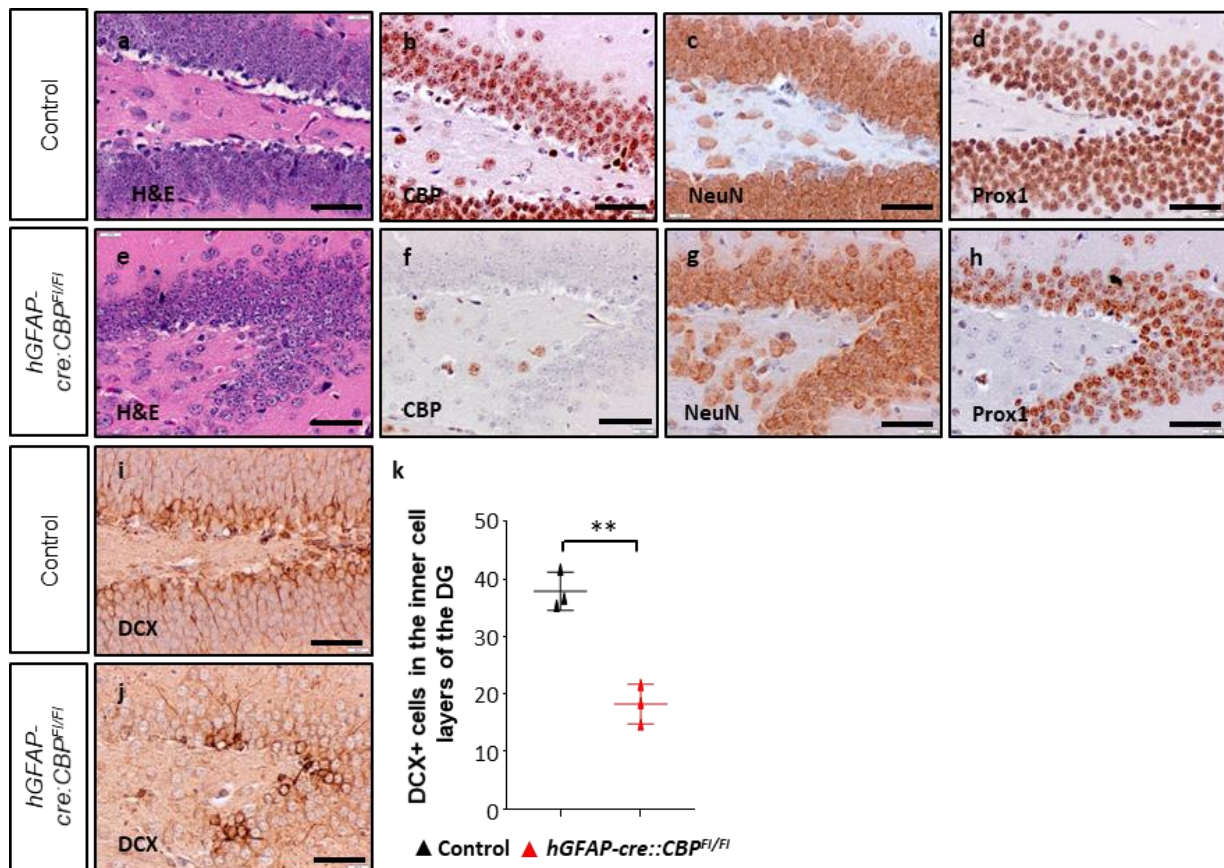
Figure 6: *hGFAP-cre::CBP^{Fl/Fl}* **mice show abnormalities in hippocampal architecture**

(a-j) The DG is severely affected by the CBP deletion. Although all granule cells of the DG do not express CBP in the mutant, cells retain their neuronal identity (NeuN + Prox1). (i,j,k) The number of DCX-positive NPCs is significantly reduced and their distribution disturbed in the mutant animals. Representative pictures, n>3. Scale bar: 50µm, **p < 0.01

3.1.2 *CBP DELETION LEADS TO CELL ACCUMULATION AT THE VENTRICULAR SITE OF THE ROSTRAL MIGRATORY STREAM*

One striking abnormality in the brain of *hGFAP-cre::CBP^{Fl/Fl}* mice is a large cell accumulation at the border of the lateral ventricle which has also been described in a previous work on *hGFAP-cre::CBP^{Fl/Fl}* mice [141]. This cell mass is visible in sagittal and frontal sections and is located below the CC at the area of the SVZ (Fig. 7 a,f). In wild type mice, the SVZ is a cell dense zone lining the ventricle. In the SVZ, adult NSCs reside and constantly produce neurons which then migrate along a defined route, the RMS, towards the OB where they replace interneurons. In order to gather information about the cell accumulation in the CBP knockout animals, we performed immunohistochemistry (Fig. 7). We first investigated the proliferation of the cells. We observed that only a small proportion of the cells in the accumulation are positive for the proliferation marker Ki67. Additionally, the proliferating cells are only present at the borders of the cell mass. This resembles the wild type situation in

which proliferating NPCs can also be found in the SVZ lining the ventricle and at the beginning of the RMS. This pattern of proliferating cells suggests that this is not a neoplastic lesion but rather an accumulation of cells (Fig. 7 b,g).

To get more information about the identity of these cells, we used the NPC marker Sox2, which is usually expressed in NPCs residing in the SVZ. In the wild type SVZ, all cells of the SVZ and at the beginning of the RMS express Sox2. In the mutant, all cells lining the ventricle are also Sox2 positive. In contrast, in the cell accumulation only a proportion of cells are expressing Sox2 (Fig. 7 c,h). Additionally, we used the neuron marker NeuN to determine cell identity. In the wild type, no cells in the SVZ express NeuN. In the mutant, a proportion of cells in the accumulation expresses NeuN (Fig. 7 d,i). As a third marker we used DCX, which usually labels migrating NPCs in the RMS. In the wild type, cells of the SVZ and the beginning RMS are positive for this marker. In the mutant, all cells of the accumulation express DCX (Fig. 7 e,j). The marker expression of cells in the accumulation suggests that NPCs are residing in the SVZ as usual but cannot leave the SVZ and therefore start to differentiate and express NeuN. Due to these results, we hypothesized a migration deficit in the CBP deficient mouse brains, which we investigated further using *in vitro* approaches.
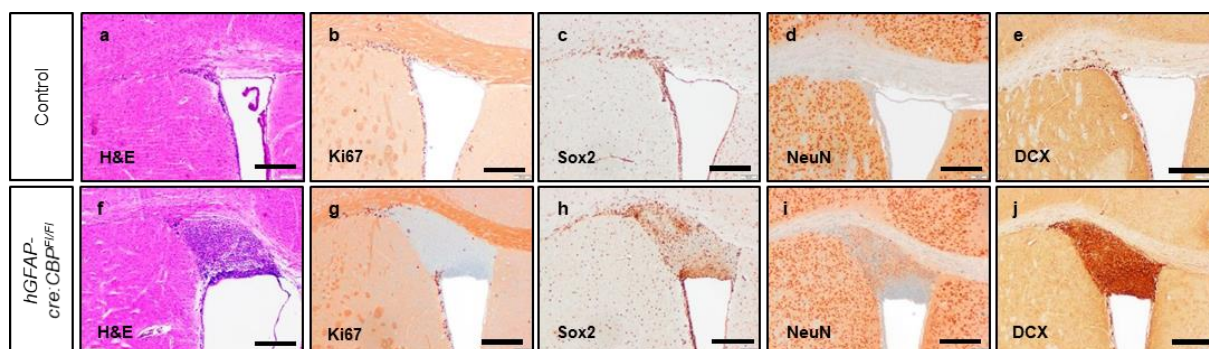

Figure 7: *hGFAP-cre::CBP^{Fl/Fl}* mice show abnormal cell accumulation at the ventricular border of the rostral migratory stream

(a,f) Frontal sections of adult mouse brains reveal a cell accumulation at the lateral ventricle of CBP deficient mice. (b,g) Normal proliferation can be observed upon Ki67 staining. (c-d;h-i) The cell accumulation comprises two different cell populations, one progenitor population expressing Sox2 and one neural differentiated expressing NeuN. (e,j) All cells express DCX as an NPC marker. Representative pictures, n>3. Scalebar: 100 µm.

3.2 CBP INFLUENCES NEURONAL MORPHOLOGY AND FUNCTION

Neuronal morphology is considered to influence neuron function and disturbed neuron morphology is described for different ID syndromes [20, 21]. The basic cell morphology is conserved between species and depends on the specific neuron class und localization [23,

24]. The overall cell morphology includes dendrites and dendritic spines but also the ultrastructure with postsynaptic densities. These represent the synapses at which neural communication takes place [18]. Therefore, we analyzed the effects of a CBP loss on neuron morphology.

3.2.1 DEFICIENCY OF CBP CAUSES AN ABNORMAL NEURON MORPHOLOGY

In order to visualize the whole neuronal cell body with its extensions, we employed Golgi-Cox staining. This technique was first described in 1891 by W.H. Cox and bases on the impregnation of mercury by a random proportion of neurons [142]. It is developed as an improvement of the Golgi staining described in 1873 which used silver nitrate instead of mercury [143]. Those staining techniques enabled Ramon y Cajal to describe neuron morphology in detail and was used for his famous studies of the different neurons in the brain. In 1906 Camillo Golgi and Ramon y Cajal earned the Nobel Prize in physiology and medicine for their studies of the nervous system.

As a first parameter of neuron morphology, we measured the length of the apical dendrite which extends from the cell soma towards the cortical surface. We studied the large pyramidal cells from layer V of the cortex. In the CBP deficient cortices, these dendrites were significantly shorter than in their wild type counterparts with only half of their length (129 µm vs. 229 µm in the control, Fig. 8 a5).

Additionally, we measured the branches per dendrite. It is described that in some ID disorders, the length of the dendrite is reduced and probably as a compensation mechanism, the number of branches is increased. However, we did not detect a difference between wild type and CBP deficient neurons (0.44 in the mutant vs 0.41 in the control, Fig. 8 a6). This in turn means that the total number of branches is reduced in the mutant due to the shorter dendrite, which will most likely have consequences on neural connectivity and thus neuron function and intellectual ability.

In addition to the dendrite and its branches, we also analyzed the number of dendritic spines. These protrusions of the neuronal cell are the location of neuronal connections, the synapses. We determined the number of spines per µm dendrite and measured a reduction of one third of the number of spines on the apical dendrite of layer V pyramidal neurons in mutant animals (0.4 in the mutant vs 0.6 in the control, Fig. 8 a7). Next to the relative reduction, the absolute number of spines is even more reduced due to the shortage of the dendrite in CBP deficient neurons.

3.2.2 CBP *LOSS HAS CONSEQUENCES ON THE NEURONAL ULTRASTRUCTURE*

The Golgi-Cox staining revealed disturbed neuron morphology without a functional CBP. We therefore wanted to investigate neuron morphology in even more detail and used electron microscopy to make the neuronal connections visible.

We focused on the same regions as in the analysis of the overall morphology and first counted the number of post synaptic densities (PSDs). This analysis revealed a reduction of PSDs in CBP deficient mice which is in perfect line with the reduced number of dendritic spines. The number of PSDs is reduced by two thirds, which suggests massive consequences for neuronal function (1.2 PSDs/10 µm² in the mutant vs 3.2 PSDs/10 µm² in the control, Fig. 8 b3).

In the analysis of electron microscopic images, we observed abnormal structures in the mutant cortex. They appear like large and mostly empty membrane enclosed spaces (Figure 8 c). In order to reveal if these structures might be axonal swellings, we employed a staining for neurofilament structures and stained the cortex of adult wild type and *hGFAP-cre::CBP^Fl/Fl* mice. The number of neurofilament positive filaments in the cortex of CBP deficient mice is significantly reduced compared to wild type animals (101 positive filaments/slide vs 448 positive filaments/slide in the control, Fig. 8 d3). The reduction in neurofilament does not allow the characterization of the structures as axonal swellings, but together, both findings further support the hypothesis that the overall cortical cell architecture is disturbed in the CBP deficient cortex.
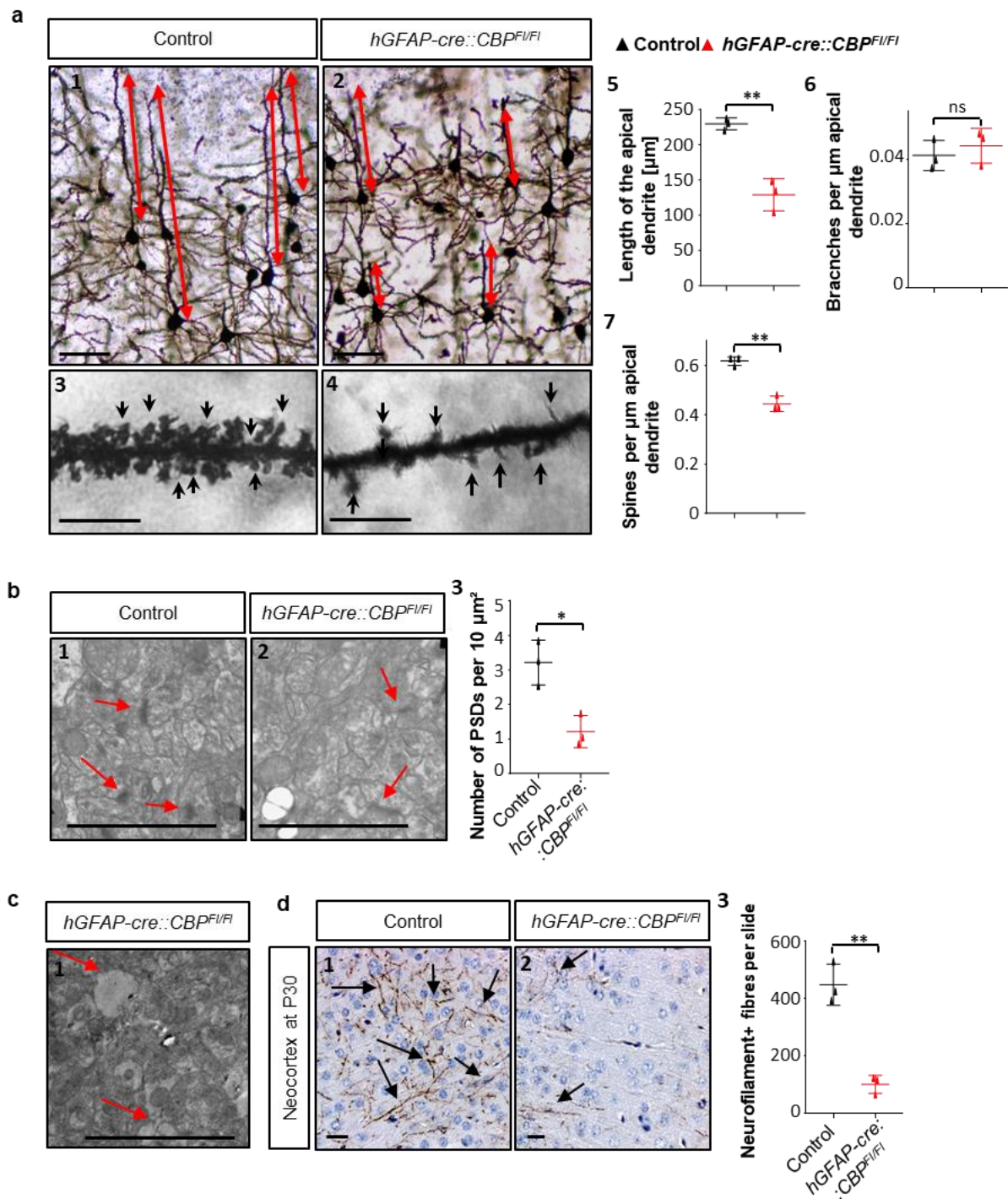
Figure 8: Neocortical layer V pyramidal cells have disturbed neuron morphology and alterations in spine density upon CBP loss

(a1-4) Golgi-Cox impregnated pyramidal neurons in layer V show severe abnormalities and maturation deficits in *hGFAP-cre::CBP^{Fl/Fl}* mice. Arrows illustrate the length of the apical dendrite. (a5,6) The apical dendrite is significantly shorter whereas the relative number of branches is unchanged. Additionally, less dendritic spines can be observed. (b1-3) Analysis of electron microscopic images of layer V neurons show that the number of PSDs is significantly diminished in the cerebral cortex of *hGFAP-cre::CBP^{Fl/Fl}* mice. Arrows point towards the visible PSDs. (c) Electron microscopic analysis revealed the existence of abnormal structures in the CBP deficient cortex. Arrows point towards two of

such structures. (d) Immunostaining revealed a reduced number of neurofilament positive fibres in the mutant, further supporting the disturbed morphology of the cortex. Arrows point towards the analyzed neurofilament positive fibres. Scale bar: 50 µm (a1-4), 100 µm (c1-2), 10 µm (c3-4), 5 µm (d1-2); *p < 0.05, **p < 0.01, ns: not significant

3.3 CBP DEFICIENCY IMPACTS NEURONAL MIGRATION

Neuronal migration is one key mechanism in brain development and differentiation of neurons. Most, if not all, neurons in the brain originate from stem cells residing in specialized stem cell niches and travel towards their final destination [25].

One famous migration route in the rodent brain is the RMS which is established during embryonic development and is present throughout the whole life of the animal. The responsible stem cells are residing in the SVZ lining the lateral ventricle. Those cells produce TAPs by asymmetric division, which then migrate through the RMS towards the OB, where they differentiate into interneurons of the granular or periglomerular layer [26].

In CBP deficient mice, a large cell accumulation at the border of the SVZ was visible. We hypothesized from immunohistochemical characterization that the cells have a migration deficit and cannot migrate normally through the RMS towards their destination but accumulate at their origin (Fig. 7).

3.3.1 CELL INTRINSIC MIGRATION OF SVZ PRECURSOR CELLS IS UNAFFECTED BY CBP LOSS

To investigate the hypothesized migration deficit further, we employed an *in vitro* experiment using primary cells from control and mutant mice. It was described in 1997 that NPCs from the SVZ of young postnatal mice are able to migrate in chains in the extracellular matrix Matrigel and recapitulate the migration in the RMS *in vivo* [136]. With this experimental design, it was shown that different factors are essential for the migration of NPCs [144-151].

For the *in vitro* migration assay, young postnatal mice were employed, their SVZ freshly dissected and small pieces of the SVZ were placed into Matrigel. Those explants were analyzed after 48 h of culture and the migration distance of the chains of NPCs was measured. We observed, contrary to what we expected, no difference in the migration of CBP deficient cells compared to their wild type counterparts. Cells of CBP deficient mice established normal chains of migrating cells and were able to travel the same distance as the cultivated control cells (415 µm in mutant cells vs 398 µm in control cells, Fig. 9 a3).

3.3.2 EXTRINSIC FACTORS FROM THE OLFACTORY BULB ARE RESPONSIBLE FOR THE MIGRATION DEFICIT OF CBP DEFICIENT SVZ PRECURSOR CELLS

We observed that the intrinsic migration ability of cells from the SVZ of *hGFAP-cre::CBP*[Fl/Fl] mice was indistinguishable from the wild type cells despite the migration deficit seen *in vivo*. Therefore, we hypothesized that an extrinsic factor might be responsible for the phenotype of the animals. The migration of NPCs is a process regulated by a multitude of different factors secreted by the SVZ, astrocytes, blood vessels and also the OB.

Hack et al. used a co-culture of SVZ and OB explants to shown that Reelin is important for the exit of migrating NPCs from their chains in the OB [149]. Therefore, we used the same experimental design to investigate if CBP is important for the final step in RMS migration. For the co-culture experiment, we used SVZ explants of wild type or *hGFAP-cre::CBP*[Fl/Fl] mice as well as OB tissue explants of both genotypes. Using this experimental approach, we showed that the mutant OB is not able to induce the exit of cells from their migration chains. In the control situation of a co-culture of SVZ and OB, cells are leaving the migration chains and can be identified as single cells surrounding the SVZ explant. The number of those single cells was significantly reduced in the presence of a mutant OB, regardless of the genotype of the SVZ (control SVZ: 68 single cells/mm² with a control OB vs 46 single cells/mm² with a mutant OB; mutant SVZ: 75 single cells/mm² with a control OB vs 42 single cells/mm² with a mutant OB, Fig. 9 b).

The results of our co-culture experiments prompted us to hypothesize that a secreted factor from the OB is responsible for the observed migration deficit. To test for this hypothesis, we modified our experimental setup. We prepared SVZ and OB explants in Matrigel as in the other experiments but in separate wells. After 24 hours of tissue culture, we exchanged the medium of the OB with the medium of the SVZ explants. We used wild type SVZ explants and medium conditioned by wild type or CBP deficient OB tissue and counted the number of single cells surrounding the SVZ explant as in the co-culture experiments. Thereby, we saw that the conditioned medium from the control OB is able to induce an exit of cells from the migration chains whereas the medium from the CBP deficient OB does not (55 single cells/mm² in the presence of control OB medium vs 43 single cells/mm² with medium from a mutant OB, Fig. 9 b). This strongly supports the hypothesis that an extracellular signaling molecule is responsible for the observed migration deficit *in vivo*.
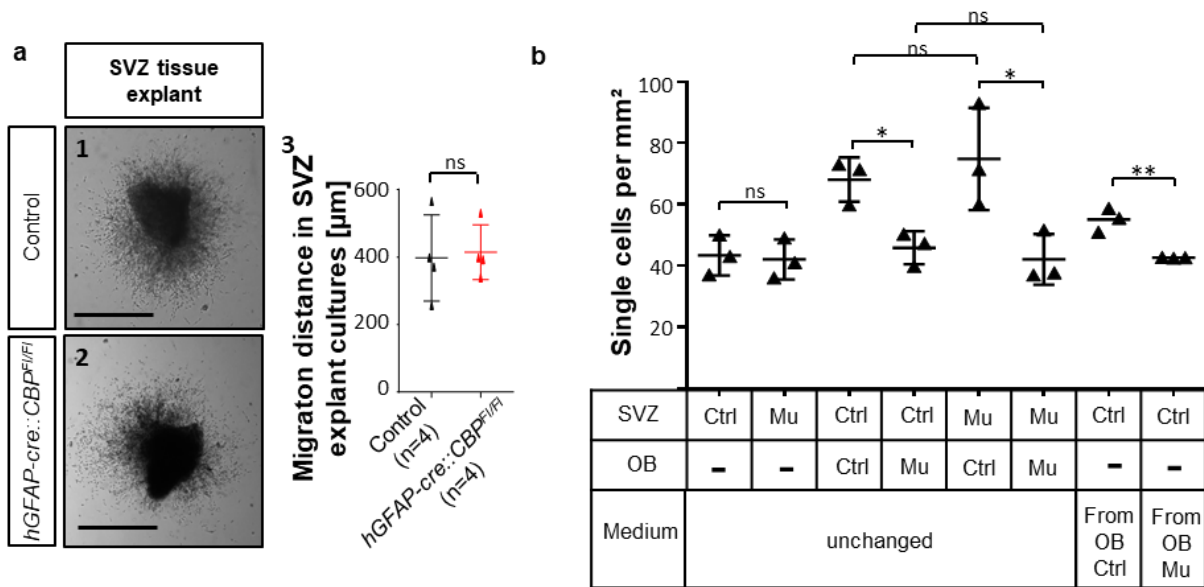
Figure 9: The migration deficit observed in *hGFAP-cre::CBP^{Fl/Fl}* mice is mediated by an extracellular signal from the OB

(a1-3) The intrinsic migration potential of SVZ derived NPCs is independent of CBP function, shown through the culture of SVZ explants in the extracellular matrix Matrigel. (b) The number of single cells was measured around explants of the SVZ cultured in Matrigel. A piece of OB from the wild type induces an exit of neuroblasts from their migratory chains and thereby an increase in single cells. The mutant OB is unable to induce this effect. The same effect can be observed with medium conditioned by tissue from the OB of wild type or mutant mice. Scale bar: 1 mm; ns: not significant, * p < 0.05, ** p < 0.01

To determine this extracellular factor, we used gene expression analyses of the stimulated SVZ explants, aiming to understand which pathways are responding to the stimulus. For this purpose, we extracted RNA from wild type SVZ explants stimulated for 24 h with medium from OB tissue of wild type or *hGFAP-cre::CBP^{Fl/Fl}* mice and sequenced the mRNA.

We compared the sequencing results for SVZ explants cultivated in wild type and CBP deficient OB medium and analyzed the differentially expressed genes (DEGs) in order to get some insight into the affected signaling pathways. We analyzed the DEGs for their involvement in cell migration, which revealed a clustering according to the genotype of the OB (gene ontology (GO) term 0016477, cell migration) (Fig. 10 a).

Additionally, we analyzed the DEGs, which have the highest log2-fold changes. In general, the log2-fold changes between the two conditions were relatively low. This was likely due to the short stimulation time and the low percentage of cells which are migrating out of the explant and respond to the stimulus provided by the medium. We analyzed the 15 most differentially expressed genes and studied the literature for promising candidates among those genes. One gene which caught our attention was the *insulin-like growth factor binding*

protein 5 (*Igfbp5),* an important protein in IGF1 signaling. IGF1 is a growth factor which has been described to be involved in NPC migration. IGF1 knockout mice, described in 2009, show a similar phenotype compared to our CBP deficient animals [152]. In the IGF1 knockout situation, the cells are also accumulating in the RMS. Further, it was shown that the dissemination from the RMS is disturbed in those mice, whereas the migration ability itself is conserved. Taken together, this prompted us to investigate the correlation and we analyzed our gene expression data for genes implicated in IGF signaling. Using the respective GO term (0005520, Insulin-like growth factor binding), we could cluster the samples according to the genotype of the OB which stimulated the medium (Fig. 10 c).

We used our *in vitro* migration experiment to test the hypothesis that IGF1 is implicated in the migration deficit observed in *hGFAP-cre::CBP^Fl/Fl* mice. For this, we again stimulated medium with OB tissue of wild type and CBP deficient mice and analyzed the response of wild type SVZ explants. Additionally, we added IGF1 to the stimulated medium to see if an addition of this growth factor could rescue the migration deficit. To exclude that this effect was growth factor and not IGF1 specific, we performed the same experiment with BDNF, another soluble growth factor implicated in brain development.

The addition of IGF1 rescued the migration deficit in our *in vitro* setting (78 single cells/mm² with medium of control OB+IGF1 vs. 80 single cells/mm² with OB medium of mutant OB+IGF1, Fig. 10 d), whereas no effect of BDNF addition was observed (87 single cells with medium of control OB+BDNF vs. 50 single cells/mm² with medium of mutant OB+BDNF, Fig. 10 d).

These results indicate that the migration deficit in the forebrain is different from the migration deficit observed in the cerebellum of CBP deficient mice described by Merk et al. in 2018 as they could show that an addition of BDNF is able to rescue this effect [115]. A possible explanation is that CBP is involved in many different migration processes in the developing and adult brain, but the effector proteins depend on the cellular context. This would highlight the global role of CBP once more and support the notion of CBP as an integrator of signals.

We also investigated if the amount of IGF1 is reduced in the medium of CBP deficient OB tissue by ELISA. The results of this did not reveal any significant changes in the IGF1 content but a trend towards reduced IGF1 in the mutant medium (65 pg/mL in control medium vs. 57 pg/mL in mutant medium, Fig. 10 e).
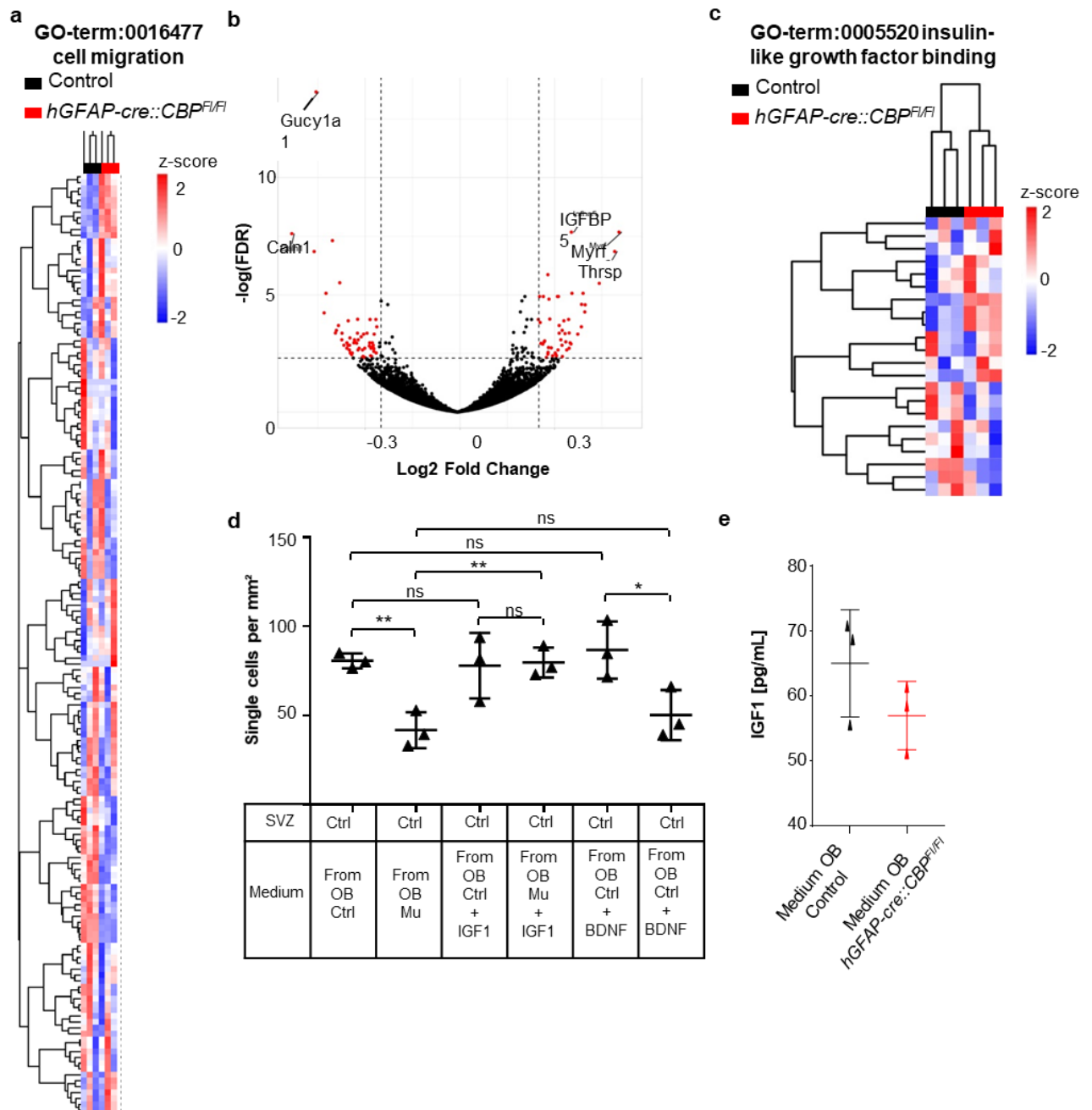
Figure 10: IGF1 as an extracellular signaling molecule is involved in the migration deficit observed in *hGFAP-cre::CBP^{Fl/Fl}* mice

(a) Clustering of DEGs, revealed by RNA sequencing of stimulated SVZ explants with OB medium involved in cell migration reveals a clustering according to the genotype of the OB. (b) RNA sequencing of SVZ explants, which were stimulated with medium conditioned from the OB of control or *hGFAP-cre::CBP^{Fl/Fl}*. In total, 106 genes are statistically different between control and mutant with a log2-fold change ≥ 0.25 and a FDR < 0.1. Genes with high log2-fold changes are annotated. (c) RNA sequencing reveals a difference in IGF signaling between control and mutant. Clustering of RNA sequencing data by the GO-term "0005520 insulin-like growth factor binding" reveals clustering according to the genotype. (d) IGF1 is able to rescue the effect of the CBP deletion on the exit of neuroblasts from chain migration. The addition of recombinant IGF1 to medium conditioned by the OB

of control mice has no effect on the number of single cells. In contrast, the number of single cells in the presence of medium conditioned by a CBP deficient OB tissue supplemented with IGF1 is comparable to the number of single cells from wild type medium. The addition of BDNF has no effect on the migration of NPCs. (e) The amount of IGF1 is reduced in medium stimulated by the OB of CBP deficient mice, shown by ELISA assay. ns: not significant, *p < 0.05, **p < 0.01

3.4 CBP AND TUMORS OF THE CENTRAL NERVOUS SYSTEM

RSTS patients are considered to have a tumor predisposition especially for CNS tumors [75]. Additionally, CBP has been described to be involved in the development of a multitude of different cancers and an analysis of registered mutations in the COSMIC database revealed CBP mutations in 3 % of human tumors [109, 110]. This suggests a function of CBP in tumor development and as many loss-of-function mutations are described, CBP is believed to be a tumor suppressor in most malignancies.

It has been shown before that CBP is frequently mutated in adult SHH MB. Work of Daniel Merk et al. suggests that CBP has a time dependent role in the development of SHH MBs and that it only has a tumor suppressive function when mutated after cerebellar development [115]. This is in line with the observation that *CBP* is significantly more frequently mutated in adult than in infant SHH MBs [119]. An open question is the role of a *CBP* mutation in the predisposition for CNS tumors. Already in the first descriptions of a tumor predisposition in RSTS, patients with MB were included [75]. Also in the large scale screening of MB samples, RSTS patients appeared but the MBs described in those patients were not SHH MBs but group 3 and group 4 MBs [119]. This finding led to the hypothesis that RSTS predisposes to Non-WNT/Non-SHH (group 3 and 4) MBs [76].

Due to the unclear role of CBP in the development of MBs, we decided to use our mouse model, which mimics aspects of RSTS, to study brain tumor development. In order to model the situation in Non-WNT/Non-SHH tumors, we combined the loss of CBP function with an amplification of the well-known oncogene *MYCN* (Fig. 11 a).

We generated *hGFAP-cre::CBP^{Fl/Fl} lsl-MYCN^{Fl/wt}* mice and analyzed them for tumor development. We observed the animals for up to half a year and detected brain tumor formation in a subset of these animals (27 %, within 176 days, Fig. 11 b). We also bred double homozygous mice (*hGFAP-cre::CBP^{Fl/Fl} lsl-MYCN^{Fl/Fl}*) and these mice developed tumors with a shorter latency and a higher frequency than the *hGFAP-cre::CBP^{Fl/Fl} lsl-MYCN^{Fl/wt}* mice (40 % within 130 days). They often presented with abnormalities in their fur and other tumor related symptoms. This supports the idea of an important role for N-myc in the formation of tumors and a dose-dependent effect of the oncogene.

The mice developed large solid lesions in the OB of the affected animals. In addition to these large lesions, we found more diffuse proliferating lesions in the mid- and hindbrain, especially in *hGFAP-cre::CBP^{Fl/Fl} lsl-NMYC^{Fl/Fl}* mice. Those proliferating cells seemed to be associated with blood vessels and/or the brain surface (Fig. 11 c,d,e).
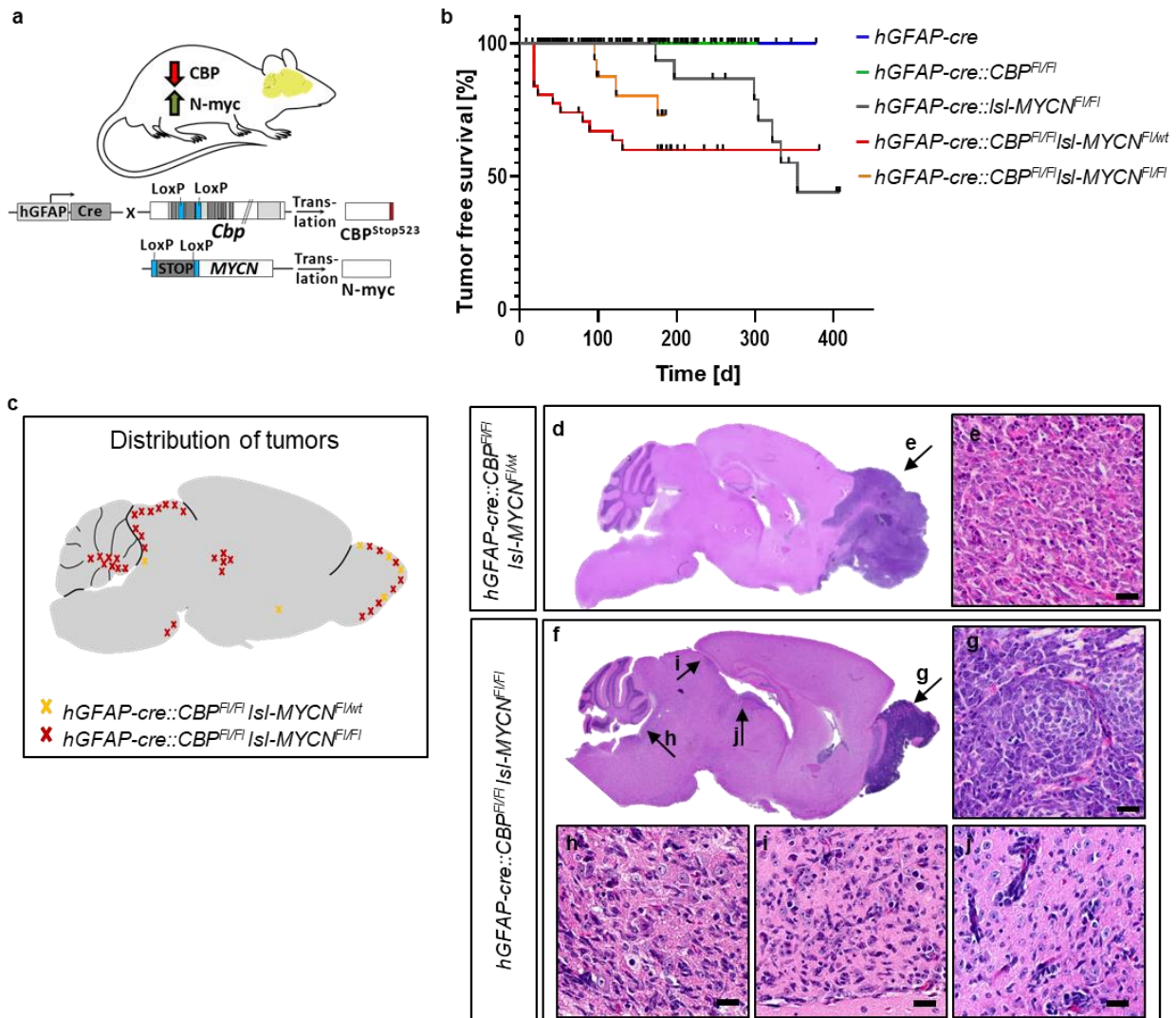

Figure 11: CBP and N-myc cooperate to drive brain tumor growth in mice

(a) Schematic drawing of the genetics of our brain tumor model combining the deletion of *Cbp* with an amplification of *MYCN* driven by the cre-loxP system in a CNS specific manner. Recombination upon *hGFAP*-driven cre activity induces recombination between the loxP sites (blue) flanking exon 7 in the *Cbp* gene and a STOP-codon in front of the *MYCN* gene. Translation leads to a severely shortened and thus no longer functional CBP protein and the expression of N-myc. (b) Kaplan-Meyer survival curves for the different mouse models. Data of the *hGFAP-cre::lsl-MYCN^{Fl/Fl}* mice was generated by Kathrin Fielitz [153]. The numbers of animals for the survival analysis are: *hGFAP-cre* n=75, *hGFAP-cre::CBP^{Fl/Fl}* n=167, *hGFAP-cre::lsl-MYCN^{Fl/Fl}* n=16, *hGFAP-cre::CBP^{Fl/Fl} lsl-MYCN^{Fl/wt}* n=35, *hGFAP-cre::CBP^{Fl/Fl} lsl-MYCN^{Fl/Fl}* n=31. Mice carrying both transgenes develop tumors earlier than mice overexpressing only N-myc. Additional, mice carrying two copies of the *MYCN* transgene have an earlier onset of disease and a higher penetrance. (c) Schematic drawing as an overview where

tumors develop in the brains of mice carrying both transgenes. Tumors of mice having one copy of the *MYCN* oncogene are depicted in yellow and are almost exclusively found in the OB whereas tumors driven by two copies of *MYCN* develop in the OB as well as in the mid- and hindbrain. (d-e) Representative H&E staining of the entire brain and a magnification of an OB tumor from a *hGFAP-cre::CBP^{Fl/Fl} lsl-MYCN^{Fl/wt}* mouse. The arrow points towards the region displayed in (e). (f-j) Representative H&E staining of the tumor bearing brain of a *hGFAP-cre::CBP^{Fl/Fl} lsl-MYCN^{Fl/Fl}* mouse. The arrows point towards the multiple lesion within the brain which are magnified in the insets (g-j). Scale bar: 20µm.

3.4.1 CBP AND N-MYC DRIVEN TUMORS

In order to gain more information on the tumor and tumor-like lesions, we used immunohistochemistry.

The large solid tumors of the OB consisted of small, densely packed cells with large pleomorphic nuclei. This morphological phenotype is described for highly aggressive tumors of embryonic origin [121]. The tumor cells proliferate strongly, shown by Ki67 positivity of most tumor cells and are negative for CBP staining and strongly positive for N-myc (Fig. 12).
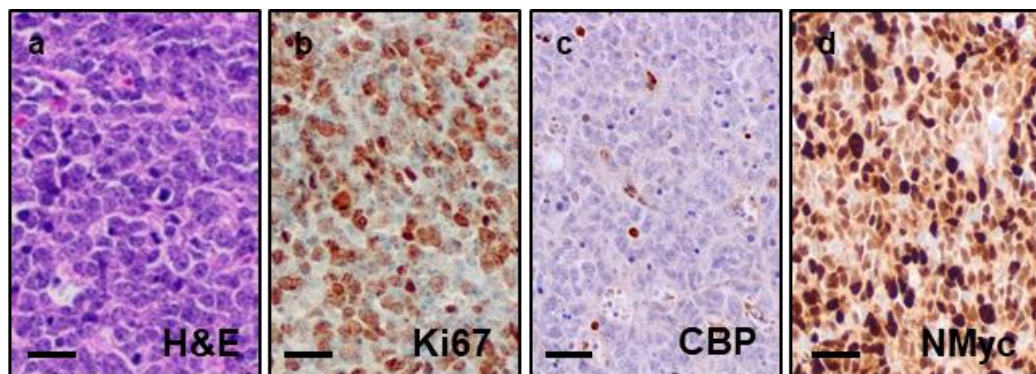

Figure 12: Tumors of the OB consist of strongly proliferating densely packed cells
(a) H&E staining of a tumor of the OB of a *hGFAP-cre::CBP^{Fl/Fl} lsl-MYCN^{Fl/wt}* mouse also depicted in Fig. 11 d. The tumor cells have densely packed pleomorphic nuclei. (b) The tumors proliferate strongly, indicated by Ki67-positivity of a large proportion of cells. (c) The tumor cells do not express CBP but express N-myc as expected by their genotype. Scale bar: 25 µm

In order to learn more about the origin of the OB tumors, younger mice were analyzed and thereby, small lesions, which mark the beginning of tumor development, could be detected. Those lesions are located in the outermost layer of the OB, the periglomerular layer. The interneurons in this cell layer, PGs, are one of the two cell populations in the adult OB which are continuously replaced by new adult born cells. The stem cells responsible for the generation of the PGs reside in the SVZ lining the lateral ventricle. Those cells produce

progenitor cells which migrate towards their destination in the OB through the RMS, a process which we describe to be disturbed in *hGFAP-cre::CBP^{Fl/Fl}* mice.

We analyzed the small lesions further by immunohistochemistry. We stained the tumors for tumor markers like GFAP, Map2c, Sox2 and S100, each being a characteristic marker for a neural or astroglial origin of the tumor (data not shown). None of those markers allowed a clear classification of the tumors. The tumor cells were negative for GFAP and S100, positive for Sox2 and mildly positive for Map2c. We also used the histochemical marker proteins Olig2 and Otx2 to collect more information about the tumors and saw that the tumor cells express Olig2 and are completely negative for Otx2 expression (Fig. 13 e,f).

In the analysis of double homozygous mice carrying a complete loss of *Cbp* together with an amplification of *MYCN* on both alleles, we noted proliferating cells in the mid- and hindbrain of mice. The cells seem to cluster along blood vessels and the brain surface and were found in the white matter of the cerebellum, in the hindbrain close to the cerebellum as well as in the midbrain.

We also analyzed these lesions immunohistochemically in order to compare them to the tumors in the OB. We wanted to determine if the same lesions emerge in different parts of the brain or if different malignancies develop in parallel in the brain of *hGFAP-cre::CBP^{Fl/Fl} lsl-MYCN^{Fl/Fl}* mice. To answer this question, we used the same markers we used for the tumors of the OB: GFAP, Map2c, Sox2, S100, Olig2 and OTX2 (data not shown and Fig. 13 e,f). Depicted in Figure 13 is a lesion in the midbrain associated with the brain surface. Most vessel associated lesions were very diffuse and therefore hard to analyze immunohistochemically. The staining of the lesions revealed a strong proliferation and the expected loss of CBP and expression of N-myc (Fig. 13 h-j). The marker expression of GFAP, Map2c, Sox2 and S100 resembled the expression in the OB lesions and did not allow a clear classification of the lesions (data not shown). On the contrary to the OB lesions, the mid- and hindbrain lesions were expressing OTX2 but not Olig2 (Fig. 13 e,f vs k,l). Therefore, we hypothesized that the lesion in the OB and in the mid- and hindbrain are of different origin and are two independent lesions developing in parallel in the brain of *hGFAP-cre::CBP^{Fl/Fl} lsl-MYCN^{Fl/Fl}* mice.
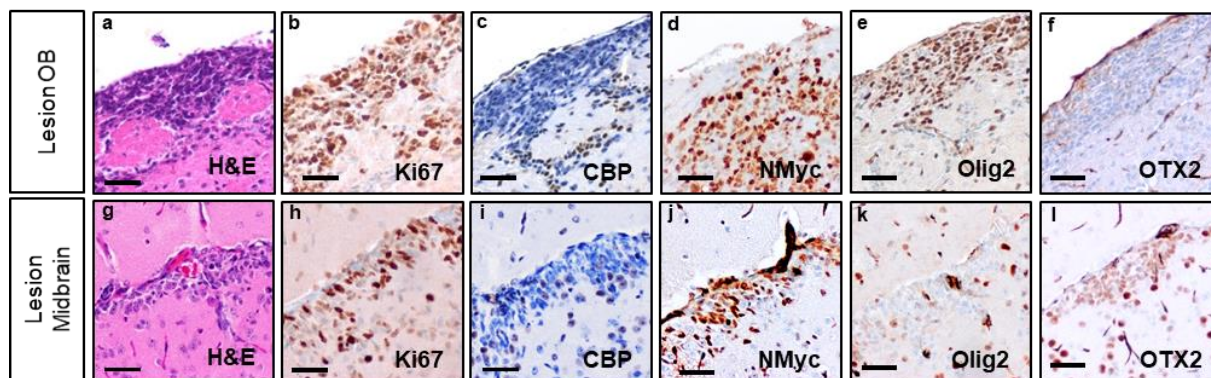
Figure 13: In *hGFAP-cre::CBP^{Fl/Fl} lsl-MYCN^{Fl/Fl}* mice, brain tumor lesions develop in the OB and the midbrain

(a) H&E staining of a lesion in the periglomerular layer of the OB. (b-f) Immunostainings of the lesion in the OB. The cells proliferate strongly and show the expected depletion of CBP and overexpression of N-myc. The lesion stain positive for Olig2 and negative for Otx2. (g) H&E stain of a midbrain lesion of a *hGFAP-cre::CBP^{Fl/Fl} lsl-MYCN^{Fl/Fl}* mouse. (h-l) Immunostainings of a midbrain lesion. The cells proliferate and show the loss of CBP and expression of N-myc. The cells do not show reactivity to Olig2 antibodies but express Otx2. Scale bar: 50µm

We wanted to characterize the lesions driven by CBP depletion and N-myc expression further. Therefore, we used fresh tumor tissue from the OB tumors for a gene expression profiling by microarray. Tissue which was visibly tumor tissue due to its whitish color and consistency was freshly extracted and the RNA was isolated. This RNA was then used for microarray analysis. We chose microarray analysis because array data for many different human tumor entities is publicly available. Due to the diffuse nature of the mid- and hindbrain lesions, we could not use fresh tumor tissue directly for gene expression analysis. However, we were interested in those lesions and in the differences between the OB and hindbrain lesions, which is why we thought about alternative approaches than using fresh mouse tissue for RNA extraction. In order to obtain a more homogenous cell population, we cultivated cells derived from *hGFAP-cre::CBP^{Fl/Fl} lsl-MYCN^{Fl/Fl}* mice. We used 3 - 4 week old *hGFAP-cre::CBP^{Fl/Fl} lsl-MYCN^{Fl/Fl}* mice without tumors visible and their wild type littermates. Because we were interested in lesions of the OB and the mid- and hindbrain, we took the entire OBs and dissected mid- and hindbrain, dissociated the tissue and cultivated it in NSC medium. The dissociated tissue of wild type OBs produced two to five small neurospheres per animal. Those appeared after a few days of culture and were most likely the product of the few adult stem and progenitor cells residing in the OB. The tissue of the mid- and hindbrain of control mice was not able to produce any viable neurospheres. In comparison, in the dissociated tissue of the mutant mice of the OBs as well as the hindbrain tissue, multiple spheres developed after a few days in culture. These spheres were proliferating strongly and

survived at least 6 weeks in culture. Furthermore, we were able to apply normal cell culture techniques like splitting, freezing and thawing.

We also analyzed the spheres immunohistochemically. As expected, the tumor spheres proliferate strongly (Fig. 14 f;i) and do not express CBP but highly express N-myc (Fig. 14 g;k;j;n). At least a proportion of the cells from both, OB and mid- and hindbrain, express Olig2 and Map2c (Fig. 14 l,m; o,p). Additionally, we could show that they express NSC markers like Nestin and Sox2 but also neuronal markers like NeuN (Fig. 14 q-v).
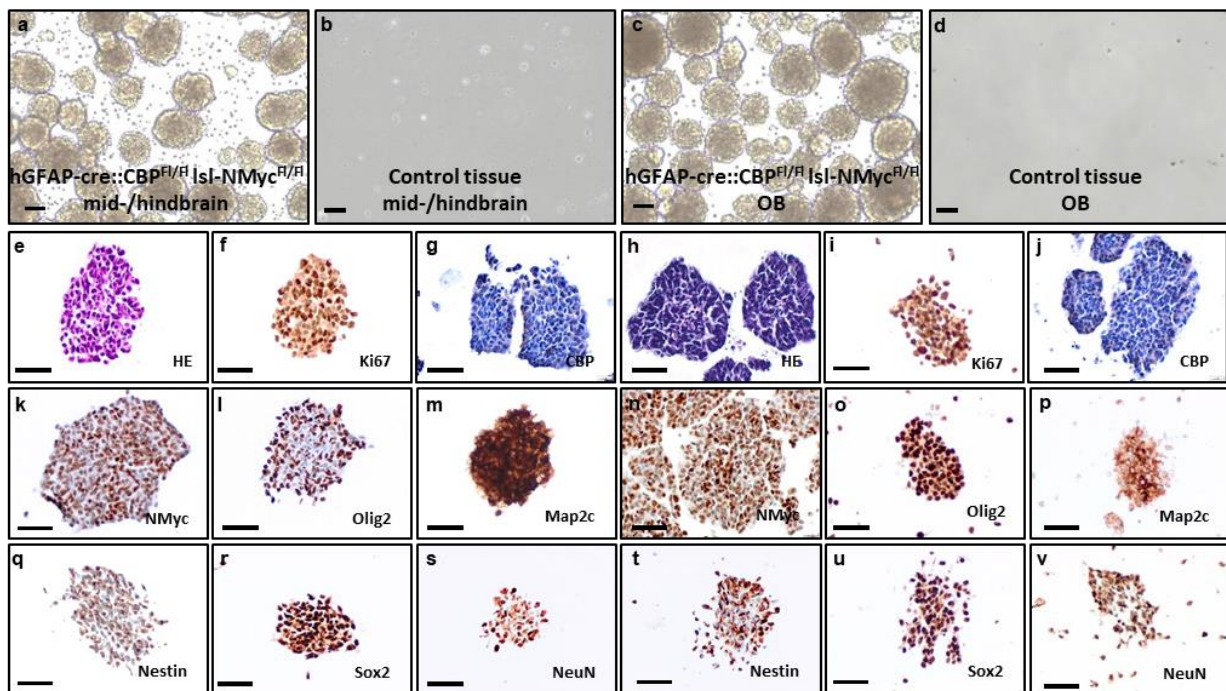

Figure 14: Tumor spheres derived from the mid-/hindbrain and the OB of *hGFAP-cre::CBP^{Fl/Fl} Isl-MYCN^{Fl/Fl}* mice grow in culture and express different histological markers

(a-d) Photos taken of tumor spheres grown in culture for 2 weeks; only very few spheres developed from tissue of control mice. (e-g; k-m; q-s) IHC stains of the developing tumor spheres from the mid-/hindbrain. The spheres proliferate strongly and show protein expression according to their genotype (negativity for CBP and expression of N-myc). The markers Olig2, Map2c, Nestin, Sox2 and NeuN did not allow a clear determination of tumor entity. (h-j; n-p; t-v) IHC stains of the developing tumor spheres from the OB. The spheres proliferate strongly and show protein expression according to their genotype (negativity for CBP and expression of N-myc). Scale bar: 50µm

In order to collect more information about the lesions, we used the tumor spheres to generate gene expressing data by RNA sequencing (Fig. 15). This data clearly shows a separation of the cells according to their origin either in the OB or the mid- and hindbrain with a number of significantly differentially expressed genes (123 down- and 87 upregulated DEGs OB- vs. mid-/hindbrain with a log2-fold change ≥ +/- 1 and a FDR <0.1., Fig. 15 a,b).

Additionally, we looked at the differential expression of known marker genes and could see that the difference in Otx2 and Olig2 positivity observed in the staining of the tumors *in vivo* is also reflected in the transcriptome data (Fig. 15 c). We also used the significantly altered DEGs for an overexpression analysis and saw a different pattern for both cell populations (Fig. 15 d,e). In the OB derived spheres, overrepresented GO-terms included neuron differentiation, neuron development, neural precursor development and other similar terms (Fig. 15 d). In contrast, in the mid-/hindbrain derived spheres, overrepresented GO-terms included terms associated with less differentiation like embryogenesis, tube development and embryonic morphogenesis (Fig. 15 e). This analysis might suggest that both cell populations consist of precursor cells and the cells originating from the hindbrain of the mice represent an even less differentiated and more embryonic cell population.
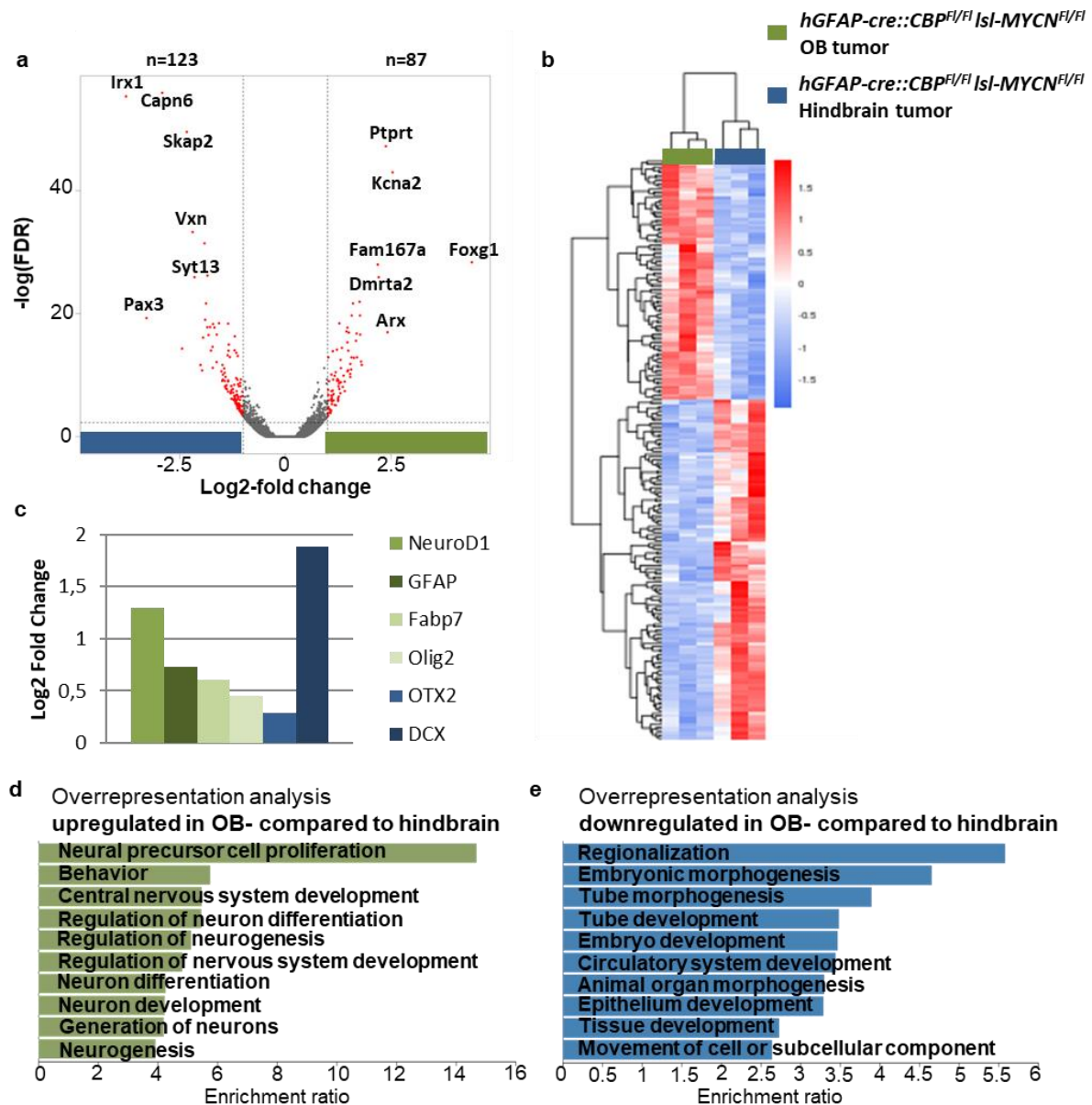
Figure 15: Lesions developing in the brains of *hGFAP-cre::CBP^{Fl/Fl} lsl-MYCN^{Fl/Fl}* mice develop independently and presumably represent different tumor entities

(a) Volcano plot of DEGs between cells generated from the mid-/hindbrain and the OB of *hGFAP-cre::CBP^{Fl/Fl} lsl-MYCN^{Fl/Fl}* mice. 123 DEGs are significantly downregulated and 87 upregulated. DEGs with a log2-fold change +/- 1 and an FDR <0.1 are marked in red. Genes with the highest log2-fold changes are annotated. (b) Unsupervised hierarchical clustering of DEGs. The different anatomic origins cluster apart from each other, supporting the difference between the two lesions. Cells derived from the OB are represented in green on the left, cells from the mid-/hindbrain on the right in blue. (c) Log2-fold changes of marker genes typically used for the characterization of brain tumors. Genes upregulated in the OB derived cells are represented in green, genes upregulated in the mid-/hindbrain derived cells in blue. The expression of Olig2 and OTX2 differs between the two cell populations. (d) Overrepresentation analysis of DEGs upregulated in the OB derived cells compared to the mid-/hindbrain derived cells revealed a differentiating neuronal signature. (e) Overrepresentation

analysis of DEGs downregulated in the OB-derived cells compared to the mid-/hindbrain, revealed a less differentiated embryonal signature in the mid-/hindbrain lesions.

4 DISCUSSION

4.1 CBP IN BRAIN DEVELOPMENT AND HOMEOSTASIS

In this work, we wanted to investigate the functions of CBP in the CNS and thereby gather information about the mechanisms of the ID of RSTS patients. CBP is a transcriptional co-activator with an additional KAT-activity and is ubiquitously expressed in the entire body. RSTS is a neurodevelopmental disorder presenting with a multitude of symptoms always including ID. In 60 % of patients, mutations in *CBP* are responsible for the disease [69].

In order to investigate the molecular functions of CBP, we generated a tissue specific mouse model leading to the deletion of CBP in the CNS. We chose a conditional knockout mouse model, because conventional homozygous knockout animals die prenatally due to multiple developmental defects [95-97]. The decision for a homozygous knockout was based on two main reasons. Firstly, only a homozygous knockout allows the exact study of protein function because no functional copy of the gene is present in the cells. Secondly, a heterozygous knockout shows no obvious phenotypic abnormalities in our mouse model. The homozygous model is clearly not an exact model for RSTS in humans as patients always carry a heterozygous germline mutation. Most likely, homozygous deletions in the germline are prenatally lethal for humans as they are for mice.

The main advantage of our model is the possibility of a homozygous knockout in a specific cell population. Another argument for the scientific value of our model is the resemblance of aspects of RSTS like the microcephaly and also the abnormalities in the OBs and the hippocampus, which has also been described in patients [82].

Another study described a similar procedure but used the *CaMKV* promoter to drive recombination and thereby CBP loss only in postmitotic neurons [101]. This approach was thought to elucidate the postnatal functions of CBP, which should help to gather information about the possible treatment of RSTS patients. They showed that the long-term memory is disturbed in this mouse model, which suggests that a treatment of RSTS patients might be useful in order to increase their intellectual abilities. This promising finding could be investigated further in our mouse model as it shows developmental defects as well as postnatal abnormalities and might therefore be an appropriate model.

When interpreting the data of our mouse model, one has to keep in mind that there are several limitations despite the underlying genetics. The recombination of our target gene *Cbp* is driven by the *hGFAP* promoter which is active from E13 onwards, which in turn means that some structures will be more affected by the loss than others due to embryonic

developmental timing [133]. For example, the hippocampus, which is significantly altered in our mouse model, is affected throughout its entire development whereas the cortex also develops before onset of recombination. This timing differences can explain that some brain regions will be stronger affected by the loss than others and this might not always be due to a higher dependency by itself but depend on the time of the CBP loss. For example, the finding that the overall cortical architecture is intact in *hGFAP-cre::CBP^{Fl/Fl}* mice might be due to the fact that the general cortical architecture is established before loss of CBP and not because this process is independent of CBP.

Additionally, we focused our analysis on neuronal cells although glial cells are also affected by the deletion of CBP and build the largest cell population in the brain. We decided to focus on neuronal cells as these cells are responsible for the information storage and forwarding and might therefore be responsible for the ID seen in RSTS patients. Nevertheless, glial cells are also important in many brain functions and might also influence the intellectual ability. Therefore, an additional analysis of glial cells in the brain of *hGFAP-cre::CBP^{Fl/Fl}* mice would be useful.

Unfortunately, we could not test the intellectual abilities of our mouse model due to the strong phenotypic abnormalities and low stress resistance of the animals. The performed open field test already showed a strong behavioral phenotype but further tests, especially for long- and short-term memory, would have completed our analysis. It was shown before that *hGFAP-cre::CBP^{Fl/Fl}* mice behave differently in a dark-/light-box test, also suggesting an increased anxiety [141]. All mouse models generated so far, including our *hGFAP-cre::CBP^{Fl/Fl}* mice, show a behavioral phenotype and abnormalities in behavior and memory functions. This clearly shows that CBP must be important in those processes and strongly suggests a similar importance in humans.

CBP has been described to be involved in the differentiation of different cell types in mouse models. Additionally, the neuron morphology of the few described analyzed RSTS patients was described as immature [79-81]. In line with those existing reports, the neuron morphology in our mouse model is severely affected by CBP deletion. The neurons have a reduced dendrite length and spine as well as synapse density, which suggests a differentiation delay or failure. In order to collect more information on the consequences of a CBP deletion on neuron morphology, primary neurons of our mouse model were cultivated and their morphology was analyzed in another project. These experiments further support the observation that a loss of CBP leads to a more immature neuron morphology with shortened dendrites [154].

Abnormalities in neuron and especially spine morphology have been described in different syndromes of ID. We also conducted analysis on a mouse model of Pitt-Hopkins syndrome which is caused by mutations in the *Transcription factor 4* and could see abnormalities in neuron morphology. In those mice, the apical dendrite is not significantly shorter, but we observed a significant increase in branching [22]. Other intensely investigated ID syndromes like Down- and Rett-syndrome also show characteristic abnormalities in neuron morphology. In Down-syndrome, the dendritic abnormalities do not seem to be as severe as in RSTS. Neurons of Down-syndrome patients have been described to be shorter and less branched, but the changes are subtle in many mouse models and also human tissue [155-157]. Rett-syndrome, another congenital disease associated with severe ID, has also been studied for implications for neuron morphology, which could act as a morphological correlate to the ID. Also in this disease, diminished neuron lengths as well as abnormalities in spine number and morphology have been described [158-161].The finding that morphological alterations of neurons are associated with an impaired function and that neuron morphology might correlate to ID is of high importance for the understanding of ID. The results generated so far suggest that all studied syndromes share an abnormality of neuron morphology, but the exact alterations seem specific for the syndrome. This suggests that a correlation between the type of ID and the cell shape exists. Most knowledge about CBP function and implications for RSTS as well as other ID syndromes have been gained in mouse models as patient material is rare. Lately, the use of patient-derived induced pluripotent stem cells (iPSCs) has become feasible and thereby allows the study of another model system. In 2018, a first study using neurons differentiated from RSTS patient-derived iPSCs has been published and revealed morphological alterations also in this model system [162]. In order to understand the molecular mechanisms leading to the ID in patients and to understand if the correlation of neuron phenotype and symptoms is really present, it will be important to integrate data generated in mouse models, iPSCs and patient autopsies.

We observed a severe migration deficit in NPCs of the SVZ at the beginning of the RMS and showed by primary cell culture of SVZ precursor cells that this migration deficit is mediated by an extracellular signaling molecule secreted by the OB. Gene expression analysis of these SVZ derived NPCs also demonstrated a CBP dependent difference in their migration behavior. Taken together, we generated *in vivo* and *in vitro* data which imply a function of CBP in cellular migration of NPCs. These results are in line with the hypothesis that RSTS should be grouped with other neural migration disorders such as lisencephaly due to similarities in MRI abnormalities [94].

We presented further that IGF1 is able to rescue the observed migration deficit *in vitro* and hypothesized that this also plays a role *in vivo*. The hypothesis that IGF1 is important in

these processes is supported by the phenotype of IGF1 knockout mice, generated by Hurtado-Chong et al., in 2009 [152]. They observe a similar cell accumulation at the ventricular border of the RMS in their IGF1 knockout animals and proposed that this is due to an effect of IGF1 on the exit of neuroblasts from the RMS in the OB. IGF1 is a growth factor which is expressed during embryonic brain development and whose expression decreases postnatally in most regions but is kept at high levels in the adult OB and the SVZ [152, 163, 164]. We could not reveal the exact mechanisms how CBP regulates IGF1, but due to the *in vitro* experiments, the gene expression data and the strikingly similar phenotype, a crosslink between the two proteins is strongly suggested. It could be demonstrated by Merk et al. in 2018 that a loss of CBP results in a migration deficit of granular precursor cells in the cerebellum which could be rescued by the growth factor BDNF [115]. BDNF had no effect on the migration of NPCs in our *in vitro* experiments, but BDNF and IGF1 are both secreted growth factors. We therefore conclude that CBP is involved in precursor cell migration in different compartments in the brain. Although the effector molecules differ depending on the cellular context, the overall mechanism that CBP regulates the expression of secreted growth factors seems to be prevalent throughout the entire brain. It has been proposed that KATs act mainly by integrating environmental stimuli into gene expression [54]. This function is thought to explain the large phenotypic variability in RSTS patients as the environmental stimuli of patients vary during development and this might be at least in part causing the severity of the ID. The function of CBP to regulate the expression of secreted growth factors or the cellular response to those factors might be one mechanism how CBP as a KAT is able to translate signaling into gene expression. Neural migration is highly regulated by a multitude of different stimuli and CBP might be an important protein in the translation of those signals into a cellular reaction. The results generated by us and others suggest that CBP is involved in differentiation as well as neural migration, two processes which are not clearly distinguishable. Most, if not all, neurons need to migrate from their birthplace to their final destination in the CNS and differentiate on the way [165]. This further supports the importance of CBP in the CNS and its development.

In conclusion, we employed histological and functional methods to analyze a new mouse model for RSTS and provide evidence for a function of CBP in neuronal migration as well as neuronal morphology. We described the consequences of a CBP loss on the establishment of neuronal morphology, which might be a morphological correlation to the ID in RSTS patients. Additionally, we provide evidence that CBP could influence neuronal migration through the regulation of the secretion of IGF1. Taken together, our results contribute to the understanding of RSTS as a complex neurodevelopmental disorder, which will hopefully ultimately help to improve the patient care.

4.2 CBP AND N-MYC COOPERATE TO INDUCE BRAIN TUMOR FORMATION IN MICE

CBP is frequently mutated in human cancers, especially of the CNS. In the last years, large sequencing studies were performed and it could be shown that SHH-MBs regularly carry *CBP* mutations [115, 119]. It has been described before that CBP acts as a tumor suppressor in different tumor entities. Therefore, it was hypothesized that CBP might also act as a tumor suppressor in SHH-MBs. This was investigated by Merk *et al.* in 2018, who were able to reveal a highly time dependent effect of a *CBP* mutation [115]. Their results suggest that CBP is functioning as a tumor suppressor in SHH-MBs only upon mutation after early pre- and postnatal cerebellar development. This also seems to hold true for the human situation as *CBP* mutations occur significantly more often in adult SHH-MBs compared to younger patients. Noteworthy, the cases in which a germline mutation of *CBP* is described and the MB subgroup is known, no SHH-MBs develop but tumors of the Non-WNT/Non-SHH groups 3 and 4 are described [119]. Bourdeaut *et al.* thus hypothesized that RSTS might be a predisposition for this type of MBs [76]. We decided to try to model these tumors by employing our RSTS mouse model and combining it with a transgene overexpressing N-myc. N-myc is known to be frequently amplified in MBs and to drive tumor growth. The generated *hGFAP-cre::CBP^{Fl/Fl} lsl-MYCN* mice developed brain tumors in the OB. Mice carrying two alleles of the *MYCN* gene develop tumors earlier in life and with a higher penetrance then mice carrying only one copy of the oncogene. This indicated that N-myc is driving tumor formation and that the dosage of the oncogenic protein is important. It was described before by Fielitz at al. that mice carrying only the *MYCN* transgene under control of the *hGFAP* promoter develop tumors of the pituitary gland and in the pancreas later in life. In contrast to that, brain tumor formation was not observed [153]. We could recapitulate the pancreas and pituitary gland tumors in our mice in animals which do not develop brain tumors earlier in life. As our *hGFAP-cre::CBP^{Fl/Fl}* mice never develop brain tumors, the tumors in *hGFAP-cre::CBP^{Fl/Fl} lsl-MYCN^{Fl/Fl}* mice are really dependent on both, the loss of CBP and the additional expression of N-myc. Mice carrying two copies of *MYCN* developed not only tumors of the OB, but also more diffuse lesions in the mid- and hindbrain. These were associated with blood vessels or brain surfaces and seem to represent a different tumor entity than the tumors of the OB.

First, we wanted to identify the tumors by histology and then by gene expression analysis in order to learn more about their biology and comparability to human brain tumor entities. In humans, only olfactory neuroblastomas develop in the OB and surrounding tissues. Different to the mouse tumors, those neuroectodermal tumors develop from the olfactory epithelium [166, 167].

In our mice, we could show that tumors develop from PGs of the OB. We hypothesize that the anatomic location of the tumors is largely based on the differences in the biology of mice and men. Mice have an immensely larger olfactory region in the brain and the adult neurogenesis in this region is at least more prominent compared to humans in which its existence is still under debate [168-170]. The active neurogenesis makes this process vulnerable for malignant transformation and therefore, tumor development in this region is not entirely surprising. The OB as a location for mouse tumor formation is also described for other transgenic mouse tumor models like glioblastoma [171-174]. This supports the hypothesis that the OB is a more tumor prone region in mice than in humans.

In order to learn more about the biology of the lesions in our mouse model and to gain a pure population of probably malignant transformed cells, we cultivated tumor cells *in vitro*. For this purpose, we dissected the OB as well as the hind- and midbrain and dissociated the tissue. In *hGFAP-cre::CBP^{Fl/Fl} lsl-MYCN^{Fl/Fl}* mice, spheres developed after a few days in culture whereas in the control situation only very few spheres formed in the tissue from the OB. The spheres from the transgenic animals grew strongly in culture whereas the few OB spheres in the control stopped growth after a short time in culture. This fast growth *in vitro* suggests a malignant potential of the cells. Additionally, we analyzed the global gene expression of the tumor spheres to investigate the differences between cells originating from the OB and the mid- and hindbrain. Thereby, we wanted to determine if they represent two different tumor entities as suggested by immunohistochemistry. In the analysis of the DEGs, we could clearly separate the cells from both anatomic locations, which supports the hypothesis that the two lesions in the brains of *hGFAP-cre::CBP^{Fl/Fl} lsl-MYCN^{Fl/Fl}* mice develop in parallel instead of being one and the same tumor.

Swartling *et al.* recently developed a model for N-myc driven brain tumor formation [175, 176]. They showed that the overexpression of N-myc in NSCs was not sufficient to drive tumor growth but only the expression of a mutational activated N-myc [175]. Additionally, they showed that the origin of the NSC determines the developing tumor type and that NSCs of the forebrain drive forebrain tumors resembling aspects of human gliomas. We propose a model in which *MYCN* does not have to be mutated but is combined with the loss of a tumor suppressor gene to drive tumor formation. This is likely to be more common in human tumors as mutations in N-myc are rare amongst all human tumor entities, whereas amplification and elevated expression are frequently observed [109, 110, 177]. Unfortunately, we were not able to determine the human counterpart of the tumors we observed in the transgenic mice. The tumors, especially of the OB, might resemble human glioma. Swartling et al. proposed in 2012 that N-myc is able to drive different tumor entities depending on the transformed cell. They observed glioma-like tumor formation in the forebrain. Specifically, they hypothesized

that their mouse model develops tumors which resemble malignant glioma and primitive neuroectodermal-tumor like features (MG-PNET). Those tumors, were described to express N-myc or c-myc in their primitive appearing nodules [175, 178]. Additionally, the expression of Olig2 in the OB tumors supports the hypothesis that these tumors might resemble human gliomas as Olig2 is used as an immunohistochemical marker in human glioma. Moreover, its expression is also described for the murine N-myc driven forebrain tumors [175, 179]. Furthermore, mouse models of glioma frequently develop tumors in the OB. A possible explanation for this observation might be that NPCs undergo malignant transformation in the SVZ and then migrate on their natural route into the OB where they establish the tumors [180, 181]. The tumors developing in the mid- and hindbrain of the animals might also resemble gliomas, as their diffuse growth pattern and their association with blood vessels and the brain surface is also described for human glioblastoma [121, 182]. However, the expression of the TF Otx2 suggests a different tumor type. The expression of Otx2, especially in the combination with overexpression of N-myc, has been described in group 3 and group 4 MBs [183].

Taken together, although we were not able to clearly determine which human tumor entity is resembled by our mouse model, we showed clearly that the combination of a loss of CBP and the expression of N-myc can drive tumor formation. The combination of both events might also play a role in human brain tumor formation. Both, CBP mutations as well as high expression of N-myc can be found in different brain tumor entities like MB but also glioma [109, 110, 184]. Therefore, our mouse brain tumor model is worth to be further investigated although no exact matching human tumor entity might be available.

5 OUTLOOK

The RSTS is a congenital neurodevelopmental disorder which is known for 57 years now and since 25 years, the genetic cause in 70 % of patients is understood. However, despite multiple studies and the usage of different mouse models, many CBP functions, especially in brain development, remain unknown. In order to be able to identify possible treatments for RSTS patients, molecular functions of CBP need to be unraveled. Those could lead to drug target discoveries which will ultimately help to improve patient care. With this study, we describe a new conditional mouse model with a CNS-specific complete knockout of *Cbp*. We detected a function of CBP in neuronal migration and neuron morphology.

With our mouse model, we were not able to distinguish the functions of CBP in the development of the CNS from E13 onwards from the effects in the fully developed brain. In order to treat patients after developmental neurogenesis is completed, it is important to determine which effects of a *Cbp* mutation or deletion are remediable by a postnatal treatment. Therefore, it would be useful to employ an additional mouse model and compare the effects of a postnatal deletion of CBP to the results generated with our mouse model. One opportunity would be to use an inducible cre-loxP system also driven by the *hGFAP*-promoter. Such an inducible system employs a fused cre-protein which is only active upon treatment with tamoxifen as the fusion protein can only enter the nucleus upon ligand binding. Thereby, one could study the effects of CBP deletion at different postnatal stages and could also use this mouse model for clinical trials. The combination of the results generated in those mice with our data would allow the exact determination of postnatal effects as this would target the same cells.

We analyzed the effects of a loss of CBP on the neuron morphology in order to collect more information about the basis of the ID in patients. Thereby, we detected a specific profile of alterations which are different from the anomalies described for other ID-syndromes. If it holds true that the morphological alterations represent the morphological correlate to the ID, this would allow the grouping of ID syndromes and maybe a more personalized treatment. In order to gather more information to be able to make such an assumption it would be needed to collect functional data on the one hand and human data on the other hand. Data on neuron function, for example using electrophysiology, would be a useful complement to our existing data. Additionally, more patient material is urgently needed to be able to evaluate the mouse data better. Therefore, autopsies of RSTS brains are needed, especially as the only existing pathological investigations of RSTS patients were performed in the 1960s and 1970s, a time when the genetic testing of patients was not available. Furthermore, patient

derived iPSCs are a relatively new technology which will allow a more detailed analysis of specialized cells and their functions and the analysis of RSTS-patient cells has just started.

In a second part of the project, we wanted to model human brain tumors, especially those of RSTS patients. Therefore, we generated a mouse model which has a CNS specific deletion of CBP and at the same time an overexpression of N-myc. The resulting animals developed aggressive, rapidly proliferating brain tumors in the fore- and hindbrain. In order to clearly demonstrate the malignant potential of the tumors, tumor cells should be transplanted orthotopically into the brains of wild type mice and the potential tumor growth should be monitored.

Histological and location-wise, the mouse tumors did not clearly resemble a human brain tumor entity. We generated global gene expression profiles for our mouse tumors which should be compared to human brain tumor data. This may reveal which human tumor entity is most similar to the CBP and N-myc driven tumors. However, we collected evidence that two different entities emerge in the animals. The forebrain tumors might resemble human glioma. The combination of those two genetic events (mutation of *CBP* and overexpression of N-myc) need to be further investigated as we clearly showed the tumor driving potential. The two genetic modifications could also be more generalized as mutations of a chromatin modifier and overexpression or even amplification of a TF of the Myc family is a frequent event in tumors. Additionally, our mouse model is the first to demonstrate the tumorigenicity of the combination of both. Therefore, our tumor mouse model should be further investigated to identify the corresponding human tumor entity and to test possible treatment options. It was proposed that CBP mutated tumors might be targetable with KDAC-inhibitors, which could be tested in our model. Furthermore, N-myc driven tumors are an ongoing research topic so that targeted therapies might be developed for such tumors. In the development of a new drug, different model systems are needed to test the efficacy. For this, our mouse model would also be of high importance for different N-myc targeting drugs.

Additionally, it was proposed before that glioma derive from malignant transformed NSCs and that a mutationally activated N-myc expressed in NSCs is able to accelerate the proliferation of NSCs. Also, mutations in *CBP* have been proposed to increase the proliferation rate of NSCs [185]. Therefore, it would be interesting to compare the behavior and potential of NSCs derived from our different mouse models (*hGFAP-cre::CBP^{Fl/Fl}*, *hGFAP-cre::lsl-MYCN^{Fl/Fl}* and *hGFAP-cre::CBP^{Fl/Fl} lsl-MYCN^{Fl/Fl}*). If it could be shown that the combination of both genetic events is able to increase the proliferation of NSCs, together with the generated *in vivo* data, would support the hypothesis that aggressive forebrain tumors like glioma derive from transformed NSCs. In order to investigate this further, it might also be possible to design an *in vivo* experiment. For this, SVZ cells would need to be labeled for example by local application of BrdU or a GFP expressing virus. Then, the

labeled cells could be tracked and it could be investigated if these cells form the tumor in the OB. A virus or in-utero electroporation could also be used to induce the recombination only in SVZ cells. Such an experimental set-up using in-utero electroporation and a recombination driving virus was employed to show that glioblastoma could develop in the SVZ [181]. Another possibility to determine if the origin of the tumor lies within in SVZ would be to transplant SVZ cells of a transgenic mouse (*hGFAP-cre::CBP^{Fl/Fl} lsl-MYCN^{Fl/Fl}*) into the SVZ of a wild type mouse and OB cells of the same genotype into the OB and observe if these animals develop tumors.

6 ABSTRACT

The transcriptional co-activator and lysine acetyltransferase CBP is a ubiquitously expressed protein with multiple functions during development and in the adult. Mutations are the underlying cause of the congenital neurodevelopmental disorder Rubinstein-Taybi syndrome (RSTS). This is associated with different symptoms including an intellectual disability (ID). The molecular functions responsible for the ID were investigated in this study. We developed a cre-loxP driven mouse model which allowed a central nervous system specific deletion in cells from embryonic day 13.5 onwards. The resulting *hGFAP-cre::CBP*$^{Fl/Fl}$ mice were analyzed for their behavior and general brain morphology. We show that they display features of RSTS patients like microcephaly and behavioral abnormalities.

Further analysis were focused on the brain and detected abnormalities in the main neurogenic zones: the hippocampus and the subventricular zone (SVZ). The basic architecture of the hippocampus is intact upon CBP deletion but the stem cell compartment is diminished. In the SVZ, we observed a large cell accumulation due to a migration deficit of neural precursor cells. We could recapitulate the migration deficit *in vitro* and provide evidence that it is mediated by IGF1 as an extracellular signaling molecule secreted by the olfactory bulb. The migration deficit was also visible in global gene expression analysis of cultured neural precursor cells. Thereby, we were the first to collect functional evidence that CBP is important in neural migration in the forebrain.

Additionally, we analyzed the cell morphology of forebrain neurons of *hGFAP-cre::CBP*$^{Fl/Fl}$ mice and detected severe alterations. The analyzed pyramidal neurons have a diminished dendrite length as well as spine density upon CBP loss. The ultrastructure of the neurons revealed an additional reduction in synapse number. Together, these results might be the morphological correlate to the ID of RSTS patients.

Apart from the role of CBP in brain development and homeostasis, it is described to have tumor-suppressive functions in different tumor entities. Additionally, a higher tumor risk for RSTS patients has been described. In order to understand this further, we developed a mouse model combining the deletion of *Cbp* with an amplification of the oncogenic driver N-myc. The resulting *hGFAP-cre::CBP*$^{Fl/Fl}$ *lsl-MYCN* mice developed tumors of the olfactory bulb and lesions in the hindbrain. We were able to cultivate tumor cells *in vitro*. Histological and gene expression analysis of the tumors reveal the development of two different tumor entities within the brain of transgenic mice.

Taken together, our results provide evidence for a role of CBP in neuronal migration and an important function in adult neurogenesis. We propose a morphological correlate to the ID in RSTS patients as well as a tumor suppressive role of CBP in combination with the oncogenic driver N-Myc.

7 ZUSAMMENFASSUNG

Der transkriptionelle Co-Aktivator mit Lysin-Acetyltransferase Aktivität CBP ist ein ubiquitär exprimiertes Protein mit vielen Funktionen während der Entwicklung und im adulten Organismus. Mutationen in *CBP* führen zum Rubinstein-Taybi Syndrom (RSTS), einer kongenitalen neuronalen Entwicklungsstörung. RSTS ist assoziiert mit verschiedenen Symptomen, unter anderem einer mentalen Retardierung. Die Funktionen von CBP, in Hirnentwicklung und -homöostase, wurden im Rahmen dieser Arbeit untersucht. Wir haben ein cre-loxP basiertes Mausmodell entwickelt, das eine Deletion im zentralen Nervensystem ab Embryonaltag 13,5 erlaubt. Unsere *hGFAP-cre::CBP^{Fl/Fl}* Mäuse spiegeln einige Aspekte des RSTS wie Mikrozephalie und Verhaltensauffälligkeiten verlässlich wider.

Wir konnten Auffälligkeiten in den neurogenen Zonen des Gehirns, dem Hippocampus und der Subventrikulärzone (SVZ), finden. Die Architektur des Hippocampus ist auch nach Deletion von CBP intakt, allerdings scheint das Stammzellkompartiment verkleinert zu sein. In der SVZ haben wir eine große Zellansammlung durch ein Migrationsdefizit von neuronalen Vorläuferzellen beobachtet und *in vitro* rekapituliert. So konnten wir zeigen, dass vom Bulbus olfaktorius sezerniertes IGF1 als Signalmolekül zum Phänotyp beitragen könnte.

Zusätzlich konnten wir zeigen, dass die Morphologie der pyramidalen Neurone stark verändert ist. Sie haben deutlich verkürzte apikale Dendriten, eine verringerte Dichte von Dornfortsätzen sowie eine signifikante Reduktion von Synapsen.

Zusätzlich zu einer Rolle von CBP in der Gehirnentwicklung ist *CBP* auch als Tumorsuppressor in verschiedenen Tumorentitäten beschrieben. Dazu passt, dass in RSTS Patienten eine Tumorprädisposition beobachtet wurde. Um dies genauer zu verstehen, haben wir ein weiteres Mausmodell generiert, in dem wir die *Cbp* Deletion mit einer Amplifikation des bekannten Onkogens N-Myc kombiniert haben. Die generierten *hGFAP-cre::CBP^{Fl/Fl} lsl-MYCN* Mäuse haben Tumore im Vorder- und Hinterhirn entwickelt. Wir konnten zeigen, dass transgene Tumorzellen auch *in vitro* wachsen. Die Analyse von Tumorhistologie und Genexpression deutet auf eine simultane Entstehung von zwei verschiedenen Tumorentitäten hin.

Zusammenfassend liefern unsere Ergebnisse Hinweise für eine Rolle von CBP in der neuronalen Migration und der Neurogenese. Wir zeigen ein mögliches morphologisches Korrelat für die mentale Retardierung in RSTS Patienten. Zusätzlich zeigen wir, dass ein Verlust von *CBP* in Kombination mit N-myc zu der Entstehung von aggressiven Gehirntumoren führt.

8 LIST OF FIGURES

9 LIST OF TABLES

10 ABBREVIATIONS

Bromo	bromodomain
BSA	bovine serum albumin
CBP	cyclic AMP-responsive element binding protein binding protein
CC	corpus callosum
CH 1-3	cystein/histidine-rich region 1-3
CNS	central nervous system
cre	causing recombination
CREB	cyclic AMP-responsive element binding protein
DAB	3,3'-Diaminobenzidine
DAPI	4,6-Diamidin-2-phenylindol
DCX	doublecortin
DEG	differentially expressed genes
DG	dentate gyrus
DNA	deoxyribonucleic acid
E	embryonic day
ECM	extracellular matrix
ELISA	enzyme-linked immunosorbent assay
floxed	flanked by loxP
GO	gene ontology
hGFAP	human glial fibrillary acidic protein
HRP	horse-radish peroxidase
ID	intellectual disability
IGF1	insulin-like growth factor-1
IGFBP5	insulin-like growth factor binding protein 5
iPSC	induced pluripotent stem cell
KAT	lysine acetyl transferases
KDAC	lysine deacetylases
KIX	CREB binding domain
LGE	lateral ganglionic eminence
loxP	locus for crossing over(x), P1
MB	medulloblastoma
MGE	medial ganglionic eminence
MRI	magnet resonance imaging
NGS	normal goat serum
NPC	neural precursor cells

NRID	nuclear hormone receptor interaction domain
NSC	neural stem cell
OB	olfactory bulb
oSVZ	outer subventricular zone
P	postnatal day
p300	E1A Binding Protein P300
PBS	phosphate buffered saline
PFA	paraformaldehyde
PG	periglomerular cell
PHD	plant homeodomain
PSD	post synaptic density
PVDF	polyvinylidenfluorid
Q	polyglutamine stretch
RG	radial glia
RIN	RNA integrity number
RMS	rostral migratory stream
RNA	ribonucleic acid
RSTS	Rubinstein-Taybi syndrome
RT	room temperature
SDS	sodium dodecyl sulfate
SDS PAGE	sodium dodecyl sulfate polyacrylamide gel electrophoresis
SHH	sonic hedgehog
SVZ	subventricular zone
TAP	transit-amplifying progenitor cell
TAZ	transcriptional adapter zinc-binding domain
TBS-T	tris-buffered saline with 10 % Tween
TF	transcription factor
Trizol	guanidinium thiocyanate-phenol-chloroform extraction
TSE	turbo spin echo
VZ	ventricular zone
WNT	wingless/Int-1

11 REFERENCES

1.   research, F.f.b. *Nobel Prizes in medicine.* 2019   [cited 2020 03.02.2020]; Available from: https://fbresearch.org/medical-advances/nobel-prizes/.

2.   Cuénot, L., *Notes et revues.* Archives de zoologie expérimentale et générale, 1902.

3.   Bedell, M.A., N.A. Jenkins, and N.G. Copeland, *Mouse models of human disease. Part I: techniques and resources for genetic analysis in mice.* Genes and Development, 1997. **11**(1): p. 1-10.

4.   Chinwalla, A.T., L.L. Cook, K.D. Delehaunty, G.A. Fewell, L.A. Fulton, R.S. Fulton, . . . G. Members of the Mouse Genome Analysis, *Initial sequencing and comparative analysis of the mouse genome.* Nature, 2002. **420**(6915): p. 520-562.

5.   Paigen, K., *One Hundred Years of Mouse Genetics: An Intellectual History. I. The Classical Period (1902-1980).* 2003. **163**(1): p. 1-7.

6.   Sternberg, N. and D. Hamilton, *Bacteriophage P1 site-specific recombination. I. Recombination between loxP sites.* Journal of Molecular Biology, 1981. **150**(4): p. 467-86.

7.   Sauer, B. and N. Henderson, *Site-specific DNA recombination in mammalian cells by the Cre recombinase of bacteriophage P1.* Proceedings of the National Academy of Sciences of the United States of America, 1988. **85**(14): p. 5166-5170.

8.   Gu, H., Y.R. Zou, and K. Rajewsky, *Independent control of immunoglobulin switch recombination at individual switch regions evidenced through Cre-loxP-mediated gene targeting.* Cell, 1993. **73**(6): p. 1155-64.

9.   Sakai, Y., *Neurulation in the mouse: Manner and timing of neural tube closure.* The Anatomical Record, 1989. **223**(2): p. 194-203.

10.   O'Rahilly, R. and F. Muller, *Neurulation in the normal human embryo.* Ciba Foundation Symposium, 1994. **181**: p. 70-82; discussion 82-9.

11.   Giedd, J., *Brain development, IX: human brain growth.* The American Journal of Psychiatry, 1999. **156**(1): p. 4.

12.   Semple, B.D., K. Blomgren, K. Gimlin, D.M. Ferriero, and L.J. Noble-Haeusslein, *Brain development in rodents and humans: Identifying benchmarks of maturation and vulnerability to injury across species.* Progress in Neurobiology, 2013. **106-107**: p. 1--16.

13.   Lui, Jan H., David V. Hansen, and Arnold R. Kriegstein, *Development and Evolution of the Human Neocortex.* Cell, 2011. **146**(1): p. 18-36.

14.   Rubenstein, J.L. and P.A. Beachy, *Patterning of the embryonic forebrain.* Current Opinion in Neurobiology, 1998. **8**(1): p. 18-26.

15.   Saladin, K.S., *Human Anatomy.* 2011: McGraw-Hill.

16. Brodmann, K., *Vergleichende Lokalisationslehre der Großhirnrinde; in ihren Prinzipien dargestellt auf Grund des Zellenbaues.* 1909: Joh. Ambrosius Barth, Leipzig.

17. Brodmann, K., *Beiträge zur histologischen Lokalisation der Grosshirnrinde. VI. Mitteilung: Die Cortexgliederung des Menschen.* Journal of Psychology and Neurology, 1908. **10** p. 231-246.

18. Spruston, N., *Pyramidal neurons: dendritic structure and synaptic integration.* Nature Reviews Neuroscience, 2008. **9**(3): p. 206-221.

19. Berry, K.P. and E. Nedivi, *Spine Dynamics: Are They All the Same?* Neuron, 2017. **96**(1): p. 43-55.

20. Fiala, J.C., J. Spacek, and K.M. Harris, *Dendritic Spine Pathology: Cause or Consequence of Neurological Disorders?* Brain Research Reviews, 2002. **39**(1): p. 29-54.

21. Kaufmann, W.E. and H.W. Moser, *Dendritic anomalies in disorders associated with mental retardation.* Cerebral Cortex, 2000. **10**(10): p. 981-91.

22. Schoof, M., M. Hellwig, L. Harrison, D. Holdhof, M.C. Lauffer, J. Niesen, . . . U. Schüller, *The basic helix-loop-helix transcription factor TCF4 impacts brain architecture as well as neuronal morphology and differentiation.* European Journal of Neuroscience. **n/a**(n/a).

23. Jones, E.G., *Cerebral Cortex*, in *Encyclopedia of Neuroscience*, L.R. Squire, Editor. 2004, Academic Press: Oxford. p. 769-773.

24. Vogt, C.V., O., *Allgemeinere Ergebnisse unserer Hirnforschung.* Journal of Psychology and Neurology, 1919. **25**: p. 279-462.

25. Jiang, X. and J. Nardelli, *Cellular and molecular introduction to brain development.* Neurobiology of Disease, 2016. **92**: p. 3-17.

26. Marin, O. and J.L. Rubenstein, *A long, remarkable journey: tangential migration in the telencephalon.* Nature Reviews Neuroscience, 2001. **2**(11): p. 780-90.

27. Angevine, J.B. and R.L. Sidman, *Autoradiographic study of cell migration during histogenesis of cerebral cortex in the mouse.* Nature, 1961. **192**: p. 766--8.

28. Molyneaux, B.J., P. Arlotta, J.R.L. Menezes, and J.D. Macklis, *Neuronal subtype specification in the cerebral cortex.* Nature Reviews Neuroscience, 2007. **8**(6): p. 427--437.

29. Anthony, T.E., C. Klein, G. Fishell, and N. Heintz, *Radial glia serve as neuronal progenitors in all regions of the central nervous system.* Neuron, 2004. **41**(6): p. 881-90.

30. Rakic, P., *Evolution of the neocortex: a perspective from developmental biology.* Nature Reviews Neuroscience, 2009. **10**(10): p. 724-735.

31. Bentivoglio, M. and P. Mazzarello, *The history of radial glia.* Brain Research Bulletin, 1999. **49**(5): p. 305-15.

32. Rakic, P., *Guidance of neurons migrating to the fetal monkey neocortex.* Brain Research, 1971. **33**(2): p. 471-6.

33. Rakic, P., *Mode of cell migration to the superficial layers of fetal monkey neocortex.* J Comp Neurol, 1972. **145**(1): p. 61-83.

34. Hatten, M.E., *Central Nervous System Neuronal Migration.* Annual Review of Neuroscience, 1999. **22**(1): p. 511--539.

35. Marín, O. and J. Rubenstein, *Cell migration in the forebrain.* Annual Review of Neuroscience, 2003. **26**: p. 441-483.

36. Kwan, K.Y., N. Sestan, and E.S. Anton, *Transcriptional co-regulation of neuronal migration and laminar identity in the neocortex.* Development, 2012. **139**(9): p. 1535-46.

37. Lois, C. and A. Alvarez-Buylla, *Long-distance neuronal migration in the adult mammalian brain.* Science 1994. **264**(5162): p. 1145--8.

38. Kornack, D.R. and P. Rakic, *Cell proliferation without neurogenesis in adult primate neocortex.* Science, 2001. **294**(5549): p. 2127-30.

39. Curtis, M.A., M. Kam, U. Nannmark, M.F. Anderson, M.Z. Axell, C. Wikkelso, . . . P.S. Eriksson, *Human neuroblasts migrate to the olfactory bulb via a lateral ventricular extension.* Science 2007. **315**(5816): p. 1243-1249.

40. Altman, J., *Autoradiographic and histological studies of postnatal neurogenesis. IV. Cell proliferation and migration in the anterior forebrain, with special reference to persisting neurogenesis in the olfactory bulb.* The Journal of Comparative Neurology, 1969. **137**(4): p. 433-457.

41. Nam, S.C., Y. Kim, D. Dryanovski, A. Walker, G. Goings, K. Woolfrey, . . . F.G. Szele, *Dynamic features of postnatal subventricular zone cell motility: a two-photon time-lapse study.* The Journal of Comparative Neurology, 2007. **505**(2): p. 190-208.

42. Luskin, M.B., *Restricted proliferation and migration of postnatally generated neurons derived from the forebrain subventricular zone.* Neuron, 1993. **11**(1): p. 173-89.

43. Noctor, S.C., V. Martnez-Cerdeo, L. Ivic, and A.R. Kriegstein, *Cortical neurons arise in symmetric and asymmetric division zones and migrate through specific phases.* Nature Neuroscience, 2004. **7**(2): p. 136--144.

44. Gheusi, G., H. Cremer, H. McLean, G. Chazal, J.D. Vincent, and P.M. Lledo, *Importance of newly generated neurons in the adult olfactory bulb for odor discrimination.* Proceedings of the National Academy of Sciences of the United States of America, 2000. **97**(4): p. 1823-8.

45. Pencea, V. and M.B. Luskin, *Prenatal development of the rodent rostral migratory stream.* The Journal of Comparative Neurology, 2003. **463**(4): p. 402-418.

46. Law, A.K., V. Pencea, C.R. Buck, and M.B. Luskin, *Neurogenesis and neuronal migration in the neonatal rat forebrain anterior subventricular zone do not require GFAP-positive astrocytes.* Developmental Biology, 1999. **216**(2): p. 622-34.

47. Doetsch, F., *A niche for adult neural stem cells.* Current Opinion in Genetics and Development, 2003. **13**(5): p. 543-50.

48. Sun, W., H. Kim, and Y. Moon, *Control of neuronal migration through rostral migration stream in mice.* Anatomy and Cell Biology, 2010. **43**(4): p. 269-279.

49. Lennington, J.B., Z. Yang, and J.C. Conover, *Neural stem cells and the regulation of adult neurogenesis.* Reproductive Biology and Endocrinology 2003. **1**: p. 99-99.

50. Alvarez-Buylla, A. and J.M. García-Verdugo, *Neurogenesis in Adult Subventricular Zone.* The Journal of Neuroscience, 2002. **22**(3): p. 629-634.

51. Chrivia, J.C., R.P.S. Kwok, N. Lamb, M. Hagiwara, M.R. Montminy, and R.H. Goodman, *Phosphorylated CREB binds specifically to the nuclear protein CBP.* Nature, 1993. **365**(6449): p. 855--859.

52. Bedford, D.C., L.H. Kasper, T. Fukuyama, and P.K. Brindle, *Target gene context influences the transcriptional requirement for the KAT3 family of CBP and p300 histone acetyltransferases.* Epigenetics, 2010. **5**(1): p. 9--15.

53. Ogryzko, V.V., R.L. Schiltz, V. Russanova, B.H. Howard, and Y. Nakatani, *The transcriptional coactivators p300 and CBP are histone acetyltransferases.* Cell, 1996. **87**(5): p. 953--9.

54. Sheikh, B.N. and A. Akhtar, *The many lives of KATs - detectors, integrators and modulators of the cellular environment.* Nature Reviews Genetics, 2019. **20**(1): p. 7-23.

55. Verdone, L., M. Caserta, and E.D. Mauro, *Role of histone acetylation in the control of gene expression.* Biochemistry and Cell Biology, 2005. **83**(3): p. 344-353.

56. Chen, L., W. Fischle, E. Verdin, and W.C. Greene, *Duration of nuclear NF-kappaB action regulated by reversible acetylation.* Science, 2001. **293**(5535): p. 1653-7.

57. Tang, Y., W. Zhao, Y. Chen, Y. Zhao, and W. Gu, *Acetylation is indispensable for p53 activation.* Cell, 2008. **133**(4): p. 612-626.

58. Schroder, S., E. Herker, F. Itzen, D. He, S. Thomas, D.A. Gilchrist, . . . M. Ott, *Acetylation of RNA polymerase II regulates growth-factor-induced gene transcription in mammalian cells.* Molecular Cell, 2013. **52**(3): p. 314-24.

59. Valor, L.M., J. Viosca, J.P. Lopez-Atalaya, and A. Barco, *Lysine Acetyltransferases CBP and p300 as Therapeutic Targets in Cognitive and Neurodegenerative Disorders.* Current Pharmaceutical Design, 2013. **19**(28): p. 5051-64.

60. Korzus, E., *Rubinstein-Taybi Syndrome and Epigenetic Alterations.* Advances in Experimental Medicine and Biology, 2017. **978**: p. 39-62.

61. Rubinstein, J.H. and H. Taybi, *Broad thumbs and toes and facial abnormalities. A possible mental retardation syndrome.* American Journal of Diseases of Children 1963. **105**: p. 588--608.

62. Milani, D., F.M.P. Manzoni, L. Pezzani, P. Ajmone, C. Gervasini, F. Menni, and S. Esposito, *Rubinstein-Taybi syndrome: clinical features, genetic basis, diagnosis, and management.* Italian Journal of Pediatrics, 2015. **41**: p. 4.

63. Petrij, F., R.H. Giles, H.G. Dauwerse, J.J. Saris, R.C. Hennekam, M. Masuno, . . . et al., *Rubinstein-Taybi syndrome caused by mutations in the transcriptional co-activator CBP.* Nature, 1995. **376**(6538): p. 348-51.

64. Roelfsema, J.H., S.J. White, Y. Ariyrek, D. Bartholdi, D. Niedrist, F. Papadia, . . . D.J.M. Peters, *Genetic heterogeneity in Rubinstein-Taybi syndrome: mutations in both the CBP and EP300 genes cause disease.* American Journal of Human Genetics, 2005. **76**(4): p. 572--80.

65. Hennekam, R.C., E.J. Lommen, and J.L.a. Strengers, *Rubinstein-Taybi syndrome in a mother and son.* European Journal of Pediatrics, 1989. **148**(5): p. 439-441.

66. Marion, R.W., D.M. Garcia, and J.B. Karasik, *Apparent dominant transmission of the Rubinstein-Taybi syndrome.* American Journal of Medical Genetics, 1993. **46**(3): p. 284-287.

67. Petrij, F., J.C. Dorsman, H.G. Dauwerse, R.H. Giles, T. Peeters, R.C. Hennekam, . . . D.J. Peters, *Rubinstein-Taybi syndrome caused by a De Novo reciprocal translocation t(2;16)(q36.3;p13.3).* American Journal of Medical Genetics, 2000. **92**(1): p. 47-52.

68. Coupry, I., C. Roudaut, M. Stef, M.A. Delrue, M. Marche, I. Burgelin, . . . B. Arveiler, *Molecular analysis of the CBP gene in 60 patients with Rubinstein-Taybi syndrome.* Journal of Medical Genetics, 2002. **39**(6): p. 415-421.

69. Bartsch, O., S. Schmidt, M. Richter, S. Morlot, and Seemanov, *DNA sequencing of CREBBP demonstrates mutations in 56 % of patients with Rubinstein-Taybi syndrome (RSTS) and in another patient with incomplete RSTS.* Human Genetics, 2005. **117**(5): p. 485-493.

70. Lopez-Atalaya, J.P., L.M. Valor, and A. Barco, *Epigenetic factors in intellectual disability: the Rubinstein-Taybi syndrome as a paradigm of neurodevelopmental disorder with epigenetic origin.* Progress in Molecular Biology and Translational Science, 2014. **128**: p. 139-76.

71. Roelfsema, J.H. and D.J. Peters, *Rubinstein-Taybi syndrome: clinical and molecular overview.* Expert Reviews in Molecular Medicine, 2007. **9**(23): p. 1-16.

72. Stevens, C.A. and M.G. Bhakta, *Cardiac abnormalities in the Rubinstein-Taybi syndrome.* American Journal of Medical Genetics, 1995. **59**(3): p. 346--348.

73. Hennekam, R.C. and C.A. Stevens, *Etiology and recurrence risk in Rubinstein-Taybi syndrome.* American Journal of Medical Genetics, 1990. **6**: p. 56-64.

74. Cazalets, J.R., E. Bestaven, E. Doat, M.P. Baudier, C. Gallot, A. Amestoy, . . . D. Lacombe, *Evaluation of Motor Skills in Children with Rubinstein–Taybi Syndrome.* Journal of Autism and Developmental Disorders, 2017. **47**(11): p. 3321-3332.

75. Miller, R.W. and J.H. Rubinstein, *Tumors in Rubinstein-Taybi syndrome.* American Journal of Medical Genetics, 1995. **56**(1): p. 112-115.

76. Bourdeaut, F., C. Miquel, W. Richer, J. Grill, M. Zerah, C. Grison, . . . O. Delattre, *Rubinstein-Taybi syndrome predisposing to non-WNT, non-SHH, group 3 medulloblastoma.* Pediatric Blood and Cancer, 2014. **61**(2): p. 383-6.

77. Hennekam, R.C., A.C. Baselier, E. Beyaert, A. Bos, J.B. Blok, H.B. Jansma, . . . H. Veerman, *Psychological and speech studies in Rubinstein-Taybi syndrome.* American Journal of Mental Retardation, 1992. **96**(6): p. 645--60.

78. Cantani, A. and D. Gagliesi, *Rubinstein-Taybi syndrome. Review of 732 cases and analysis of the typical traits.* European Review for Medical and Pharmacological Sciences, 1998. **2**(2): p. 81-7.

79. Pogacar, S., N.F. Nora, and T.L. Kemper, *Neuropathological findings in the Rubinstein-Taybi syndrome.* Rhode Island Medical Journal, 1973. **56**(3): p. 114-121.

80. Coffin, G.S., *Brachydactyly, peculiar facies and mental retardation.* American Journal of Diseases of Children, 1964. **108**: p. 351-359.

81. Fukunaga, N., S. Suda, Y. Ebihara, N. Laovoravit, and M. Laovoravit, *Rubinstein-Taybi's syndrome - a case report.* Acta Pathologica Japonica, 1969. **19**(4): p. 501-510.

82. Ajmone, P.F., S. Avignone, C. Gervasini, A. Giacobbe, F. Monti, A. Costantino, . . . D. Milani, *Rubinstein-Taybi syndrome: New neuroradiological and neuropsychiatric insights from a multidisciplinary approach.* American Journal of Medical Genetics Part B: Neuropsychiatric Genetics, 2018. **177**(4): p. 406--415.

83. Rebel, V.I., A.L. Kung, E.A. Tanner, H. Yang, R.T. Bronson, and D.M. Livingston, *Distinct roles for CREB-binding protein and p300 in hematopoietic stem cell self-renewal.* Proceedings of the National Academy of Sciences of the United States of America, 2002. **99**(23): p. 14789--14794.

84. Wang, J., I.C.G. Weaver, A. Gauthier-Fisher, H. Wang, L. He, J. Yeomans, . . . F.D. Miller, *CBP Histone Acetyltransferase Activity Regulates Embryonic Neural Differentiation in the Normal and Rubinstein-Taybi Syndrome Brain.* Developmental Cell, 2010. **18**(1): p. 114-125.

85. Tsui, D., A. Voronova, D. Gallagher, D.R. Kaplan, F.D. Miller, and J. Wang, *CBP regulates the differentiation of interneurons from ventral forebrain neural precursors during murine development.* Developmental Biology, 2014. **385**(2): p. 230-241.

86. Lopez-Atalaya, J.P., A. Ciccarelli, J. Viosca, L.M. Valor, M. Jimenez-Minchan, S. Canals, . . . A. Barco, *CBP is required for environmental enrichment-induced neurogenesis and cognitive enhancement.* The EMBO Journal, 2011. **30**(20): p. 4287-98.

87. Bourtchouladze, R., R. Lidge, R. Catapano, J. Stanley, S. Gossweiler, D. Romashko, . . . T. Tully, *A mouse model of Rubinstein-Taybi syndrome: Defective long-term memory is ameliorated by inhibitors of phosphodiesterase 4.* Proceedings of the National Academy of Sciences of the United States of America, 2003. **100**(18): p. 10518-10522.

88. Alarcón, J.M., G. Malleret, K. Touzani, S. Vronskaya, S. Ishii, E.R. Kandel, and A. Barco, *Chromatin Acetylation, Memory, and LTP Are Impaired in CBP+/− Mice: A Model for the Cognitive Deficit in Rubinstein-Taybi Syndrome and Its Amelioration.* Neuron, 2004. **42**(6): p. 947-959.

89. Korzus, E., J. Torchia, D.W. Rose, L. Xu, R. Kurokawa, E.M. McInerney, . . . M.G. Rosenfeld, *Transcription factor-specific requirements for coactivators and their acetyltransferase functions.* Science 1998. **279**(5351): p. 703--7.

90. Schoof, M., M. Launspach, D. Holdhof, L. Nguyen, V. Engel, S. Filser, . . . U. Schüller, *The transcriptional coactivator and histone acetyltransferase CBP regulates neural precursor cell development and migration.* Acta Neuropathologica Communications, 2019. **7**(1): p. 199.

91. Tanaka, Y., I. Naruse, T. Maekawa, H. Masuya, T. Shiroishi, and S. Ishii, *Abnormal skeletal patterning in embryos lacking a single Cbp allele: a partial similarity with Rubinstein-Taybi syndrome.* Proceedings of the National Academy of Sciences of the United States of America, 1997. **94**(19): p. 10215--20.

92. Kung, A.L., V.I. Rebel, R.T. Bronson, L.E. Ch'ng, C.A. Sieff, D.M. Livingston, and T.P. Yao, *Gene dose-dependent control of hematopoiesis and hematologic tumor suppression by CBP.* Genes and Development, 2000. **14**(3): p. 272-277.

93. Oike, Y., A. Hata, T. Mamiya, T. Kaname, Y. Noda, M. Suzuki, . . . K. Yamamura, *Truncated CBP protein leads to classical Rubinstein-Taybi syndrome phenotypes in mice: implications for a dominant-negative mechanism.* Human Molecular Genetics, 1999. **8**(3): p. 387-396.

94. Ateca-Cabarga, J.C., A. Cosa, V. Pallarés, J.P. López-Atalaya, Á. Barco, S. Canals, and D. Moratal, *Brain size regulations by cbp haploinsufficiency evaluated by in-vivo MRI based volumetry.* Scientific Reports, 2015. **5**: p. 16256.

95.   Yao, T.P., S.P. Oh, M. Fuchs, N.D. Zhou, L.E. Ch'ng, D. Newsome, . . . R. Eckner, *Gene dosage-dependent embryonic development and proliferation defects in mice lacking the transcriptional integrator p300.* Cell, 1998. **93**(3): p. 361--72.

96.   Oike, Y., N. Takakura, A. Hata, T. Kaname, M. Akizuki, Y. Yamaguchi, . . . T. Suda, *Mice homozygous for a truncated form of CREB-binding protein exhibit defects in hematopoiesis and vasculo-angiogenesis.* Blood, 1999. **93**(9): p. 2771-9.

97.   Tanaka, Y., I. Naruse, T. Hongo, M. Xu, T. Nakahata, T. Maekawa, and S. Ishii, *Extensive brain hemorrhage and embryonic lethality in a mouse null mutant of CREB-binding protein.* Mechanisms of Development, 2000. **95**(1-2): p. 133-145.

98.   Roth, J.F., N. Shikama, C. Henzen, I. Desbaillets, W. Lutz, S. Marino, . . . R. Eckner, *Differential role of p300 and CBP acetyltransferase during myogenesis: p300 acts upstream of MyoD and Myf5.* The EMBO Journal, 2003. **22**(19): p. 5186-96.

99.   Kasper, L.H., F. Boussouar, P.A. Ney, C.W. Jackson, J. Rehg, J.M. van Deursen, and P.K. Brindle, *A transcription-factor-binding surface of coactivator p300 is required for haematopoiesis.* Nature, 2002. **419**(6908): p. 738-43.

100.   Kasper, L.H., F. Boussouar, K. Boyd, W. Xu, M. Biesen, J. Rehg, . . . P.K. Brindle, *Two transactivation mechanisms cooperate for the bulk of HIF-1-responsive gene expression.* The EMBO Journal, 2005. **24**(22): p. 3846-3858.

101.   Valor, L.M., M.M. Pulopulos, M. Jimenez-Minchan, R. Olivares, B. Lutz, and A. Barco, *Ablation of CBP in Forebrain Principal Neurons Causes Modest Memory and Transcriptional Defects and a Dramatic Reduction of Histone Acetylation But Does Not Affect Cell Viability.* The Journal of Neuroscience, 2011. **31**(5): p. 1652-1663.

102.   del Blanco, B., D. Guiretti, R. Tomasoni, M.T. Lopez-Cascales, R. Muñoz-Viana, M. Lipinski, . . . A. Barco, *CBP and SRF co-regulate dendritic growth and synaptic maturation.* Cell Death and Differentiation, 2019.

103.   Borrow, J., V.P. Stanton, J.M. Andresen, R. Becher, F.G. Behm, R.S.K. Chaganti, . . . Dub, *The translocation t(8;16)(p11;p13) of acute myeloid leukaemia fuses a putative acetyltransferase to the CREB–binding protein.* Nature Genetics, 1996. **14**(1): p. 33--41.

104.   Panagopoulos, I., T. Fioretos, M. Isaksson, U. Samuelsson, R. Billstrom, B. Strombeck, . . . B. Johansson, *Fusion of the MORF and CBP genes in acute myeloid leukemia with the t(10;16)(q22;p13).* Human Molecular Genetics, 2001. **10**(4): p. 395-404.

105.   Rowley, J.D., S. Reshmi, O. Sobulo, T. Musvee, J. Anastasi, S. Raimondi, . . . N. Zeleznik-Le, *All patients with the T(11;16)(q23;p13.3) that involves MLL and CBP have treatment-related hematologic disorders.* Blood, 1997. **90**(2): p. 535--41.

106. Sobulo, O.M., J. Borrow, R. Tomek, S. Reshmi, A. Harden, B. Schlegelberger, . . . N.J. Zeleznik-Le, *MLL is fused to CBP, a histone acetyltransferase, in therapy-related acute myeloid leukemia with a t(11;16)(q23;p13.3).* Proceedings of the National Academy of Sciences of the United States of America, 1997. **94**(16): p. 8732-8737.

107. Mullighan, C.G., J. Zhang, L.H. Kasper, S. Lerach, D. Payne-Turner, L.A. Phillips, . . . J.R. Downing, *CREBBP mutations in relapsed acute lymphoblastic leukaemia.* Nature, 2011. **471**(7337): p. 235--239.

108. Pasqualucci, L., D. Dominguez-Sola, A. Chiarenza, G. Fabbri, A. Grunn, V. Trifonov, . . . R. Dalla-Favera, *Inactivating mutations of acetyltransferase genes in B-cell lymphoma.* Nature, 2011. **471**(7337): p. 189--195.

109. Tate, J.G., S. Bamford, H.C. Jubb, Z. Sondka, D.M. Beare, N. Bindal, . . . S.A. Forbes, *COSMIC: the Catalogue Of Somatic Mutations In Cancer.* Nucleic Acids Research, 2018. **47**(D1): p. D941-D947.

110. COSMIC, S.I. *cancer.sanger.ac.uk.* 08.01.20].

111. Vyazunova, I., V.I. Maklakova, S. Berman, I. De, M.D. Steffen, W. Hong, . . . L.S. Collier, *Sleeping Beauty mouse models identify candidate genes involved in gliomagenesis.* PLoS One, 2014. **9**(11): p. e113489.

112. Brennan, Cameron W., Roel G.W. Verhaak, A. McKenna, B. Campos, H. Noushmehr, Sofie R. Salama, . . . R. McLendon, *The Somatic Genomic Landscape of Glioblastoma.* Cell, 2013. **155**(2): p. 462-477.

113. Jones, D.T.W., N. Jger, M. Kool, T. Zichner, B. Hutter, M. Sultan, . . . P. Lichter, *Dissecting the genomic complexity underlying medulloblastoma.* Nature, 2012. **488**(7409): p. 100--5.

114. Robinson, G., M. Parker, T.A. Kranenburg, C. Lu, X. Chen, L. Ding, . . . R.J. Gilbertson, *Novel mutations target distinct subgroups of medulloblastoma.* Nature, 2012. **488**(7409): p. 43--48.

115. Merk, D.J., J. Ohli, N.D. Merk, V. Thatikonda, S. Morrissy, M. Schoof, . . . U. Schller, *Opposing Effects of CREBBP Mutations Govern the Phenotype of Rubinstein-Taybi Syndrome and Adult SHH Medulloblastoma.* Developmental Cell, 2018. **44**(6): p. 709-724.e6.

116. Sturm, D., S. Bender, D.T.W. Jones, P. Lichter, J. Grill, O. Becher, . . . S.M. Pfister, *Paediatric and adult glioblastoma: multiform (epi)genomic culprits emerge.* Nature Reviews Cancer, 2014. **14**(2): p. 92-107.

117. Northcott, P.A., A.M. Dubuc, S. Pfister, and M.D. Taylor, *Molecular subgroups of medulloblastoma.* Expert Review of Neurotherapeutics, 2012. **12**(7): p. 871-884.

118. Azzarelli, R., B.D. Simons, and A. Philpott, *The developmental origin of brain tumours: a cellular and molecular framework.* Development, 2018. **145**(10).

119. Northcott, P.A., I. Buchhalter, A.S. Morrissy, V. Hovestadt, J. Weischenfeldt, T. Ehrenberger, . . . P. Lichter, *The whole-genome landscape of medulloblastoma subtypes.* Nature, 2017. **547**(7663): p. 311-317.

120. Ostrom, Q.T., H. Gittleman, G. Truitt, A. Boscia, C. Kruchko, and J.S. Barnholtz-Sloan, *CBTRUS Statistical Report: Primary Brain and Other Central Nervous System Tumors Diagnosed in the United States in 2011-2015.* Neuro-Oncology, 2018. **20**(suppl_4): p. iv1-iv86.

121. Louis DN, O.H., Wiestler OD, Cavenee WK, *WHO Classification of Tumours of the Central Nervous System.* Revised 4th Edition ed. WHO Classification of Tumours. Vol. Volume 1. 2016: WHO Press.

122. MacKenzie, D.J., *A Classification of the Tumours of the Glioma Group on a Histogenetic Basis With a Correlated Study of Prognosis.* Canadian Medical Association Journal, 1926. **16**(7): p. 872-872.

123. Okubo, T., P.S. Knoepfler, R.N. Eisenman, and B.L. Hogan, *Nmyc plays an essential role during lung development as a dosage-sensitive regulator of progenitor cell proliferation and differentiation.* Development, 2005. **132**(6): p. 1363-74.

124. Wilde, B.R. and D.E. Ayer, *Interactions between Myc and MondoA transcription factors in metabolism and tumourigenesis.* British Journal of Cancer, 2015. **113**(11): p. 1529-33.

125. Ruiz-Pérez, M.V., A.B. Henley, and M. Arsenian-Henriksson, *The MYCN Protein in Health and Disease.* Genes, 2017. **8**(4): p. 113.

126. Schwab, M., K. Alitalo, K.H. Klempnauer, H.E. Varmus, J.M. Bishop, F. Gilbert, . . . J. Trent, *Amplified DNA with limited homology to myc cellular oncogene is shared by human neuroblastoma cell lines and a neuroblastoma tumour.* Nature, 1983. **305**(5931): p. 245-8.

127. Charron, J., B.A. Malynn, P. Fisher, V. Stewart, L. Jeannotte, S.P. Goff, . . . F.W. Alt, *Embryonic lethality in mice homozygous for a targeted disruption of the N-myc gene.* Genes and Development, 1992. **6**(12a): p. 2248-2257.

128. Sawai, S., A. Shimono, Y. Wakamatsu, C. Palmes, K. Hanaoka, and H. Kondoh, *Defects of embryonic organogenesis resulting from targeted disruption of the N-myc gene in the mouse.* Development, 1993. **117**(4): p. 1445-55.

129. Knoepfler, P.S., P.F. Cheng, and R.N. Eisenman, *N-myc is essential during neurogenesis for the rapid expansion of progenitor cell populations and the inhibition of neuronal differentiation.* Genes and Development, 2002. **16**(20): p. 2699-2712.

130. Rickman, D.S., J.H. Schulte, and M. Eilers, *The Expanding World of N-MYC–Driven Tumors.* Cancer Discovery, 2018. **8**(2): p. 150-163.

131. Chomczynski, P., *A reagent for the single-step simultaneous isolation of RNA, DNA and proteins from cell and tissue samples.* Biotechniques, 1993. **15**(3): p. 532-4, 536-7.

132. Brenner, M. and A. Messing, *METHODS: A Companion to Methods in GFAP Transgenic Mice.* Enzymology, 1996. **10**: p. 351--364.

133. Zhuo, L., M. Theis, I. Alvarez-Maya, M. Brenner, K. Willecke, and A. Messing, *hGFAP-cre transgenic mice for manipulation of glial and neuronal function in vivo.* Genesis, 2001. **31**(2): p. 85--94.

134. Zhang, Z., C. Hofmann, E. Casanova, G. Schutz, and B. Lutz, *Generation of a conditional allele of the CBP gene in mouse.* Genesis, 2004. **40**(2): p. 82--89.

135. Althoff, K., A. Beckers, E. Bell, M. Nortmeyer, T. Thor, A. Sprussel, . . . J.H. Schulte, *A Cre-conditional MYCN-driven neuroblastoma mouse model as an improved tool for preclinical studies.* Oncogene, 2015. **34**(26): p. 3357-68.

136. Wichterle, H., J.M. Garcia-Verdugo, and A. Alvarez-Buylla, *Direct evidence for homotypic, glia-independent neuronal migration.* Neuron, 1997. **18**(5): p. 779-91.

137. Andrews, S. *FASTQC. A quality control tool for high throughput sequence data'.* Available online at: http://www.bioinformatics.babraham.ac.uk/projects/fastqc 2010 [cited 2020 25.02.2020].

138. Dobin, A., C.A. Davis, F. Schlesinger, J. Drenkow, C. Zaleski, S. Jha, . . . T.R. Gingeras, *STAR: ultrafast universal RNA-seq aligner.* Bioinformatics, 2012. **29**(1): p. 15-21.

139. Love, M.I., W. Huber, and S. Anders, *Moderated estimation of fold change and dispersion for RNA-seq data with DESeq2.* Genome Biology, 2014. **15**(12): p. 550.

140. Alvarez-Buylla, A. and D.A. Lim, *For the long run: maintaining germinal niches in the adult brain.* Neuron, 2004. **41**(5): p. 683--6.

141. Launspach, M., *The Role of CBP in Forebrain Development - A Mouse-Model for Rubinstein-Taybi-Syndrome.* Dissertation Medizin, Ludwig-Maximilians-Universität München, 2018.

142. Cox, W.H., *Imprägnation des centralen Nervensystems mit Quecksilbersalzen.* Archiv für mikroskopische Anatomie, 1891. **37**(1): p. 16-21.

143. Golgi, C., *Sulla struttura della sostanza grigia del cervello (Comunicazione preventiva).* Gazetta Medica Italiana Lombardia, 1873. **33**: p. 244-246.

144. Tseng, K.Y., J.E. Anttila, K. Khodosevich, R.K. Tuominen, M. Lindahl, A. Domanskyi, and M. Airavaara, *MANF Promotes Differentiation and Migration of Neural Progenitor Cells with Potential Neural Regenerative Effects in Stroke.* Molecular Therapy : The Journal of the American Society of Gene Therapy, 2018. **26**(1): p. 238-255.

145. Comte, I., Y. Kim, C.C. Young, J.M. van der Harg, P. Hockberger, P.J. Bolam, . . . F.G. Szele, *Galectin-3 maintains cell motility from the subventricular zone to the olfactory bulb.* Journal of Cell Science, 2011. **124**(14): p. 2438-2447.

146. Hirota, Y., T. Ohshima, N. Kaneko, M. Ikeda, T. Iwasato, A.B. Kulkarni, . . . K. Sawamoto, *Cyclin-Dependent Kinase 5 Is Required for Control of Neuroblast Migration in the Postnatal Subventricular Zone.* The Journal of Neuroscience, 2007. **27**(47): p. 12829-12838.

147. Chazal, G., P. Durbec, A. Jankovski, G. Rougon, and H. Cremer, *Consequences of Neural Cell Adhesion Molecule Deficiency on Cell Migration in the Rostral Migratory Stream of the Mouse.* The Journal of Neuroscience, 2000. **20**(4): p. 1446-1457.

148. Chiaramello, S., G. Dalmasso, L. Bezin, D. Marcel, F. Jourdan, P. Peretto, . . . S. De Marchis, *BDNF/TrkB interaction regulates migration of SVZ precursor cells via PI3-K and MAP-K signalling pathways.* European Journal of Neuroscience, 2007. **26**(7): p. 1780-1790.

149. Hack, I., M. Bancila, K. Loulier, P. Carroll, and H. Cremer, *Reelin is a detachment signal in tangential chain-migration during postnatal neurogenesis.* Nature Neuroscience, 2002. **5**: p. 939.

150. Kim, W.R., Y. Kim, B. Eun, O.-h. Park, H. Kim, K. Kim, . . . W. Sun, *Impaired Migration in the Rostral Migratory Stream But Spared Olfactory Function after the Elimination of Programmed Cell Death in Bax Knock-Out Mice.* The Journal of Neuroscience, 2007. **27**(52): p. 14392-14403.

151. Wang, Y., N. Kaneko, N. Asai, A. Enomoto, M. Isotani-Sakakibara, T. Kato, . . . M. Takahashi, *Girdin Is an Intrinsic Regulator of Neuroblast Chain Migration in the Rostral Migratory Stream of the Postnatal Brain.* The Journal of Neuroscience, 2011. **31**(22): p. 8109-8122.

152. Hurtado-Chong, A., M.J. Yusta-Boyo, E. Vergaño-Vera, A. Bulfone, F. De Pablo, and C. Vicario-Abejón, *IGF-I promotes neuronal migration and positioning in the olfactory bulb and the exit of neuroblasts from the subventricular zone.* European Journal of Neuroscience, 2009. **30**(5): p. 742-755.

153. Fielitz, K., K. Althoff, K. De Preter, J. Nonnekens, J. Ohli, S. Elges, . . . U. Schuller, *Characterization of pancreatic glucagon-producing tumors and pituitary gland tumors in transgenic mice overexpressing MYCN in hGFAP-positive cells.* Oncotarget, 2016. **7**(46): p. 74415-74426.

154. Nguyen, L., *Morphologische Veränderungen von Neuronen beim Rubinstein-Taybi-Syndrom anhand eines Mausmodells.* Dissertation Medizin, Universitätsklinikum Hamburg-Eppendorf, unpublished, 2020.

155. Dierssen, M., R. Benavides-Piccione, C. Martinez-Cue, X. Estivill, J. Florez, G.N. Elston, and J. DeFelipe, *Alterations of neocortical pyramidal cell phenotype in the Ts65Dn mouse model of Down syndrome: effects of environmental enrichment.* Cerebral Cortex, 2003. **13**(7): p. 758-764.

156. Huo, H.Q., Z.Y. Qu, F. Yuan, L. Ma, L. Yao, M. Xu, . . . Y. Liu, *Modeling Down Syndrome with Patient iPSCs Reveals Cellular and Migration Deficits of GABAergic Neurons.* Stem Cell Reports, 2018. **10**(4): p. 1251-1266.

157. Haas, M.A., D. Bell, A. Slender, E. Lana-Elola, S. Watson-Scales, E.M. Fisher, . . . F. Guillemot, *Alterations to dendritic spine morphology, but not dendrite patterning, of cortical projection neurons in Tc1 and Ts1Rhr mouse models of Down syndrome.* PLoS One, 2013. **8**(10): p. e78561.

158. Kishi, N. and J.D. Macklis, *MECP2 is progressively expressed in post-migratory neurons and is involved in neuronal maturation rather than cell fate decisions.* Molecular and Cellular Neuroscience, 2004. **27**(3): p. 306-21.

159. Belichenko, N.P., P.V. Belichenko, H.H. Li, W.C. Mobley, and U. Francke, *Comparative study of brain morphology in Mecp2 mutant mouse models of Rett syndrome.* The Journal of Comparative Neurology, 2008. **508**(1): p. 184-195.

160. Belichenko, P.V., E.E. Wright, N.P. Belichenko, E. Masliah, H.H. Li, W.C. Mobley, and U. Francke, *Widespread changes in dendritic and axonal morphology in Mecp2-mutant mouse models of Rett syndrome: evidence for disruption of neuronal networks.* The Journal of Comparative Neurology, 2009. **514**(3): p. 240-58.

161. Rietveld, L., D.P. Stuss, D. McPhee, and K.R. Delaney, *Genotype-specific effects of Mecp2 loss-of-function on morphology of Layer V pyramidal neurons in heterozygous female Rett syndrome model mice.* Frontiers in Cellular Neuroscience, 2015. **9**: p. 145.

162. Alari, V., S. Russo, B. Terragni, P.F. Ajmone, A. Sironi, I. Catusi, . . . L. Larizza, *iPSC-derived neurons of CREBBP- and EP300-mutated Rubinstein-Taybi syndrome patients show morphological alterations and hypoexcitability.* Stem Cell Research, 2018. **30**: p. 130-140.

163. Bondy, C., H. Werner, C.T. Roberts, Jr., and D. LeRoith, *Cellular pattern of type-I insulin-like growth factor receptor gene expression during maturation of the rat brain: comparison with insulin-like growth factors I and II.* Neuroscience, 1992. **46**(4): p. 909-23.

164. Russo, V.C., P.D. Gluckman, E.L. Feldman, and G.A. Werther, *The insulin-like growth factor system and its pleiotropic functions in brain.* Endocrine Reviews, 2005. **26**(7): p. 916-43.

165. Marín, O., M. Valiente, X. Ge, and L.-H. Tsai, *Guiding neuronal cell migrations.* Cold Spring Harbor Perspectives in Biology, 2010. **2**(2): p. a001834-a001834.

166. Bak, M. and R.O. Wein, *Esthesioneuroblastoma: A Contemporary Review of Diagnosis and Management.* Hematology/Oncology Clinics of North America, 2012. **26**(6): p. 1185-1207.

167. Engel, N.W., J.E. Neumann, J. Ahlfeld, A.K. Wefers, D.J. Merk, J. Ohli, and U. Schüller, *Canonical Wnt Signaling Drives Tumor-Like Lesions from Sox2-Positive Precursors of the Murine Olfactory Epithelium.* PloS one, 2016. **11**(11): p. e0166690-e0166690.

168. Curtis, M.A., M. Kam, U. Nannmark, M.F. Anderson, M.Z. Axell, C. Wikkelso, . . . P.S. Eriksson, *Human Neuroblasts Migrate to the Olfactory Bulb via a Lateral Ventricular Extension.* Science, 2007. **315**(5816): p. 1243.

169. Petrik, D. and J.M. Encinas, *Perspective: Of Mice and Men – How Widespread Is Adult Neurogenesis?* Frontiers in Neuroscience, 2019. **13**(923).

170. Sanai, N., T. Nguyen, R.A. Ihrie, Z. Mirzadeh, H.H. Tsai, M. Wong, . . . A. Alvarez-Buylla, *Corridors of migrating neurons in the human brain and their decline during infancy.* Nature, 2011. **478**(7369): p. 382-6.

171. Olson, M.V., D.G. Johnson, H. Jiang, J. Xu, M.M. Alonso, K.D. Aldape, . . . J. Fueyo, *Transgenic E2F1 Expression in the Mouse Brain Induces a Human-Like Bimodal Pattern of Tumors.* Cancer Research, 2007. **67**(9): p. 4005.

172. Alcantara Llaguno, S., J. Chen, C.H. Kwon, E.L. Jackson, Y. Li, D.K. Burns, . . . L.F. Parada, *Malignant astrocytomas originate from neural stem/progenitor cells in a somatic tumor suppressor mouse model.* Cancer Cell, 2009. **15**(1): p. 45-56.

173. Vitte, J., F. Gao, G. Coppola, A.R. Judkins, and M. Giovannini, *Timing of Smarcb1 and Nf2 inactivation determines schwannoma versus rhabdoid tumor development.* Nature Communications, 2017. **8**(1): p. 300.

174. Reilly, K.M., D.A. Loisel, R.T. Bronson, M.E. McLaughlin, and T. Jacks, *Nf1;Trp53 mutant mice develop glioblastoma with evidence of strain-specific effects.* Nature Genetics, 2000. **26**(1): p. 109-113.

175. Swartling, F.J., V. Savov, A.I. Persson, J. Chen, C.S. Hackett, P.A. Northcott, . . . W.A. Weiss, *Distinct neural stem cell populations give rise to disparate brain tumors in response to N-MYC.* Cancer Cell, 2012. **21**(5): p. 601-613.

176. Swartling, F.J., M.R. Grimmer, C.S. Hackett, P.A. Northcott, Q.W. Fan, D.D. Goldenberg, . . . L. Chesler, *Pleiotropic role for MYCN in medulloblastoma.* Genes and Development, 2010. **24**(10): p. 1059-1072.

177. Schaub, F.X., V. Dhankani, A.C. Berger, M. Trivedi, A.B. Richardson, R. Shaw, . . . C. Grandori, *Pan-cancer Alterations of the MYC Oncogene and Its Proximal Network across the Cancer Genome Atlas.* Cell Systems, 2018. **6**(3): p. 282-300.e2.

178. Perry, A., C.R. Miller, M. Gujrati, B.W. Scheithauer, S.C. Zambrano, S.C. Jost, . . . M.K. Rosenblum, *Malignant gliomas with primitive neuroectodermal tumor-like components: a clinicopathologic and genetic study of 53 cases.* Brain Pathology, 2009. **19**(1): p. 81-90.

179. Ligon, K.L., J.A. Alberta, A.T. Kho, J. Weiss, M.R. Kwaan, C.L. Nutt, . . . D.H. Rowitch, *The Oligodendroglial Lineage Marker OLIG2 Is Universally Expressed in Diffuse Gliomas.* Journal of Neuropathology and Experimental Neurology, 2004. **63**(5): p. 499-509.

180. Kroonen, J., J. Nassen, Y.-G. Boulanger, F. Provenzano, V. Capraro, V. Bours, . . . B. Rogister, *Human glioblastoma-initiating cells invade specifically the subventricular zones and olfactory bulbs of mice after striatal injection.* International Journal of Cancer, 2011. **129**(3): p. 574-585.

181. Lee, J.H., J.E. Lee, J.Y. Kahng, S.H. Kim, J.S. Park, S.J. Yoon, . . . J.H. Lee, *Human glioblastoma arises from subventricular zone cells with low-level driver mutations.* Nature, 2018. **560**(7717): p. 243-247.

182. Scherer, H.J., *The forms of growth in gliomas and their practical significance* Brain, 1940. **63**(1): p. 1-35.

183. Lu, Y., C.M. Labak, N. Jain, I.J. Purvis, M.R. Guda, S.E. Bach, . . . K.K. Velpula, *OTX2 expression contributes to proliferation and progression in Myc-amplified medulloblastoma.* American Journal of Cancer Research, 2017. **7**(3): p. 647-656.

184. Grobner, S.N., B.C. Worst, J. Weischenfeldt, I. Buchhalter, K. Kleinheinz, V.A. Rudneva, . . . S.M. Pfister, *The landscape of genomic alterations across childhood cancers.* Nature, 2018. **555**(7696): p. 321-327.

185. Feldman, H.M., C.M. Toledo, S. Arora, P. Hoellerbauer, P. Corrin, L. Carter, . . . P.J. Paddison, *Neural G0: a quiescent-like state found in neuroepithelial-derived cells and glioma.* bioRxiv, 2019: p. 446344.

12 DANKSAGUNG

13 PUBLICATIONS

The basic helix-loop-helix transcription factor TCF4 impacts brain architecture as well as neuronal morphology and differentiation.
Schoof M, Hellwig M, Harrison L, Holdhof D, Lauffer MC, Niesen J, Virdi S, Indenbirken D, Schüller U.
European Journal of Neuroscience 2020 Jan 9. doi: 10.1111/ejn.14674. [Epub ahead of print]

The transcriptional coactivator and histone acetyltransferase CBP regulates neural precursor cell development and migration.
Schoof M, Launspach M, Holdhof D, Nguyen L, Engel V, Filser S, Peters F, Immenschuh J, Hellwig M, Niesen J, Mall V, Ertl-Wagner B, Hagel C, Spohn M, Lutz B, Sedlacik J, Indenbirken D, Merk DJ, Schüller U.
Acta Neuropathologica Communications 2019 Dec 5;7(1):199. doi: 10.1186/s40478-019-0849-5.

hGFAP-Positive Stem Cells Depend on Brg1 for Proper Formation of Cerebral and Cerebellar Structures.
Holdhof D, **Schoof M**, Hellwig M, Holdhof NH, Niesen J, Schüller U.
Cerebral Cortex. 2019 Sep 3. pii: bhz173. doi: 10.1093/cercor/bhz173. [Epub ahead of print]

TCF4 (E2-2) harbors tumor suppressive functions in SHH medulloblastoma.
Hellwig M, Lauffer MC, Bockmayr M, Spohn M, Merk DJ, Harrison L, Ahlfeld J, Kitowski A, Neumann JE, Ohli J, Holdhof D, Niesen J, **Schoof M**, Kool M, Kraus C, Zweier C, Holmberg D, Schüller U.
Acta Neuropathologica 2019 Apr;137(4):657-673. doi: 10.1007/s00401-019-01982-5. Epub 2019 Mar 4.

Opposing Effects of CREBBP Mutations Govern the Phenotype of Rubinstein-Taybi Syndrome and Adult SHH Medulloblastoma.
Merk DJ, Ohli J, Merk ND, Thatikonda V, Morrissy S, **Schoof M**, Schmid SN, Harrison L, Filser S, Ahlfeld J, Erkek S, Raithatha K, Andreska T, Weißhaar M, Launspach M, Neumann JE, Shakarami M, Plenker D, Marra MA, Li Y, Mungall AJ, Moore RA, Ma Y, Jones SJM, Lutz B, Ertl-Wagner B, Rossi A, Wagener R, Siebert R, Jung A, Eberhart CG, Lach B, Sendtner M, Pfister SM, Taylor MD, Chavez L, Kool M, Schüller U.
Developmental Cell. 2018 Mar 26;44(6):709-724.e6. doi: 10.1016/j.devcel.2018.02.012. Epub 2018 Mar 15.

The target landscape of clinical kinase drugs.

Klaeger S, Heinzlmeir S, Wilhelm M, Polzer H, Vick B, Koenig PA, Reinecke M, Ruprecht B, Petzoldt S, Meng C, Zecha J, Reiter K, Qiao H, Helm D, Koch H, **Schoof M**, Canevari G, Casale E, Depaolini SR, Feuchtinger A, Wu Z, Schmidt T, Rueckert L, Becker W, Huenges J, Garz AK, Gohlke BO, Zolg DP, Kayser G, Vooder T, Preissner R, Hahne H, Tõnisson N, Kramer K, Götze K, Bassermann F, Schlegl J, Ehrlich HC, Aiche S, Walch A, Greif PA, Schneider S, Felder ER, Ruland J, Médard G, Jeremias I, Spiekermann K, Kuster B. Science. 2017 Dec 1;358(6367). pii: eaan4368. doi: 10.1126/science.aan4368.

14 CURRICULUM VITAE

Der Lebenslauf wurde aus datenschutzrechtlichen Gründen entfernt.

15 EIDESSTATTLICHE VERSICHERUNG

Ich versichere ausdrücklich, dass ich die Arbeit selbständig und ohne fremde Hilfe verfasst, andere als die von mir angegebenen Quellen und Hilfsmittel nicht benutzt und die aus den benutzten Werken wörtlich oder inhaltlich entnommenen Stellen einzeln nach Ausgabe (Auflage und Jahr des Erscheinens), Band und Seite des benutzten Werkes kenntlich gemacht habe.

Ferner versichere ich, dass ich die Dissertation bisher nicht einem Fachvertreter an einer anderen Hochschule zur Überprüfung vorgelegt oder mich anderweitig um Zulassung zur Promotion beworben habe.

Ich erkläre mich einverstanden, dass meine Dissertation vom Dekanat der Medizinischen Fakultät mit einer gängigen Software zur Erkennung von Plagiaten überprüft werden kann.

Unterschrift: ....